Proton Magnetic Resonance and Molecular Orbital Studies of the Conformational Behaviour of Some Substituted Anisoles and Alkylbenzenes

by

LINA BIG-LIN LEE

A Thesis

Submitted to the Faculty of Graduate Studies

in Partial Fulfillment of the Requirements for

the Degree of

MASTER OF SCIENCE

Department of Chemistry

University of Manitoba

Winnipeg, Manitoba

Canada

August 1991

ISBN 0-315-76915-7

PROTON MAGNETIC RESONANCE AND MOLECULAR ORBITAL STUDIES OF THE CONFORMATIONAL BEHAVIOUR OF SOME SUBSTITUTED ANISOLES AND ALKYLBENZENES

BY

LINA BIG-LIN LEE

A thesis submitted to the Faculty of Graduate Studies of the University of Manitoba in partial fulfillment of the requirements of the degree of

MASTER OF SCIENCE

Acknowledgements

I would like to thank Dr. Ted Schaefer for giving me the opportunity of working in his laboratory. I am very grateful for his advice, guidance, and patience during the course of this work.

I thank Mr. Rudy Sebastian for his instructions in operating the spectrometer and workstation, and in using some of the computer programs related to this research. His help with the 3-21G MO computations on 1,3-dimethoxybenzene is greatly appreciated.

To Mr. Kirk Marat and Mr. Terry Wolowiec, I express thanks for their assistance in the use of the spectrometer and the workstation.

I thank all the graduate students for their friendship, and for making my stay at the university a cherishable memory.

I would like to thank my family, whose love and support have always been an invaluable source of encouragement to me.

Finally, I would like to thank my fiancé, Terence Chu, who is also my best friend, for his encouragement, patience and understanding.

Table of Contents

List of Tables

List of Figures

Abstract

The ^1H nmr spectra of 3-iodoanisole, 1,3-dimethoxybenzene and 5-chloro-1,3-dimethoxybenzene in CS_2 and acetone-d_6, at 300 K, are completely analyzed to yield the long-range coupling constants between the *ortho* ring protons and the methoxy protons, $^5J_o(H,CH_3)$. The values of $^5J_o(H,CH_3)$ imply that the *cis* conformer of 3-iodoanisole is slightly more stable than the *trans* conformer with a fractional population of 0.57(1) and 0.54(1), respectively, in these solutions. For 1,3-dimethoxybenzene, the values of $^5J_o(H,CH_3)$ give certain sums of the fractional populations of the conformers. From these, the *cis-cis* conformer is found to be about 20% more abundant than the *trans-trans* conformer in both solvents. The substitution of a chlorine atom at the *meta* position does not appear to change the population differences. Geometry-optimized STO-3G MO calculations for the free molecule are reported for the rotation of the methoxy group(s) in 3-iodoanisole and 1,3-dimethoxybenzene. The calculations predict that the *trans* conformer of 3-iodoanisole is more stable than the *cis* by 0.26 kJ mol^{-1}, suggesting a slight shift of the *cis/trans* equilibrium in solution. The calculated population distribution of 1,3-dimethoxybenzene indicates that the *cis-cis* conformer is 7% less than the *trans-trans* conformer, in contrast to the behaviour in solution.

The parameters of the fully analyzed ^1H nmr spectra of

isobutylbenzene and 3-phenylpentane in CS_2 at 300 K are reported, together with the geometry-optimized molecular orbital results. The long-range coupling constants between the *para* ring proton and the α-proton(s) in the side chain, $^6J_p(H,H)$, are used to determine the minimum energy conformations and to derive the apparent twofold rotational barriers about the C_{sp^2}-C_{sp^3} bonds of these molecules. Isobutylbenzene has the isopropyl group perpendicular to the aromatic plane in the conformation of lowest energy, and an apparent twofold barrier of 10.4(1) kJ mol^{-1}, which compares very closely with the STO-3G barrier, but not with the AM1. Comparison with the results of ethylbenzene at these two levels indicates that the STO-3G basis set may give a better approximation to the internal rotational barriers of other α-alkyl substituted toluenes. The value of $^3J(H,H)$ in isobutylbenzene indicates a predominant *gauche* orientation of the methine C-H bond and the ring. 3-phenylpentane has the minimum energy conformation with the methine C-H bond in the plane of the ring. The AM1 barrier agrees well with the apparent twofold barrier of 14.9(1) kJ mol^{-1}. The agreement seems to hold for other α,α-dialkyl substituted toluenes, eg., isopropylbenzene. The values of $^3J(H,H)$ in 3-phenylpentane indicate that the free energy difference between the TT and TG^+(or G^-T) conformations is 1.0(4) kJ mol^{-1}, favouring the latter. However the enthalpy of the TT conformer is lower than that of the doubly degenerate TG^+(or G^-T) conformer. The sign of $^4J(CH_3,H)$ is determined as

determined as negative, and the coupling is consistent with the TT and TG^{+}(or $G^{-}T$) conformations.

The use of stereospecific long-range spin-spin coupling constants between the side chain nuclei and the benzene ring nuclei has been successful in studies of molecular conformation and internal dynamics (1-19). In this thesis, two types of long-range coupling constants are used to determine the conformational behaviour of some substituted anisoles and alkylbenzenes in solution. For 3-iodoanisole, 1,3-dimethoxybenzene and 5-chloro-1,3-dimethoxybenzene, the coupling constants between the methoxy protons and the *ortho* ring protons, $^5J_o(H,CH_3)$, are used. The coupling constants between the benzylic or benzalic proton(s) and the *para* ring proton, $^6J_p(H,H)$, are used for isobutylbenzene and 3-phenylpentane. Molecular orbital calculations are also performed for all of these molecules except for 5-chloro-1,3-dimethoxybenzene.

The application of these coupling constants as conformational indicators relies on the fact that they are stereospecific. Therefore, a description of their conformational dependence is given in Chapter 1. However, the interpretation of such coupling constants in terms of conformer populations and of internal rotational potentials, requires detailed discussion and is illustrated by that in Chapter 4. In Chapter 2, the experimental procedures are outlined. All the experimental and computational results are reported in Chapter 3. Chapter 4 contains three sections, in which the substituted anisoles are discussed under three subsections within Section 4.1; isobutylbenzene and

3-phenylpentane are discussed in Section 4.2 and 4.3, respectively. A suggestion of some interesting future work is outlined in Chapter 5.

1. INTRODUCTION

Coupling constants can be discussed in terms of three mechanisms: the σ mechanism, the π mechanism and the proximate or through-space mechanism (20). The σ mechanism involves the transmission of spin state information by the σ electrons. The maximum coupling requires a zig-zag pathway through the intervening bonds between the coupling nuclei. In the π mechanism, the contribution by the π electrons results from the σ-π overlap of σ orbitals of the side chain and the π orbitals of the benzene moiety. The through-space mechanism involves the direct interaction of electrons in orbitals on atoms carrying the spatially proximate nuclei. The magnitude of the coupling is very sensitive to the internuclear distances between the coupled nuclei.

1.1. Stereospecific $^5J_o(H,CH_3)$ in anisole derivatives

The long-range spin-spin coupling constants between the *ortho* ring protons and the methoxy protons, $^5J_o(H,CH_3)$, in anisole and its derivatives are stereospecific (1-4). A detailed set of INDO MO FPT computations performed by Schaefer and Laatikainen (1) has shown that the magnitude of $^5J_o(H,CH_3)$ is strongly dependent on the torsional angle, θ, and

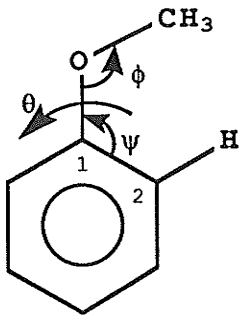

$\theta = 0^\circ$

is dominated by the through-space mechanism. The coupling is calculated as -0.292 Hz for the *cis* conformation of the *ortho* C-H bond and the methoxy group ($\theta=0^\circ$). For the *trans* conformation, $^5J_o(H,CH_3)$ is computed as 0.037 Hz ($\theta=180^\circ$). The coupling is effectively zero as θ approaches 60°, and is 0.037 Hz for θ values between 90° and 180°. The computed values of $^5J_o(H,CH_3)$ can be reproduced by a $\cos^4\theta$ function in the region of $\theta=0^\circ$ to 60° as

$$^5J_o(H,CH_3) = -0.292\cos^4\theta \text{ (Hz)} \qquad [1]$$

where $^5J_o(H,CH_3)$ is the coupling for the methoxy group twisted out of the benzene plane by an angle of θ (3).

The rapid decrease in the magnitude of $^5J_o(H,CH_3)$ as θ increases demonstrates the through-space mechanism. An examination (1), using the procedures of Barfield, shows that the sign of the coupling is determined by the proximate interaction of the methyl carbon valence orbitals and the *ortho* hydrogen 1s orbital. This negative contribution dominates the positive contribution from proximate interactions between the hydrogen orbitals. The sign of $^5J_o(H,CH_3)$ was first determined for 2,4-dibromoanisole in CCl_4 solution as -0.33(2) Hz at ambient temperature (21).

The partially restricted molecular orbital (PRMO) calculations on 2-methoxybenzaldehyde by de Kowalewski et al. (22), at the INDO FPT level, suggested that $^5J_o(H,CH_3)$ is dominated by the through-space mechanism when the methoxy protons are coupled only to the *ortho* protons. However, a π electron mechanism might also be involved, depending on the geometry of the methoxy group and the electronic effect of other substituents on the ring (22). An alternative interpretation of all long-range coupling constants involving the methoxy protons in anisole and some derivatives, consistent with experiment, is available (23).

Computations (1) also have indicated an increase in the magnitude of $^5J_o(H,CH_3)$ as the geometry around the methoxy group and the *ortho* ring proton is compressed. For $\theta=0^\circ$, a decrease of 1° in Ψ or ϕ will lead to a decrease of 0.031 or 0.018 Hz in $^5J_o(H,CH_3)$, respectively. An increase of 1° in Ψ increases the coupling algebraically by 0.025 Hz. The change

of 0.01 Å in the lengths of the C_{sp^2}-O, O-C_{sp^3} and C_{sp^3}-H bonds will only cause a change of ≤0.005 Hz in $^5J_o(H,CH_3)$ (1). The presence of a bulky *ortho* substituent may shorten the average distance between the methyl protons and the *ortho* proton, leading to a larger magnitude of $^5J_o(H,CH_3)$ than in anisole (3). However, none of the groups, OH, SH, SCH_3, OCH_3, CH_2OH, CH_2OCH_3 and $CH_3C{=}O$ at the *ortho* position, seem to change the geometry appreciably. $^5J_o(H,CH_3)$ ranges from -0.288(1) Hz for the OH substituent to -0.270(10) Hz for CH_2OCH_3 (3).

Since $^5J_o(H,CH_3)$ is calculated as -0.292 Hz at $\theta=0^\circ$ and 0.037 Hz at $\theta=180^\circ$, a planar conformation implies that the value of $^5J_o(H,CH_3)$ is $\frac{1}{2}(-0.292+0.037)=-0.13$ Hz (1). If $^5J_o(H,CH_3)$ vanishes at $\theta=180^\circ$, the computed value of 0.037 Hz being considered as an artifact of the computation, then $^5J_o(H,CH_3)$ becomes $-0.292/2=-0.146$ Hz. $^5J_o(H,CH_3)$ in CS_2 and acetone-d_6 at 300 K is -0.152(0) and -0.155(0) Hz, respectively (23), consistent with a substantial barrier to internal rotation and a planar conformation of the methoxy group. The presence of a substituent may increase or decrease the double bond character in the C_{sp^2}-O bond, leading to a decrease or increase in the bond length. The decrease in double bond character will lower the rotational barrier. A decrease in barrier implies a larger torsional amplitude about the bond and a smaller magnitude of $^5J_o(H,CH_3)$, and therefore a larger expectation value of θ, $\langle\theta\rangle$ (2). Substitution of a π electron acceptor, such as CHO, at the 4-position of 1,2-dimethoxybenzene leaves the value of

$^5J_o(H,CH_3)$ unchanged for H-3 and decreases it to -0.308(5) Hz for H-6 (3). Substitution of a π electron donor, such as OCH_3, at the 4-position increases the value of $^5J_o(H,CH_3)$ to -0.232(5) Hz for H-6 (1,3). However, these early data probably need reexamination with modern instrumentation.

The decrease in the magnitude of $^5J_o(H,CH_3)$ can be considered as indicative of an increase in the amplitude of oscillation of the 1-methoxy group in 1,2,4-trimethoxybenzene as compared to 1,2-dimethoxybenzene. By using the $\cos^4\theta$ function in [1], $^5J_o(H,CH_3)$ corresponds to a θ of 20° (3), and can be considered as a change in the rms amplitude of about 10° from its value in anisole (3). A rigorous approach to get $\langle\theta\rangle$ from $^5J_o(H,CH_3)$ requires the knowledge of the potential function for the rotation about the C_{sp^2}-O bond (3,24)[§].

$^5J_o(H,CH_3)$ does not give quantitative information on the rotational barrier about the C_{sp^2}-O bond. The stereospecific couplings between the methoxy carbon and the *para* carbon or

---

[§] For a simple n-fold potential with barrier, B, much larger than kT, a classical averaging procedure (24) gives

$$\langle\theta^2\rangle \sim \frac{2RT}{Bn^2}\ (\text{rad}^2)$$
$$\sim \frac{2RT}{Bn^2}\left(\frac{180}{\pi}\right)^2\ (\text{deg}^2)$$

This expression originates from the relation of the sinusoidal potential function of a librating group, with a small vibration amplitude, and the quadratic force constant, $f=\frac{RT}{\langle\theta^2\rangle}$ kJ mol^{-1} rad^{-2}, which is $V=\frac{1}{2}B(1-\cos n\theta)=\frac{1}{4}Bn^2\theta^2\sim\frac{1}{2}f\theta^2$ (neglecting all terms higher than quadratic in the expanded series). Then $B\sim\frac{2RT}{\langle\theta^2\rangle}$ (24). The barrier of 25.1 kJ mol^{-1} for anisole at 305 K gives $\langle\theta^2\rangle^{1/2}=13°$ for n=2 and $\langle\theta^2\rangle^{1/2}=6°$ for n=4 (3). However, the barrier in anisole is a mixture of twofold and fourfold components (5,7,25,26).

proton, $^{5}J(^{13}C,^{13}C)$ (6,8) and $^{6}J_{p}(^{1}H,^{13}C)$ (5,7,8), employing the J-method, have proved useful in this respect (for the J-method, see Section 1.2). Both $^{5}J(^{13}C,^{13}C)$ and $^{6}J_{p}(^{1}H,^{13}C)$ are σ-π electron couplings and are proportional to $\sin^{2}\theta$, as in [2] and [3],

$$^{5}J(^{13}C,^{13}C) = (0.98\pm0.03)\langle\sin^{2}\theta\rangle \text{ (Hz)} \qquad [2]$$

$$^{6}J_{p}(^{1}H,^{13}C) = (0.625\pm0.005)\langle\sin^{2}\theta\rangle \text{ (Hz)} \qquad [3]$$

where $\langle\sin^{2}\theta\rangle$ is the the expectation values of $\sin^{2}\theta$.

For *meta* substituted anisoles (eg. 3-fluoroanisole (4)), the sum of $^{5}J_{o}(H,CH_{3})$ for H-2 and H-6 is taken as $^{5}J_{c}(H,CH_{3})$ for the *cis* orientation and $^{5}J_{t}(H,CH_{3})$ for the *trans* is assumed to vanish (see Section 4.1.2).

$$^{5}J_{c}(H,CH_{3}) = {}^{5}J_{o}(H2,CH_{3}) + {}^{5}J_{o}(H6,CH_{3}) \text{ (Hz)} \qquad [4]$$

1.2. $^{n}J(H,H)$ for n=4,5,6 in alkylbenzenes and the J-method

The long-range spin-spin coupling constants between the ring protons and the benzylic or benzalic protons in the side chain, $^{n}J(H,H)$, for n=4,5,6, in benzene derivatives are useful in conformational studies (9-19). These couplings depend on θ, the angle by which the C_α-H bond containing the coupled proton in the side chain is twisted out of the plane of the

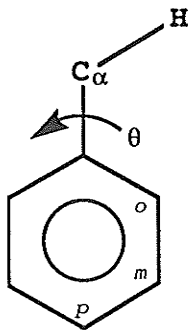

ring. The conformational dependence and the mechanism of the methyl-ring proton couplings in toluene, *o*-, *m*- and *p*-xylene have been studied with INDO MO FPT computations by Wasylishen and Schaefer (27).

$^{6}J_{p}(H,H)$ and the J-Method

It has been proved in numerous studies that $^{6}J_{p}(H,H)$ is useful in the determination of the minimum energy conformation and of the internal rotational barrier of the side chain in alkylbenzenes (9,10,12-19). $^{6}J_{p}(H,H)$ in toluene is calculated as -0.075 Hz at $\theta=0^{\circ}$ and -1.219 Hz at $\theta=90^{\circ}$

(27). The computed values closely obey a $\sin^2\theta$ dependence, implying a sole π electron mechanism for $^6J_p(H,H)$. Experimentally, $^6J_p(H,H)$ for toluene in CS_2 at 300 K is -0.602(2) Hz (9), and $^7J_p(CH_3,CH_3)$ for *p*-xylene is +0.60(3) Hz (10), in good agreement with the π electron mechanism for the methyl group replacement model. The coupling is written as

$$^6J_p(H,H) = {}^6J_0 + {}^6J^{\pi}_{90}\langle\sin^2\theta\rangle \text{ (Hz)} \qquad [5]$$

where $^6J_0$ is negligibly small (13,14), $^6J^{\pi}_{90}$ is -1.204(4) Hz from toluene (9), and $\langle\sin^2\theta\rangle$ is the average of $\sin^2\theta$ over the populated rotational states. $^6J_p(H,H)$ is insensitive to ring substitution (9). The methyl group rotational barrier in toluene is 0.06 kJ mol^{-1} (12); therefore toluene has $\langle\sin^2\theta\rangle$ as 0.5 for an effectively zero barrier. For an α-substituted toluene, the rotational barrier is larger than zero and $\langle\sin^2\theta\rangle$ is different from 0.5.

The method of using $\langle\sin^2\theta\rangle$, deduced from the measured $^6J_p(H,H)$ if $^6J^{\pi}_{90}$ is known, to give the apparent twofold rotational barrier about the C_{sp^2}-C_{sp^3} bond in an α-substituted toluene (also applicable to some other benzene derivatives) is called the J-method (12,29). The procedure involves solution of the hindered rotor problem in terms of the free rotor basis, and weighting the values of $\langle\sin^2\alpha\rangle$ for each state with a Boltzmann factor [7].

$$-\left(\frac{\hbar^2}{2I}\right)\left(\frac{d^2\Psi_m}{d\alpha^2}\right) + \left(\frac{V_2}{2}\right)(1-\cos^2\alpha)\Psi_m = E_m\Psi_m \qquad [6]$$

$$\langle \sin^2\alpha \rangle = \sum_{p=0}^{\infty} \langle \Psi_p | \sin^2\alpha | \Psi_p \rangle \frac{\exp(-E_p/kT)}{\sum_{p=0}^{\infty} \exp(-E_p/kT)} \qquad [7]$$

where I is the reduced moment of inertia about the C_{sp^2}-C_{sp^3} bond, α is the angle defining the orientation of the side chain relative to the benzene plane, V_2 is the magnitude of the twofold internal rotational barrier, E_m and Ψ_m are the energy and the wavefunction of the m^{th} state, and T is the temperature. The angle α may not be the same as the angle θ (defined on p.10), depending on the minimum energy conformation. For $\langle \sin^2\theta \rangle \neq \langle \sin^2\alpha \rangle$, the conversion has to be made by a trigonometric treatment (29), as in [8],

$$\begin{aligned} \langle \sin^2\theta \rangle &= \cos^2\theta_{min} \langle \sin^2\alpha \rangle + \sin^2\theta_{min} \langle \cos^2\alpha \rangle \\ &= \cos 2\theta_{min} \langle \sin^2\alpha \rangle + \sin^2\theta_{min} \end{aligned} \qquad [8]$$

where θ_{min} is defined as the angle between the C_α-H bond and the benzene plane in the minimum energy conformation.

Tables of $\langle \sin^2\theta \rangle$ and V_2 at particular values of I and T can be drawn up by the computer, enabling the barrier height to be estimated by comparison. Quite often, the barrier to internal rotation includes higher terms than just the twofold term (16,18). Tables with values of V_2, V_4 and $\langle \sin^2\theta \rangle$, obtained by classical averaging, are also used. The ratio of the V_2 and V_4 terms cannot be estimated from the measured $^6J_p(H,H)$, but can be predicted by molecular orbital calculations. The J-method is most accurate for the

determination of rotational barriers within the range of 0.8-12.6 kJ mol^{-1}; $\langle \sin^2\theta \rangle$ is found to be insensitive to I for the molecules of interest here (12).

The minimum energy conformation of the molecule is ascertained from the value of $\langle \sin^2\theta \rangle$ deduced from the measured $^6J_p(H,H)$. For benzalic compounds, the four possible conceivable minimum energy conformations have $\theta_{min}=0^\circ$, 30°, 60° and 90° as indicated below:

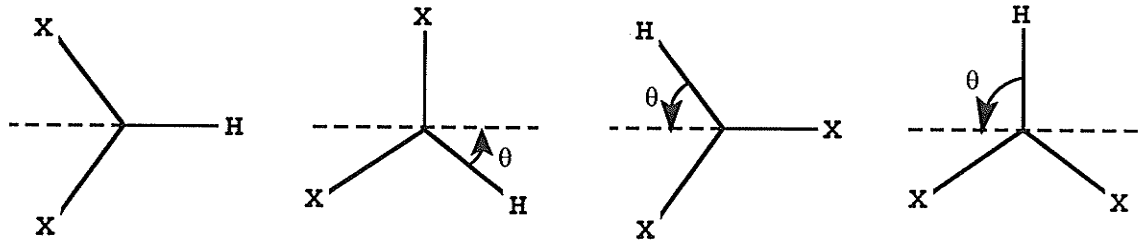

$\theta_{min}=0^\circ$	$\theta_{min}=30^\circ$	$\theta_{min}=60^\circ$	$\theta_{min}=90^\circ$
$0.5 \geq \sin^2\theta \geq 0.0$	$0.5 \geq \sin^2\theta \geq 0.25$	$0.5 \leq \sin^2\theta \leq 0.75$	$0.5 \leq \sin^2\theta \leq 1.0$
I	**II**	**III**	**IV**

The low barrier limit corresponds to a $\langle \sin^2\theta \rangle$ of 0.5 (cf. toluene). In the high barrier limit, the molecule will be locked in one of the conformations, **I**, **II**, **III** or **IV**, which have values of $\langle \sin^2\theta \rangle$ as 0.0, 0.25, 0.75 and 1.0, respectively. For a molecule with finite barrier, the value of $\langle \sin^2\theta \rangle$ fall between either one of these four values and 0.5. The minimum energy conformer is then determined by comparison with these ranges in each conformation.

For benzylic compounds, there are two θ_{min}. The $\langle \sin^2\theta \rangle$ corresponding to the high barrier limit is calculated by

averaging the expectation values at these two angles.

$$\langle \sin^2\theta \rangle = \frac{\langle \sin^2\theta_{min1} \rangle + \langle \sin^2\theta_{min2} \rangle}{2} \qquad [9]$$

The four low energy forms of benzylic compounds are **V**, **VI**, **VII** and **VIII**.

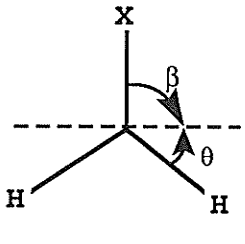

$\theta_{min}=30^\circ, 30^\circ$

$0.5 \geq \sin^2\theta \geq 0.25$

V

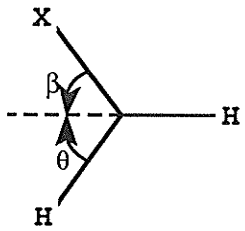

$\theta_{min}=0^\circ, 60^\circ$

$0.5 \geq \sin^2\theta \geq 0.375$

VI

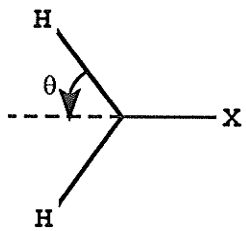

$\theta_{min}=60^\circ, 60^\circ$

$0.5 \leq \sin^2\theta \leq 0.7$

VII

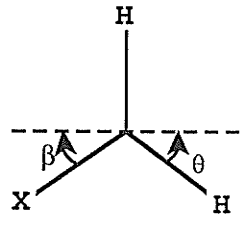

$\theta_{min}=30^\circ, 90^\circ$

$0.5 \leq \sin^2\theta \leq 0.625$

VIII

The angles θ and β are related by equation [10] for a

$$\langle \sin^2\theta \rangle = 0.75 - 0.5\langle \sin^2\beta \rangle \qquad [10]$$

tetrahedral geometry at the side chain.

^5J_m(H,H)

The calculated coupling constants between the *meta* ring protons and the α-protons in toluene (27) do not agree with a sole π electron mechanism. The angular dependence of ^5J_m(H,H) is compatible with a π electron mechanism of $\sin^2\theta$ superimposed on a σ electron mechanism of $\sin^2(\frac{\theta}{2})$, and can be written (11) as [11],

$$^5J_m(H,H) = {}^5J^{\pi}_{90}\langle\sin^2\theta\rangle + {}^5J^{\sigma}_{180}\langle\sin^2(\tfrac{\theta}{2})\rangle \text{ (Hz)} \qquad [11]$$

where $^5J^{\pi}_{90}$ is the magnitude of the σ-π electron component for $\theta=90^\circ$, and $^5J^{\sigma}_{180}$ is the magnitude of the σ electron component for $\theta=180^\circ$. $^5J^{\pi}_{90}$ vanishes at $\theta=0^\circ$ and 180°, and $^5J^{\sigma}_{180}$ vanishes at $\theta=0^\circ$. On the basis of the measured $^5J_m(H,H)$ in the 2,6-difluoro derivatives of toluene, ethylbenzene and cumene, and the values of $\langle\sin^2\theta\rangle$ obtained from the respective $^6J_p(H,H)$, and a value of 0.5 for $\langle\sin^2(\frac{\theta}{2})\rangle$, $^5J^{\pi}_{90}$ is deduced as 0.336 Hz and $^5J^{\sigma}_{180}$ as 0.540 Hz (11). Therefore,

$$^5J_m(H,H) = 0.336\langle\sin^2\theta\rangle + 0.540\langle\sin^2(\tfrac{\theta}{2})\rangle \text{ (Hz)} \qquad [12]$$

For toluene, $^5J_m(H,H)$ is 0.329(1) Hz in CS_2 at 300 K (9), which gives $^5J^{\sigma}_{180}$ as 0.322 Hz. Then,

$$^5J_m(H,H) = 0.336\langle\sin^2\theta\rangle + 0.322\langle\sin^2(\tfrac{\theta}{2})\rangle \text{ (Hz)} \qquad [13]$$

on the assumption that the σ electron component is sensitive to ring substitution. The values of $\langle\sin^2\theta\rangle$ and $\langle\sin^2(\frac{\theta}{2})\rangle$ are 0.5 for toluene because of the threefold symmetry of the methyl group, so that $^5J_m(H,H)$ cannot be used as a conformational indicator for the methyl group. However, for α-substituted toluene derivatives, the lowering of the symmetry in the side chain enables the separation of the σ and the σ-π electron components of $^5J_m(H,H)$ (11). The conformation is implied by the value of $\langle\sin^2\theta\rangle$, which is other than 0.5.

In general, substitution at the *ortho* position causes an increase, whereas substitution at the *meta* position causes a decrease, in the magnitude of $^5J_m(H,H)$. For example, the magnitude varies from 0.300(1) Hz in 3-fluorotoluene to 0.464(4) Hz in 2-fluoro-4,6-dibromotoluene (11).

$^4J_o(H,H)$

The calculated coupling constants between the *ortho* ring proton and the α-protons in toluene (27) indicate that the π electron mechanism is modified by a σ electron contribution. The experimental $^4J_o(H,H)$ for toluene in CS_2 at 300 K is -0.701(1) Hz (9) whereas $^5J_o(CH_3,CH_3)$ in *o*-xylene, considered as a measure of the magnitude of the π electron contribution for toluene, is only 0.45(2) Hz (10). However, proximate contributions to $^5J_o(CH_3,CH_3)$ are also present (27).

In another study of $^4J_o(H,H)$ by Barfield et al. (28), concerning its dependence on bond order, conformation and ring substitution in methyl aromatic compounds, the coupling is related to the mutual atom-atom polarizability, $\pi_{pp'}$, and the torsional angle, θ, as in [14].

$$^4J_o(H,H) = 6.90\pi_{pp'}\sin^2\theta - 0.32\cos^2\theta \text{ (Hz)} \qquad [14]$$

The π electron component varies as $\sin^2\theta$ and the σ electron component varies as $\cos^2\theta$. The value of $\pi_{pp'}$ for toluene is -0.157 (28); therefore,

$$^4J_o(H,H) = -1.08\langle\sin^2\theta\rangle - 0.32\langle\cos^2\theta\rangle \text{ (Hz)} \quad [15]$$

where the angular brackets indicate expectation values, and are 0.5 for toluene. The substituent dependence of $^4J_o(H,H)$ is considered unimportant (28), although $\pi_{pp'}$ changes upon ring substitution and the change in $^4J_o(H,H)$ actually can be large. The measured $^4J_o(H,H)$ in 2-fluoro, 4-fluoro and 2-chloro-5-fluorotoluene in CS_2 are -0.779(2), -0.714(3) and -0.700(3) Hz, respectively (9).

1.3. Introduction to the problems

The orientation of the methoxy group relative to the aromatic ring, being suggested to affect the psychotomimetic activities of certain methoxy compounds (49,50), has attracted much attention (1-6,25,26,36-61). The use of $^5J_o(H,CH_3)$ in the conformational studies of 1,2-dimethoxybenzene (1,8) and 3-fluoroanisole (4) has been successful. In this thesis, $^5J_o(H,CH_3)$ and molecular orbital calculations are employed to determine the conformational distributions of 3-iodoanisole and 1,3-dimethoxybenzene in polar and nonpolar media, and in the free state. Conformational studies of 1,3-dimethoxybenzene are scarce (36,37,58,74,75).

A number of conformational studies of isobutylbenzene (80,81) and 3-phenylpentane have been done (103,104). However, there is no information on the rotational barriers about their C_{sp^2}-C_{sp^3} bonds. 3-phenylpentane can be considered as a primitive model for such a barrier in polystyrene. The lowest energy conformations and the apparent twofold barriers of isobutylbenzene and 3-phenylpentane are here determined by the J-method, which has had some success in numerous internal rotational studies (9,10,12-19). These two compounds are representatives of the benzylic and benzalic types of molecules. Also, molecular orbital calculations are performed on isobutylbenzene at the AM1 and STO-3G MO levels, and on 3-phenylpentane at the AM1 level. The AM1 level

appears promising for the prediction of the barrier of 3-phenylpentane, as indicated by the computations on isopropylbenzene.

2. EXPERIMENTAL METHODS

2.1. Sample preparation

All compounds were Aldrich products, except that 3-phenylpentane was purchased from K & K Laboratories.

Samples, at concentrations of 2-5 mol%, were prepared by dissolving appropriate amounts in acetone-d_6 plus a small amount of TMS or in $CS_2/C_6D_{12}/C_6F_6$/TMS. The solvent mixture of CS_2 was prepared with 10 mol% of C_6D_{12} for an internal lock, and 0.25 mol% of each of TMS and C_6F_6 as internal references for ^1H and ^{19}F nmr, respectively; ^{19}F nmr was not used in this thesis, of course. Each sample was filtered through cotton wool, transferred to a 5 mm od nmr tube, and degassed by the freeze-pump-thaw procedure (3-5 cycles). The tube was then flame-sealed.

2.2. Spectroscopic method

All nmr spectra were run on the AM 300 Bruker spectrometer at a probe temperature of 300 K and a spectrometer frequency of 300.135_2 MHz for protons. A "sweepwidth" of 6000 Hz was used to acquire the survey spectrum for each molecule. The regions of interest were then acquired separately, using 4 K of memory for each 50 Hz spectrum. A typical acquisition time was 40.96 sec, which limits the linewidth to 0.024 Hz at half-height. 8 to 64 free induction decays (FIDs) were accumulated, depending on the intensities of the signals. The FIDs were zero-filled twice or four times before Fourier transformation. A Gaussian multiplication of 0.600 and line broadening of -0.100 were normally used for resolution enhancement.

Homonuclear double resonance experiments were performed on 1,3-dimethoxybenzene, **IX**, isobutylbenzene, **X**, and 3-phenylpentane, **XI**.

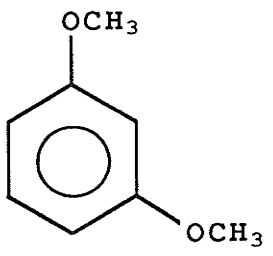

IX

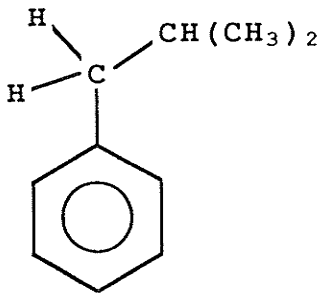

X

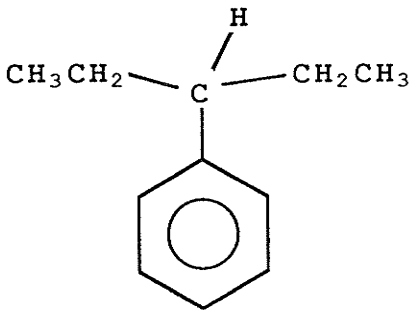

XI

The methoxy protons of **IX** were coherently decoupled to facilitate the identification of spectral parameters.

The methyl protons in isobutylbenzene were successfully decoupled but not those in 3-phenylpentane, **XI**.

2.3. Spectral analysis

Spectral analyses were done with the NUMARIT program (30) extensively modified by R. Sebastian in this laboratory. The plots coupled to the final iteration were compared visually with the experimental spectra.

The protons in isobutylbenzene and 3-phenylpentane constitute 14- and 16-spin systems, respectively, which exceed the limit of 12 spins for each single analysis in the NUMARIT program. The analysis of the methyl-decoupled spectrum of isobutylbenzene was unsuccessful due to divergence during iteration. Therefore, the analyses of the side chain and the ring were done separately. For isobutylbenzene, the side chain was analysed as an A_6BC_2DD' system (including the two *ortho* protons) and the ring as an $AB_2CC'DD'E$ system (excluding the methyl protons). The analysis of 3-phenylpentane was performed as an $A_3A'_3BB'CC'D$ system for the side chain and an $A_6BCC'DD'E$ system (excluding all methylene protons) for the ring.

2.4. Molecular orbital computations

All the molecular orbital calculations reported in this thesis were done with the GAUSSIAN-86 program (31) on the Amdahl 5870 system. The geometries were fully optimized, except that the nuclei of the benzene moieties were kept in a plane.

Computations on 3-iodoanisole and 1,3-dimethoxybenzene were performed at 15° intervals of the methoxy torsional angles between 0° and 180°, at the STO-3G level of *ab initio* molecular orbital theory. For 1,3-dimethoxybenzene, the methoxy groups were alternately kept in the plane of the ring while the other was rotated. Computations at the 3-21G MO level were also performed for the three planar conformers of 1,3-dimethoxybenzene.

The calculations on isobutylbenzene and 3-phenylpentane were performed at the AM1 level, for various geometries of the side chain, and at 15° intervals of the side chain torsional angles between 0° and 90°. Isobutylbenzene was also examined at the STO-3G MO level.

The potentials were fitted to the $\sin^2 n\theta$ series by using the SAS nonlinear regression program NLIN (32). The curves were plotted by using a spline interpolation in the SAS/GRAPH library (33). The optimized geometries were also drawn by invoking the SAS/GRAPH library.

3. EXPERIMENTAL RESULTS

3.1. Spectral parameters

3.1.1. 3-iodoanisole

Results of the analyses of the ^1H nmr spectra of 2.0 mol% solutions of 3-iodoanisole in CS_2/C_6D_{12}/TMS and acetone-d_6/TMS appear in Table 1. All signs of the coupling constants were adopted from an earlier analysis for 3-fluoroanisole (4). The spectra of the methoxy groups in both solvents appear in Figure 1.

Table 1

^{1}H nmr spectral parameters[a] for a 2.0 mol% solution of 3-iodoanisole in CS_2/C_6D_{12}/TMS and acetone-d_6/TMS at 300 K.

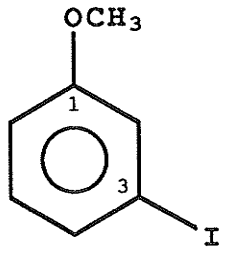

	CS_2/C_6D_{12}	acetone-d_6
$\upsilon(CH_3)$	1111.681(1)[b]	1139.315(1)[b]
υ(H2)	2137.542(1)	2189.165(1)[d]
υ(H4)	2147.512(1)[c]	2190.361(1)[d]
υ(H5)	2066.641(1)	2121.462(1)
υ(H6)	2023.230(1)	2087.200(1)
$^5J(CH_3,H2)$	-0.176(1)	-0.167(1)
$^7J(CH_3,H4)$	-0.040(1)[c]	-0.038(1)
$^6J(CH_3,H5)$	0.051(1)	0.046(1)
$^5J(CH_3,H6)$	-0.134(1)	-0.141(1)
^4J(H2,H4)	1.573(1)	1.592(2)
^5J(H2,H5)	0.257(1)	0.258(2)
^4J(H2,H6)	2.505(1)	2.517(1)
^3J(H4,H5)	7.771(1)	7.787(2)
^4J(H4,H6)	0.909(1)	0.883(1)
^3J(H5,H6)	8.346(1)	8.393(1)

transitions calculated	256	280
transitions assigned	215	243
peaks observed	106	117
largest absolute difference	0.013	0.015
RMS deviation	0.004	0.006

Notes

a. In hertz, at 300.135_2 MHz to high frequency of internal TMS.

b. Numbers in parentheses are standard deviations in the last significant digit, as given by the NUMARIT analysis.

c. υ(H4) correlates with $^7J(CH_3,H4)$ by -0.299.

d. υ(H2) correlates with υ(H4) by 0.239.

Figure 1

The methoxy proton region of a 2.0 mol% solution of 3-iodoanisole in A) CS_2/C_6D_{12}/TMS, and B) acetone-d_6/TMS.

a. observed spectrum

b. calculated spectrum

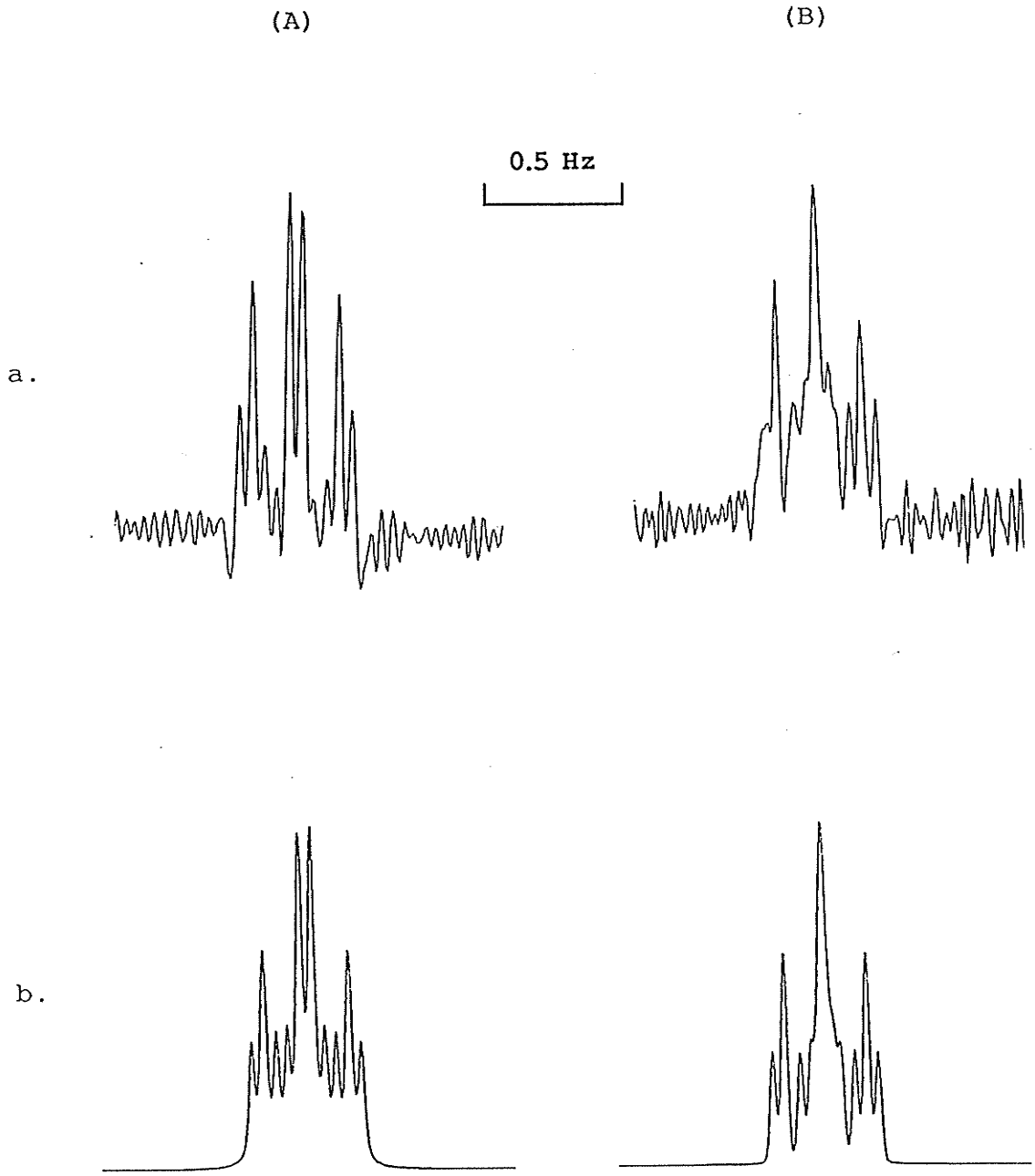

3.1.2. 1,3-dimethoxybenzene

Results of the analyses of the ^1H nmr spectra of 4.0 mol% solutions of 1,3-dimethoxybenzene in CS_2/C_6D_{12}/TMS and acetone-d_6/TMS appear in Table 2. All signs of the couplings were adopted from an earlier analysis for anisole (16). Some initial parameters were obtained by decoupling the methoxy protons in acetone-d_6/TMS. The spectra of the methoxy groups in both solvents appear in Figure 2. The spectra of the ring protons in CS_2 solution appear in Figure 3 and 4.

Table 2

^{1}H nmr spectral parameters[a] for a 4.0 mol% solution of 1,3-dimethoxybenzene in CS_2/C_6D_{12}/TMS and acetone-d_6/TMS at 300 K.

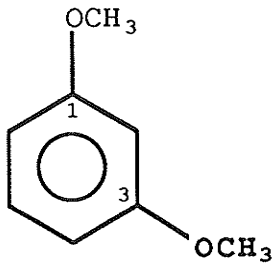

	CS_2/C_6D_{12}	acetone-d_6[f]
υ(CH_3=**CH_3**)	1097.086(0)[b,c]	1127.177(0)
υ(H2)	1879.406(0)	1942.527(0)[e]
υ(H4=H6)	1895.155(0)	1950.477(0)[e]
υ(H5)	2097.702(0)	2147.892(1)
^{8}J(CH_3,**CH_3**)	0.000(0)	0.000(0)
^{5}J(CH_3,H2)=^{5}J(**CH_3**,H2)	-0.153(0)	-0.160(0)
^{7}J(CH_3,H4)=^{7}J(**CH_3**,H6)	-0.063(1)	-0.059(1)
^{6}J(CH_3,H5)=^{6}J(**CH_3**,H5)	0.059(0)[c]	0.074(0)
^{5}J(CH_3,H6)=^{5}J(**CH_3**,H4)	-0.097(1)	-0.104(1)
^{4}J(H2,H4=H6)	2.385(0)	2.397(0)
^{5}J(H2,H5)	0.307(1)	0.319(1)[e]
^{4}J(H4,H6)	0.758[d]	0.732[d]
^{3}(H4=H6,H5)	8.213(0)	8.238(1)[e]

transitions calculated	1168	1103
transitions assigned	758	841
peaks observed	67	85
largest absolute difference	0.012	0.019
RMS deviation	0.005	0.006

Notes

a. In hertz, at 300.135_2 MHz to high frequency of internal TMS.

b. Numbers in parentheses are standard deviations in the last significant digit, as given by the NUMARIT analysis.

c. $\upsilon(CH_3)$ correlates with $^6J(CH_3,H5)$ by 0.470.

d. The values of $^4J(H4,H6)$ are calculated with the couplings in anisole (23) and benzene (34), using the additivity rule.

e. $\upsilon(H2)$ correlates with $^5J(H2,H5)$ by -0.239. $\upsilon(H4)$ correlates with $^3J(H4,H5)$ by -0.340.

f. The parameters (in Hz) for the methoxy decoupled spectrum, with 608 out of 960 transitions assigned, are:

$\upsilon(H2)=1942.342(0)$ $^4J(H2,H4=H6)=2.396(0)$

$\upsilon(H4=H6)=1950.288(0)$ $^5J(H2,H5)=0.317(0)$

$\upsilon(H5)=2147.701(0)$ $^3(H4=H6,H5)=8.236(0)$

Bloch-Siegert shifts are evident.

Figure 2

The methoxy proton region of a 4.0 mol% solution of 1,3-dimethoxybenzene in A) $CS_2/C_6D_{12}/TMS$, and B) acetone-d_6/TMS.

a. observed spectrum

b. calculated spectrum

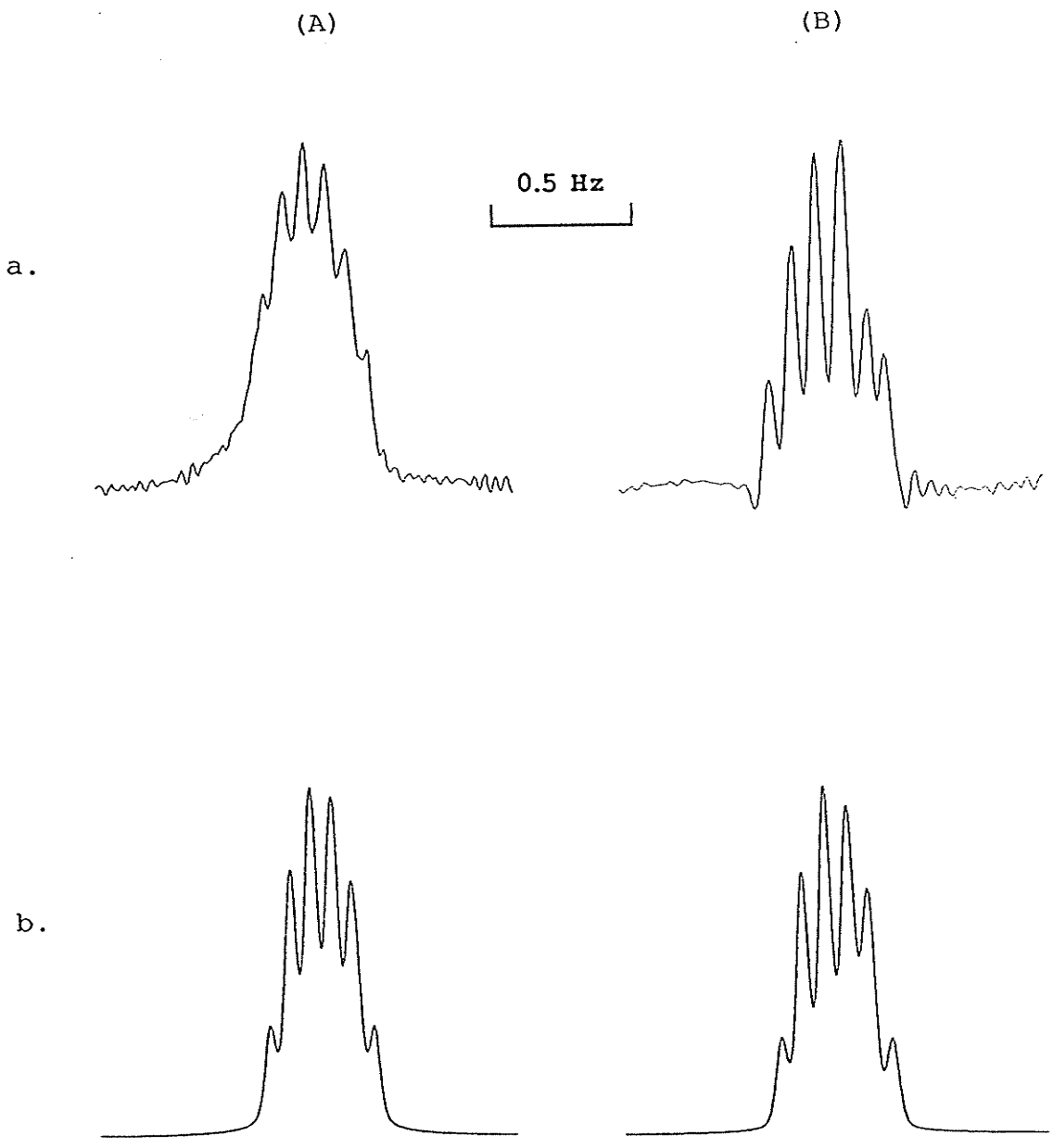

Figure 3

Spectra of H-2, H-4 and H-6 of a 4.0 mol% solution of 1,3-dimethoxybenzene in CS_2/C_6D_{12}/TMS.

a. observed spectrum

b. calculated spectrum

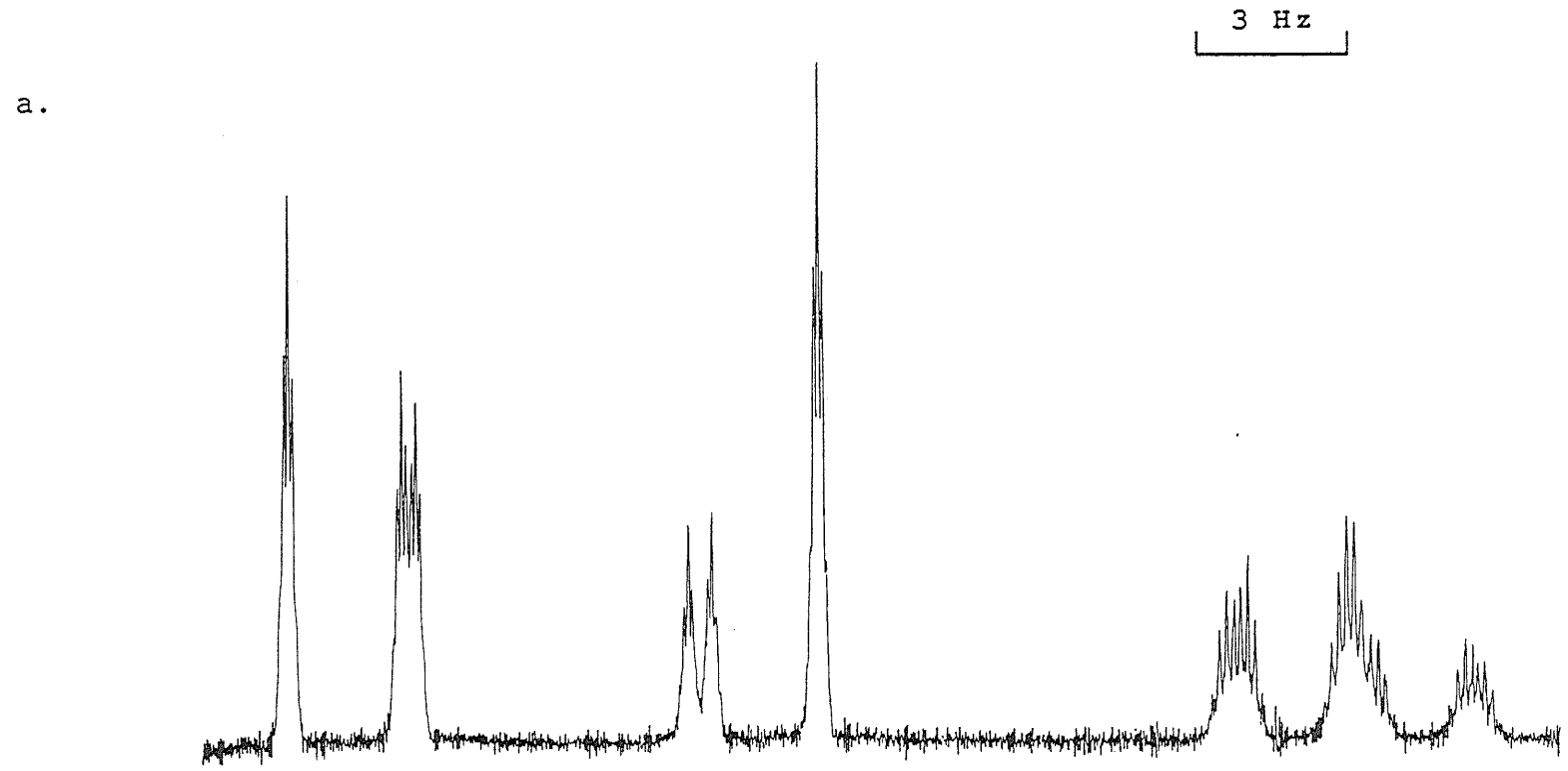

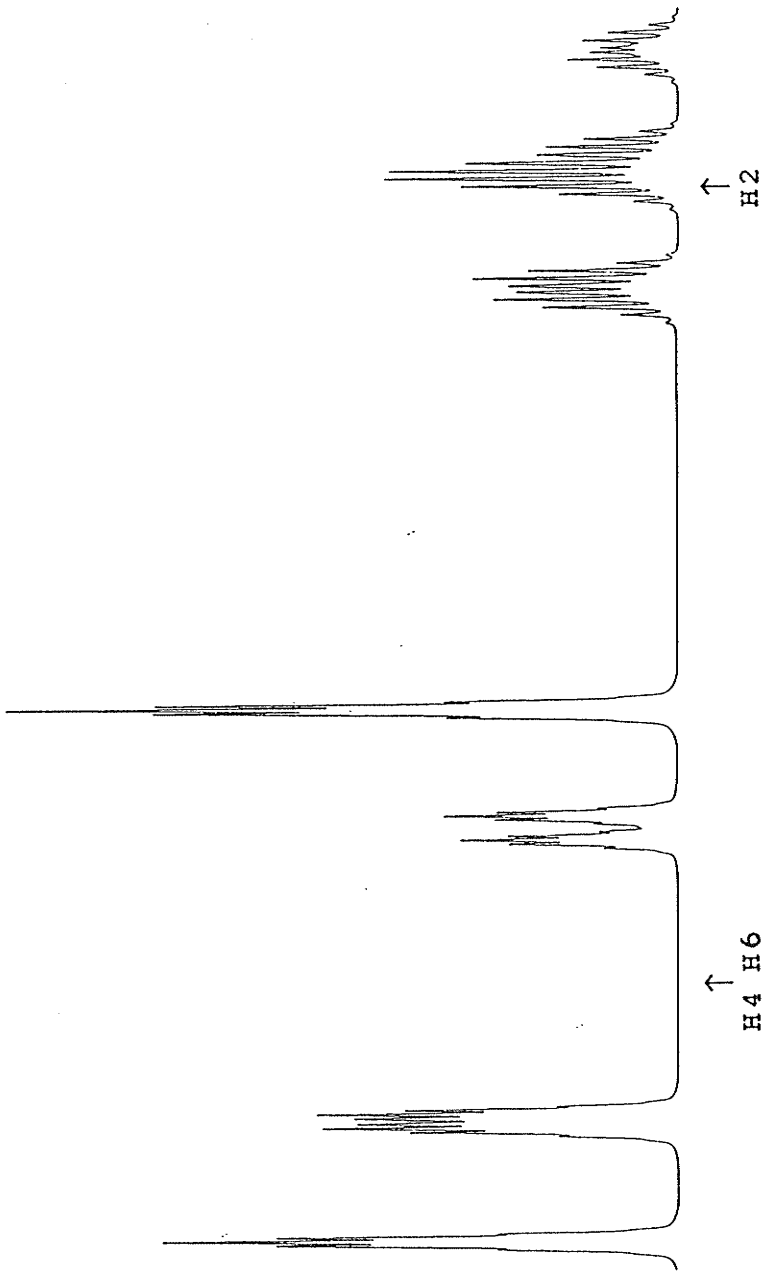

b.

Figure 4

Spectrum of H-5 of a 4.0 mol% solution of 1,3-dimethoxybenzene in CS_2/C_6D_{12}/TMS.

a. observed spectrum

b. calculated spectrum

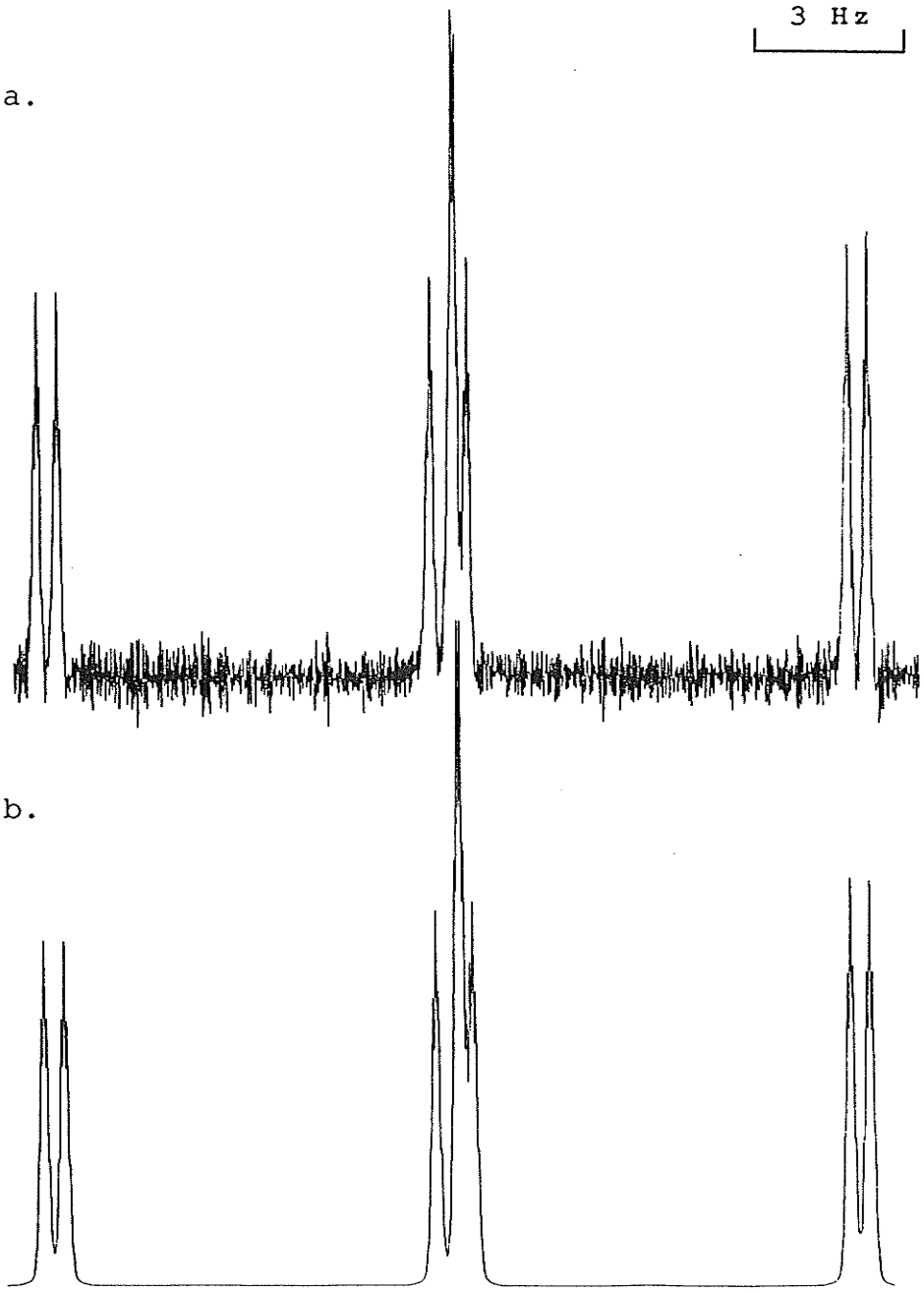

3.1.3. 5-chloro-1,3-dimethoxybenzene

Results of the analyses of the ^1H nmr spectra of 4.0 mol% solutions of 5-chloro-1,3-dimethoxybenzene in CS_2/C_6D_{12}/TMS and acetone-d_6/TMS appear in Table 3. The spectra of the methoxy groups in both solvents appear in Figure 5. The spectra of the ring protons in acetone-d_6/TMS appear in Figure 6 and 7.

Table 3

^{1}H nmr spectral parameters[a] for a 4.0 mol% solution of 5-chloro-1,3-dimethoxybenzene in CS_2/C_6D_{12}/TMS and acetone-d_6/TMS at 300 K.

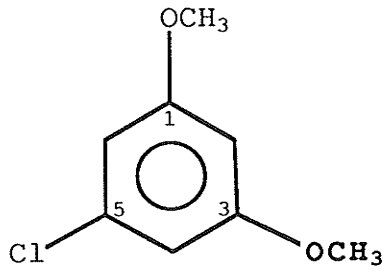

	CS_2/C_6D_{12}	acetone-d_6
$\upsilon(CH_3{=}\mathbf{CH_3})$	1103.126(0)[b]	1137.277(0)[b]
υ(H2)	1856.768(0)	1929.178(1)
υ(H4=H6)	1906.946(0)[c]	1963.164(0)
$^8J(CH_3,\mathbf{CH_3})$	-0.001(0)	-0.002(0)
$^5J(CH_3,H2)=^5J(\mathbf{CH_3},H2)$	-0.146(0)	-0.157(0)
$^7J(CH_3,H4)=^7J(\mathbf{CH_3},H6)$	-0.064(4)[c]	-0.061(3)
$^5J(CH_3,H6)=^5J(\mathbf{CH_3},H4)$	-0.098(5)	-0.100(2)
^4J(H2,H4=H6)	2.244(0)	2.231(1)
^4J(H4,H6)	1.650[d]	1.624[d]
transitions calculated	408	392
transitions assigned	279	371
peaks observed	30	30
largest absolute difference	0.010	0.014
RMS deviation	0.004	0.005

Notes

a. In hertz, at 300.135_2 MHz to high frequency of internal TMS.

b. Numbers in parentheses are standard deviations in the last significant digit, as given by the NUMARIT analysis.

c. υ(H4=H6) correlates with $^7J(CH_3,H4)$ by 0.304.

d. The values of ^4J(H4,H6) are calculated with the couplings in anisole (23), benzene (34) and chlorobenzene (35), using the additivity rule.

Figure 5

The methoxy proton region of a 4.0 mol% solution of 5-chloro-1,3-dimethoxybenzene in A) CS_2/C_6D_{12}/TMS, and B) acetone-d_6/TMS.

a. observed spectrum

b. calculated spectrum

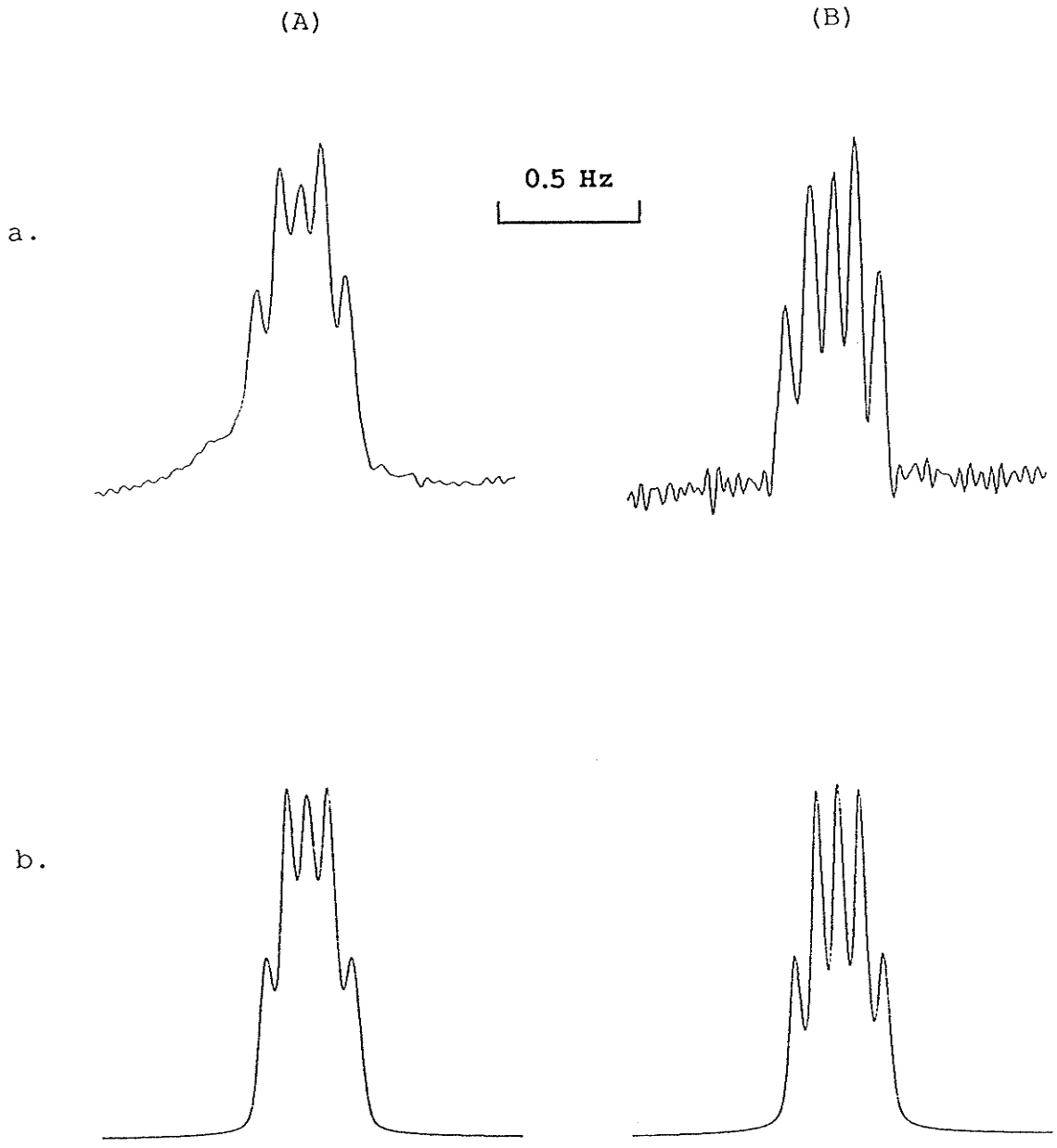

Figure 6

Spectrum of H-2 of a 4.0 mol% solution of 5-chloro-1,3-dimethoxybenzene in acetone-d_6/TMS.

a. observed spectrum

b. calculated spectrum

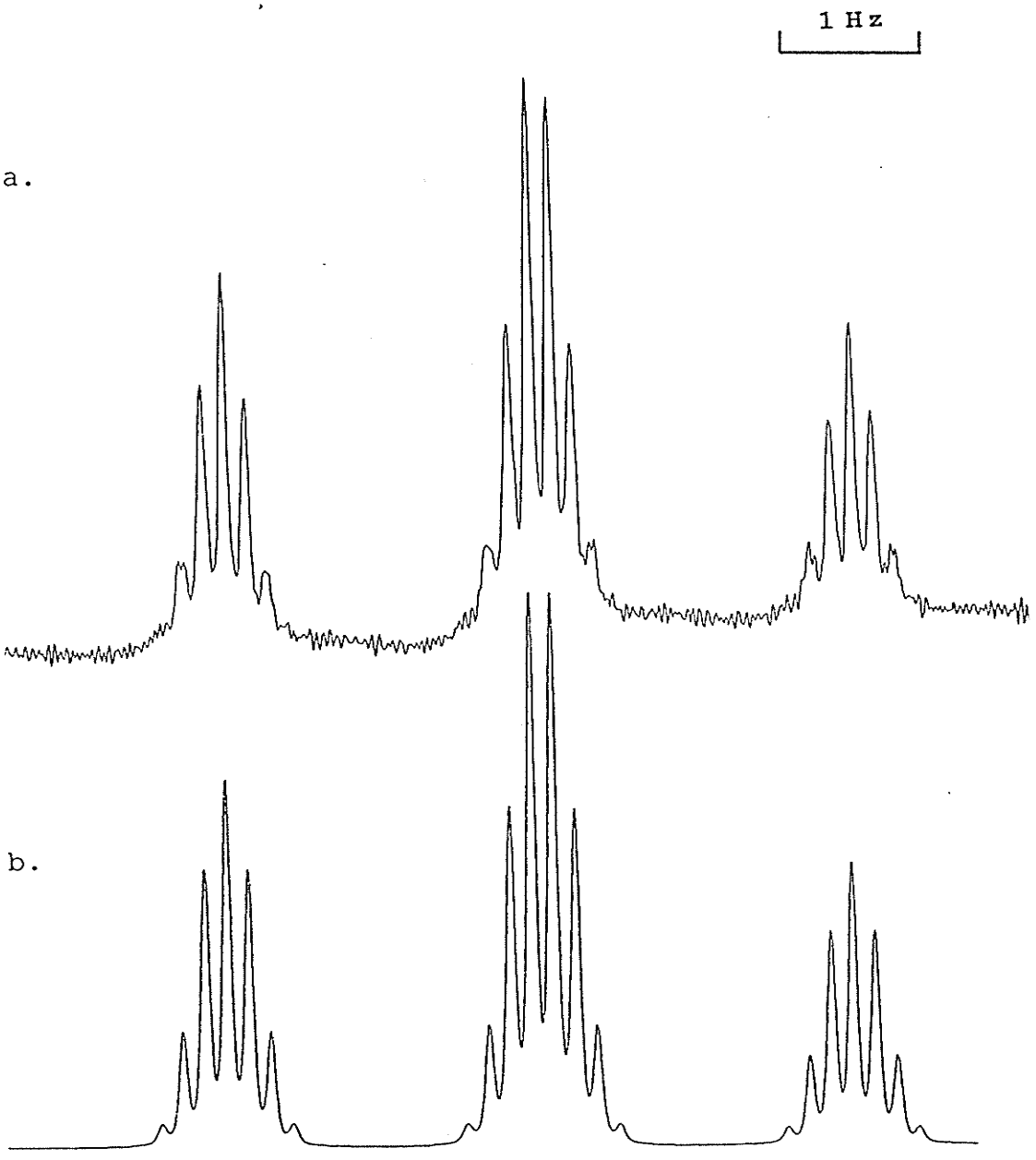

Figure 7

Spectra of H-4 and H-6 of a 4.0 mol% solution of 5-chloro-1,3-dimethoxybenzene in acetone-d_6/TMS.

a. observed spectrum

b. calculated spectrum

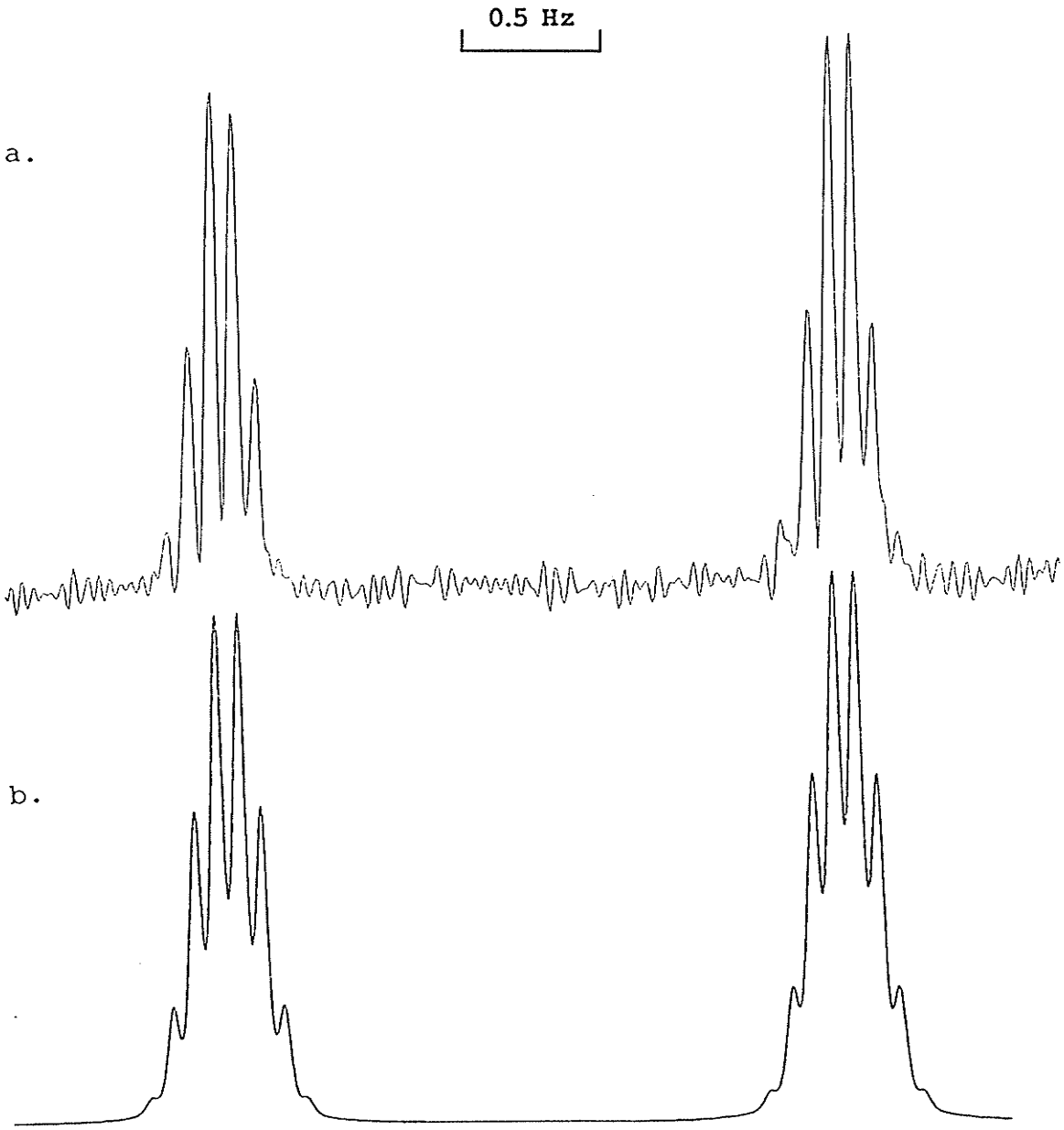

3.1.4. Isobutylbenzene

Results of the analysis of the ^1H nmr spectrum of a 4.0 mol% solution of isobutylbenzene in CS_2/C_6D_{12}/TMS appear in Table 4. The transitions of the methylene protons were not assigned. The analysis of the side chain and ring gave different values of ^5J(CH,H2), 0.038(2) and 0.015(2) Hz, respectively. The ring region appears in Figure 8. The methine proton spectrum appears in Figure 9, that of the methyl protons in Figure 10.

Table 4

^{1}H nmr spectral parameters[a] for a 4.0 mol% solution of isobutylbenzene in CS_2/C_6D_{12}/TMS at 300 K.

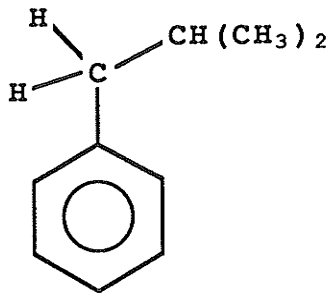

$\upsilon(CH_3)$	264.654(0)[b,c]		
$\upsilon(CH)$	543.179(2)[c]		
$\upsilon(CH_2)$	724.200[d]		
$\upsilon(H2)$	2101.218(1)		
$\upsilon(H3)$	2136.725(1)		
$\upsilon(H4)$	2109.823(1)		
$^3J(CH_3,CH)$	6.613(1)[c]	$^5J(CH_2,H3)$	0.272(1)
$^4J(CH_3,CH_2)$	-0.009(1)[c]	$^6J(CH_2,H4)$	-0.374(1)
$^6J(CH_3,H2)$	-0.001(1)	$^3J(H2,H3)$	7.644(2)
$^3J(CH,CH_2)$	7.154(1)	$^4J(H2,H4)$	1.271(1)
$^5J(CH,H2)$	0.038(2)[c,e]	$^4J(H2,H6)$	1.902(1)
$^6J(CH,H3)$	0.001(1)	$^3J(H3,H4)$	7.431(1)
$^7J(CH,H4)$	-0.001(2)	$^4J(H3,H5)$	1.452(1)
$^4J(CH_2,H2)$	-0.538(1)	$^5J(H3,H6)$	0.596(0)

transitions calculated	864[f]	539[g]
transitions assigned	215	349
peaks observed	190[h]	
largest absolute difference	0.016	0.019
RMS deviation	0.006	0.007

Notes

a. In hertz, at 300.135_2 MHz to high frequency of internal TMS.

b. Numbers in parentheses are standard deviations in the last significant digit, as given by the NUMARIT analysis.

c. $\upsilon(CH_3)$ correlates with $^3J(CH_3,CH)$ by 0.210. $\upsilon(CH_3)$ correlates with $^4J(CH_3,CH_2)$ by 0.401. $\upsilon(CH)$ correlates with $^3J(CH_3,CH)$ by 0.254. $\upsilon(CH)$ correlates with $^5J(CH,H2)$ by -0.867. $^3J(CH_3,CH)$ correlates with $^5J(CH,H2)$ by -0.205.

d. Chemical shift was not optimized.

e. $^5J(CH,H2)$ is 0.015(2) Hz from the ring analysis.

f. Number of transitions calculated for the side chain region, there being many degenerate transitions.

g. Number of transitions calculated for the ring proton region, there being many degenerate transitions.

h. Total number of peaks observed for the whole molecule.

Figure 8

The ring proton region of a 4.0 mol% solution of isobutylbenzene in CS_2/C_6D_{12}/TMS.

a. observed spectrum

b. calculated spectrum

a.

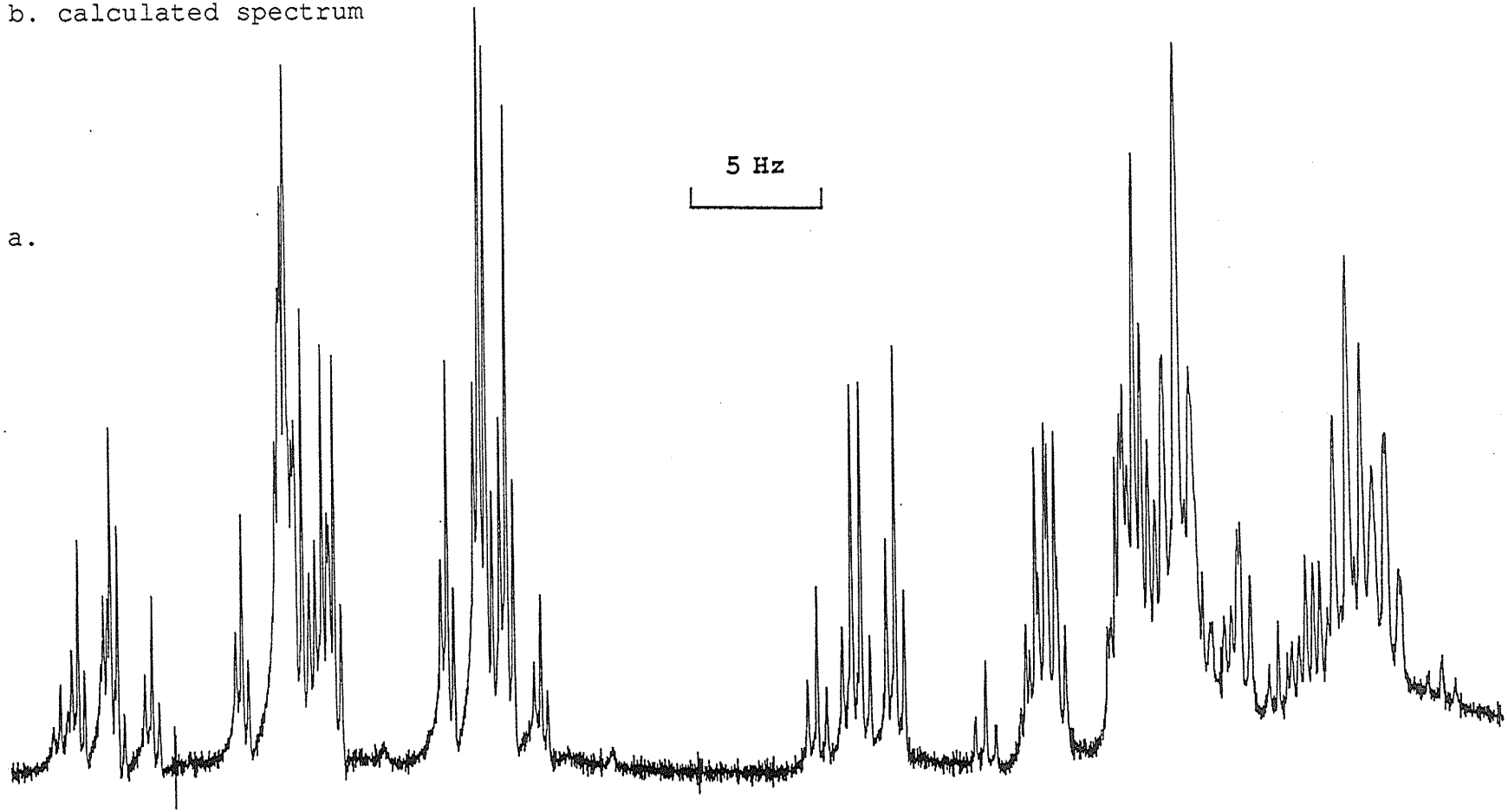

b.

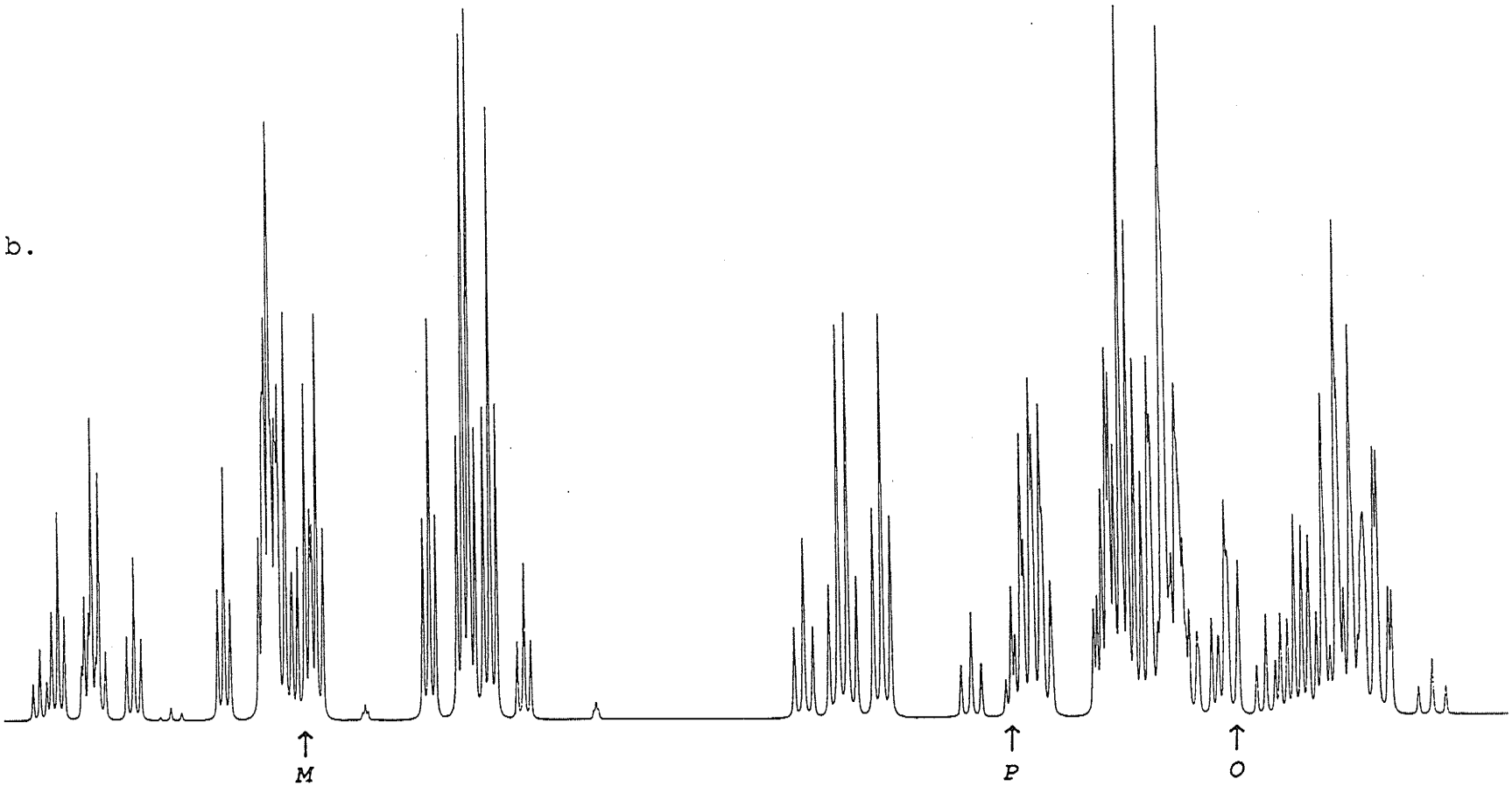

Figure 9

The methine proton region of a 4.0 mol% solution of isobutylbenzene in CS_2/C_6D_{12}/TMS.

a. observed spectrum

b. calculated spectrum

a.

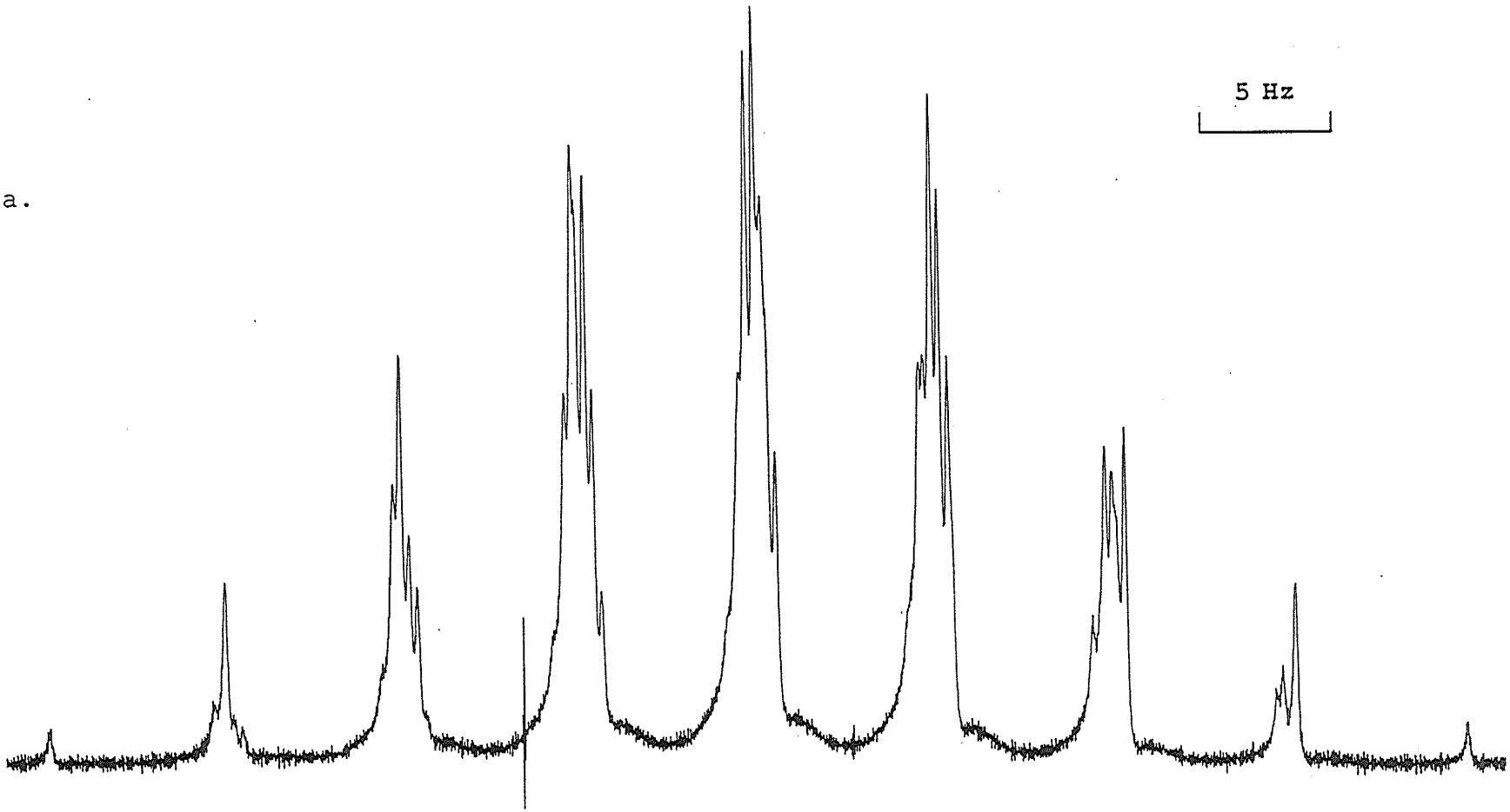

b.

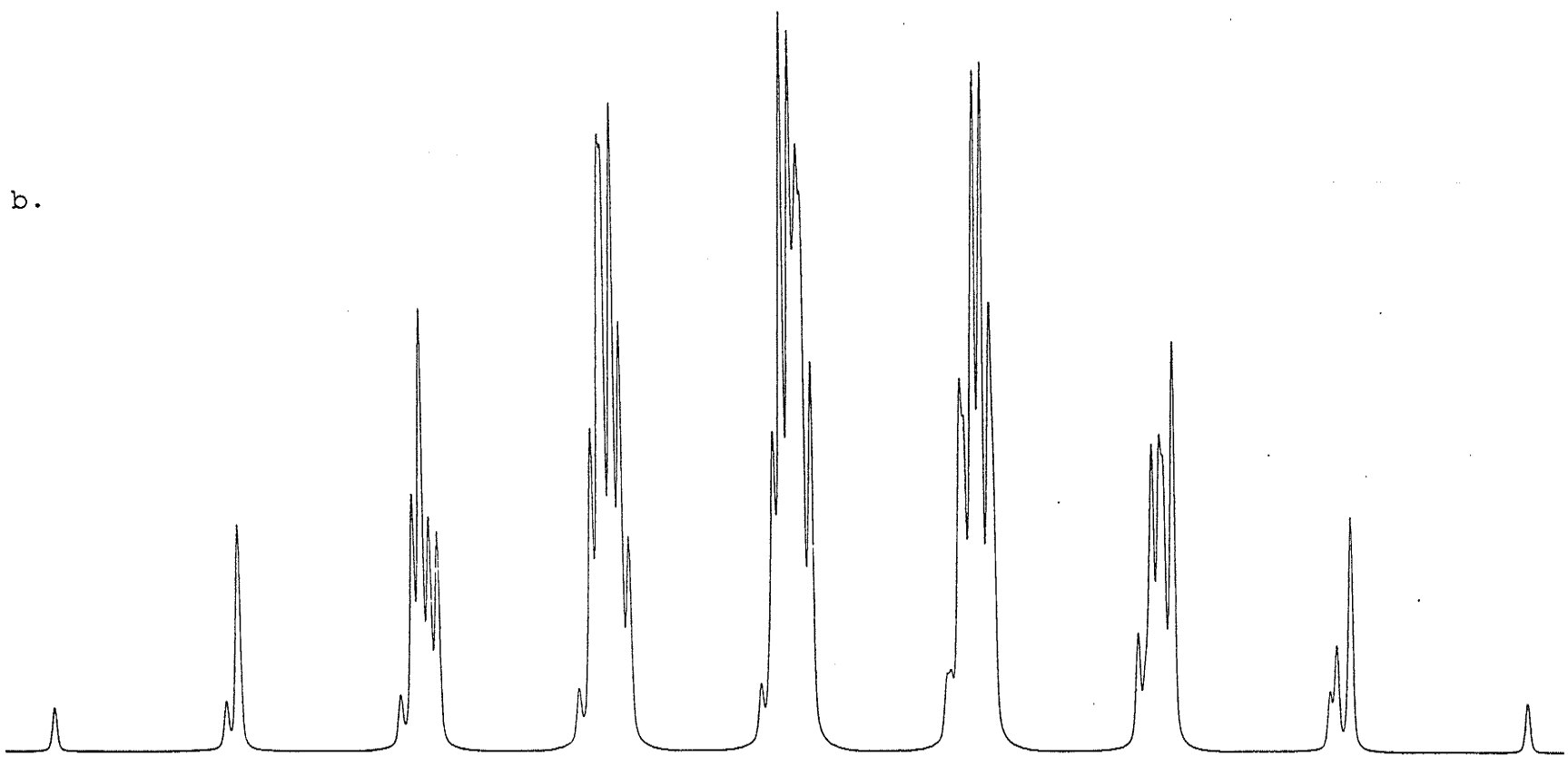

Figure 10

The methyl proton region of a 4.0 mol% solution of isobutylbenzene in CS_2/C_6D_{12}/TMS.

a. observed spectrum

b. calculated spectrum

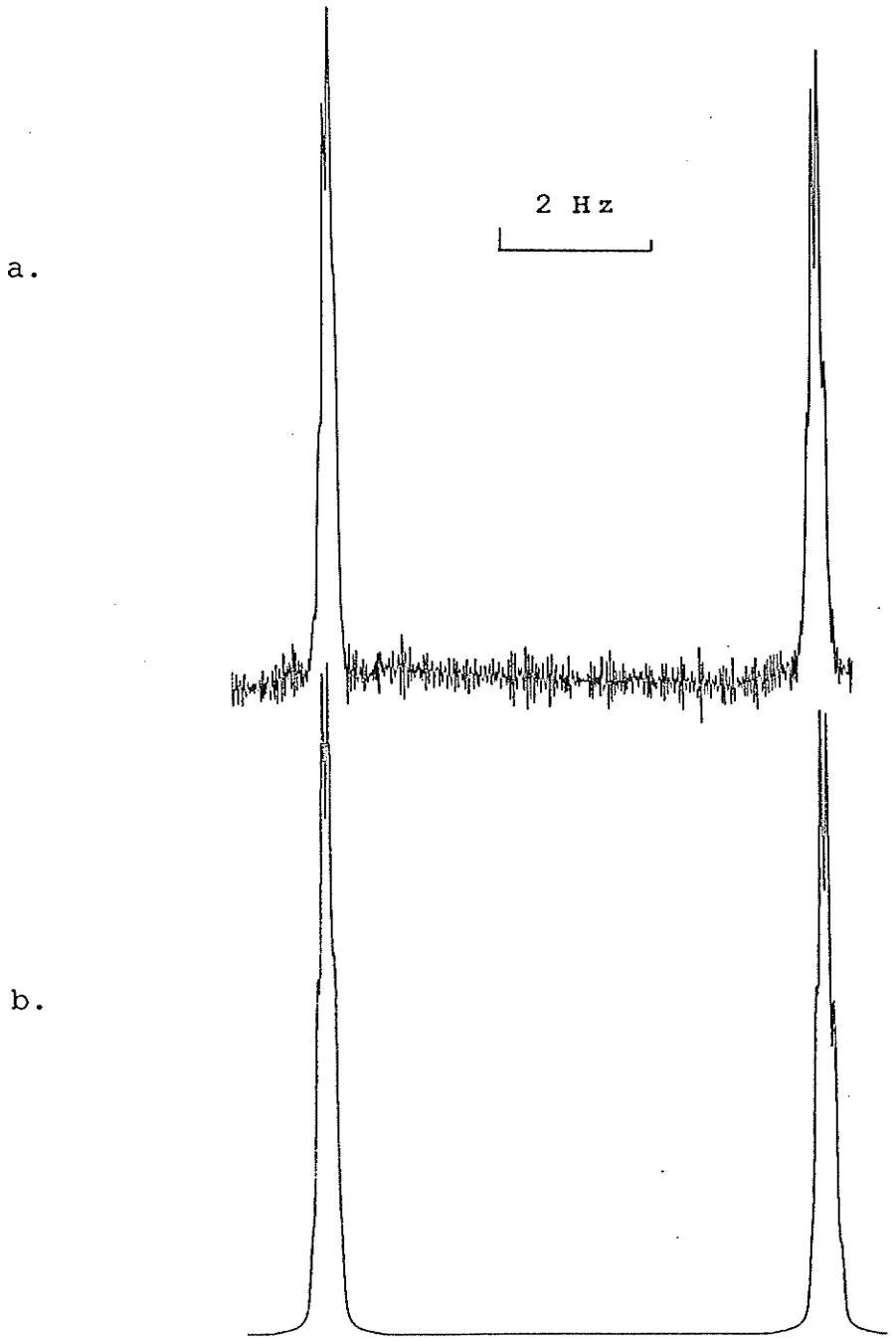

3.1.5. 3-phenylpentane

Results of the analysis of the ^1H nmr spectrum of a 4.7 mol% solution of 3-phenylpentane in CS_2/C_6D_{12}/TMS appear in Table 5. The transitions of the methine proton were not assigned. The ring region appears in Figure 11. The spectrum of the methylene protons appears in Figure 12, that of the methyl protons in Figure 13.

Table 5

^{1}H nmr spectral parameters[a] for a 4.7 mol% solution of 3-phenylpentane in CS_2/C_6D_{12}/TMS at 300 K.

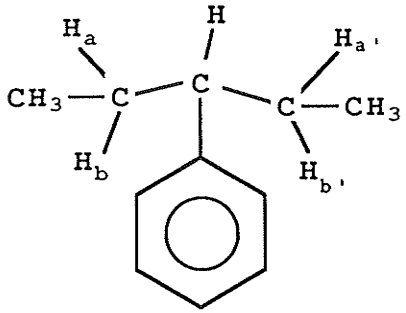

$\upsilon(CH_3)$	224.319(1)[b,c]		
$\upsilon(H_a=H_{a'})$	454.936(1)		
$\upsilon(H_b=H_{b'})$	494.989(1)[c]		
υ(CH)	673.600[e]		
υ(H2=H6)	2107.425(1)		
υ(H3=H5)	2149.092(0)		
υ(H4)	2117.605(1)[d]		
$^3J(CH_3, H_a=H_{a'})$	7.356(2)	$^3J(H_a=H_{a'}, CH)$	9.207(3)
$^3J(CH_3, H_b=H_{b'})$	7.387(2)[c]	$^3J(H_b=H_{b'}, CH)$	5.250(2)[c]
$^4J(CH_3, CH)$	-0.273(2)[c]	^4J(CH,H2=H6)	-0.454(1)
$^5J(CH_3, H_a=H_{a'})$	-0.001(0)[c]	^5J(CH,H3=H5)	0.279(1)
$^5J(CH_3, H_b=H_{b'})$	-0.001(0)	^6J(CH,H4)	-0.107(1)
^6J(CH_3,H2=H6)	0.054(0)	^3J(H2,H3)	7.710(1)
^7J(CH_3,H3=H5)	-0.001(0)	^4J(H2,H4)	1.269(1)
$^4J(H_a, H_{a'})$	-0.233(3)[c]	^4J(H2,H6)	1.925(1)
$^2J(H_a, H_b)$	-13.476(3)[c]	^3J(H3,H4)	7.395(1)[d]
$^4J(H_a, H_{b'})=^4J(H_{a'}, H_b)$	-0.231(0)[c]	^4J(H3,H5)	1.461(1)
$^4J(H_b, H_{b'})$	-0.228(2)[c]	^5J(H3,H6)	0.576(0)

transitions calculated	2596[f]	1689[g]
transitions assigned	740	1200
peaks observed	170[h]	
largest absolute difference	0.031	0.026
RMS deviation	0.016	0.010

Notes

a. In hertz, at 300.135_2 MHz to high frequency of internal TMS.

b. Numbers in parentheses are standard deviations in the last significant digit, as given by the NUMARIT analysis.

c. $\upsilon(CH_3)$ correlates with $^3J(CH_3,H_b{=}H_{b'})$ by -0.226. $\upsilon(CH_3)$ correlates with $^4J(CH_3,CH)$ by 0.275. $\upsilon(CH_3)$ correlates with $^5J(CH_3,H_a{=}H_{a'})$ by 0.285. $\upsilon(H_b{=}H_{b'})$ correlates with $^3J(H_b{=}H_{b'},CH)$ by -0.266. $^4J(H_a,H_{a'})$ correlates with $^2J(H_a,H_b)$ by 0.407. $^4J(H_a,H_{a'})$ correlates with $^4J(H_a,H_{b'})$ by -0.245. $^2J(H_a,H_b)$ correlates with $^4J(H_a,H_{b'})$ by -0.203. $^2J(H_a,H_b)$ correlates with $^4J(H_b,H_{b'})$ by 0.337. $^4J(H_a,H_{b'})$ correlates with $^4J(H_b,H_{b'})$ by -0.266.

d. υ(H4) correlates with ^3J(H3,H4) by -0.247.

e. Chemical shift was not optimized.

f. Number of transitions calculated for the side chain region, there being many degenerate transitions.

g. Number of transitions calculated for the ring proton region, there being many degenerate transitions.

h. Total number of peaks observed for the whole molecule.

Figure 11

The ring proton region of a 4.7 mol% solution of 3-phenylpentane in CS_2/C_6D_{12}/TMS.

a. observed spectrum

b. calculated spectrum

a.

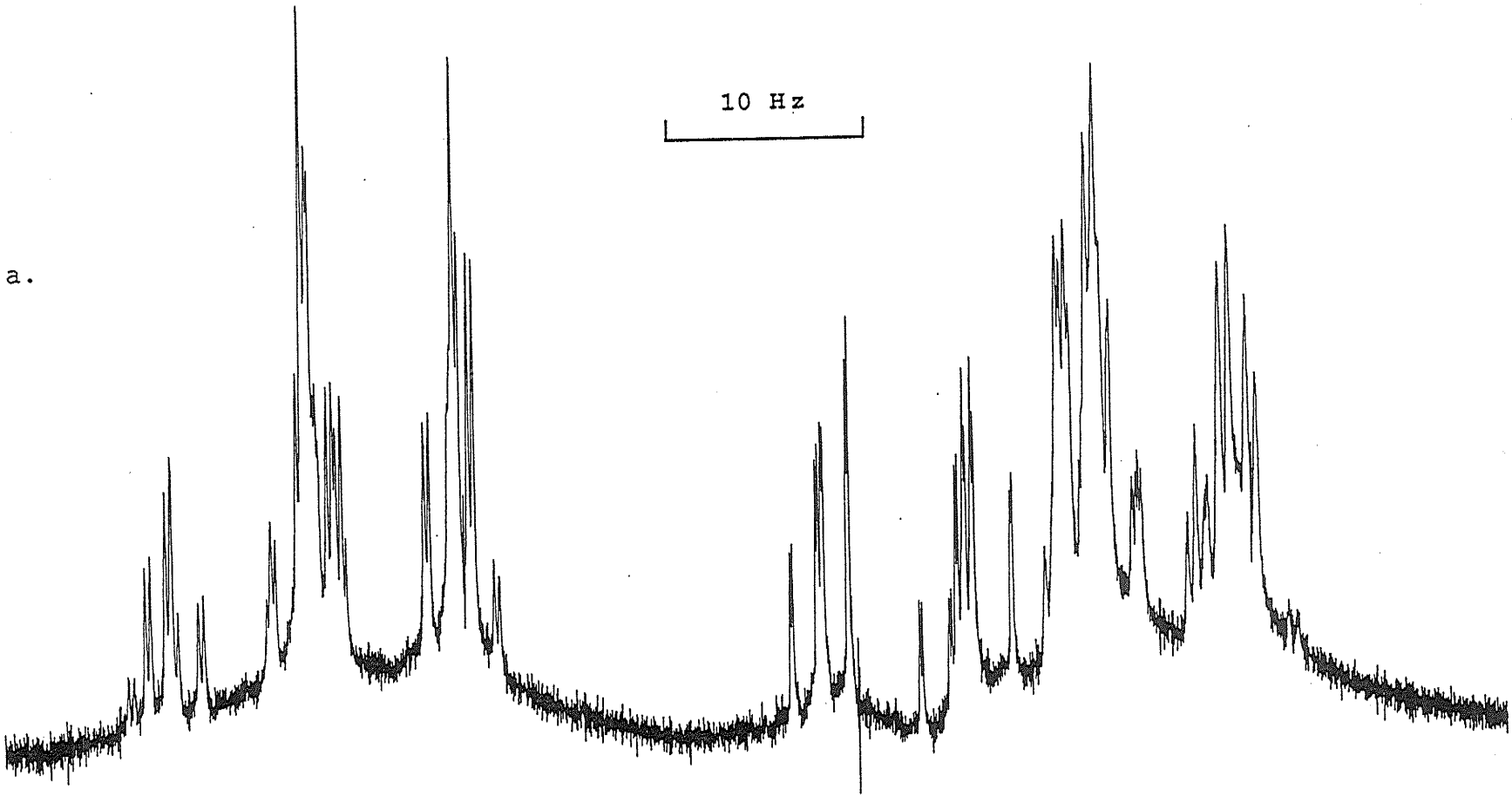

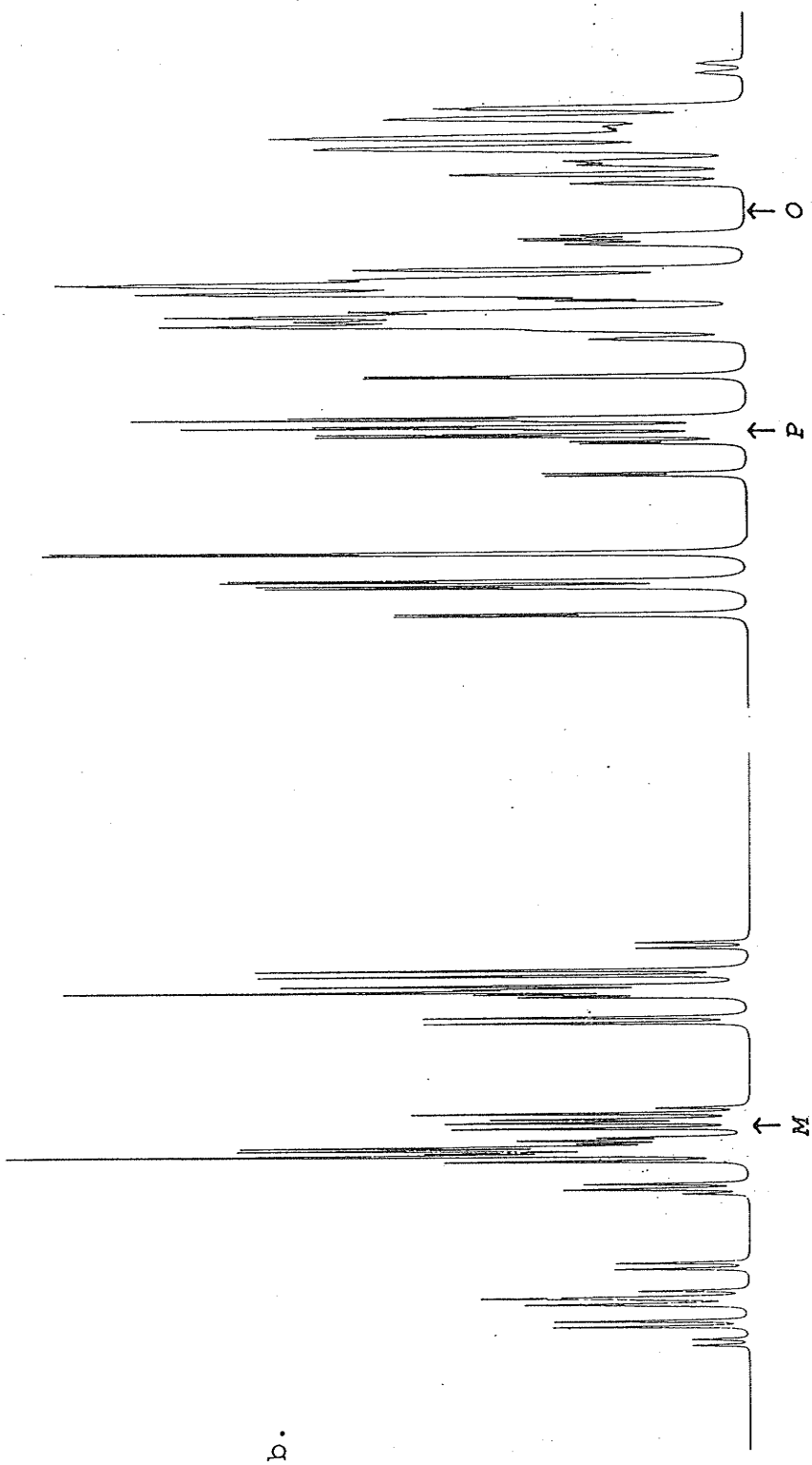

p.

Figure 12

The methylene proton region of a 4.7 mol% solution of 3-phenylpentane in CS_2/C_6D_{12}/TMS.

a. observed spectrum

b. calculated spectrum

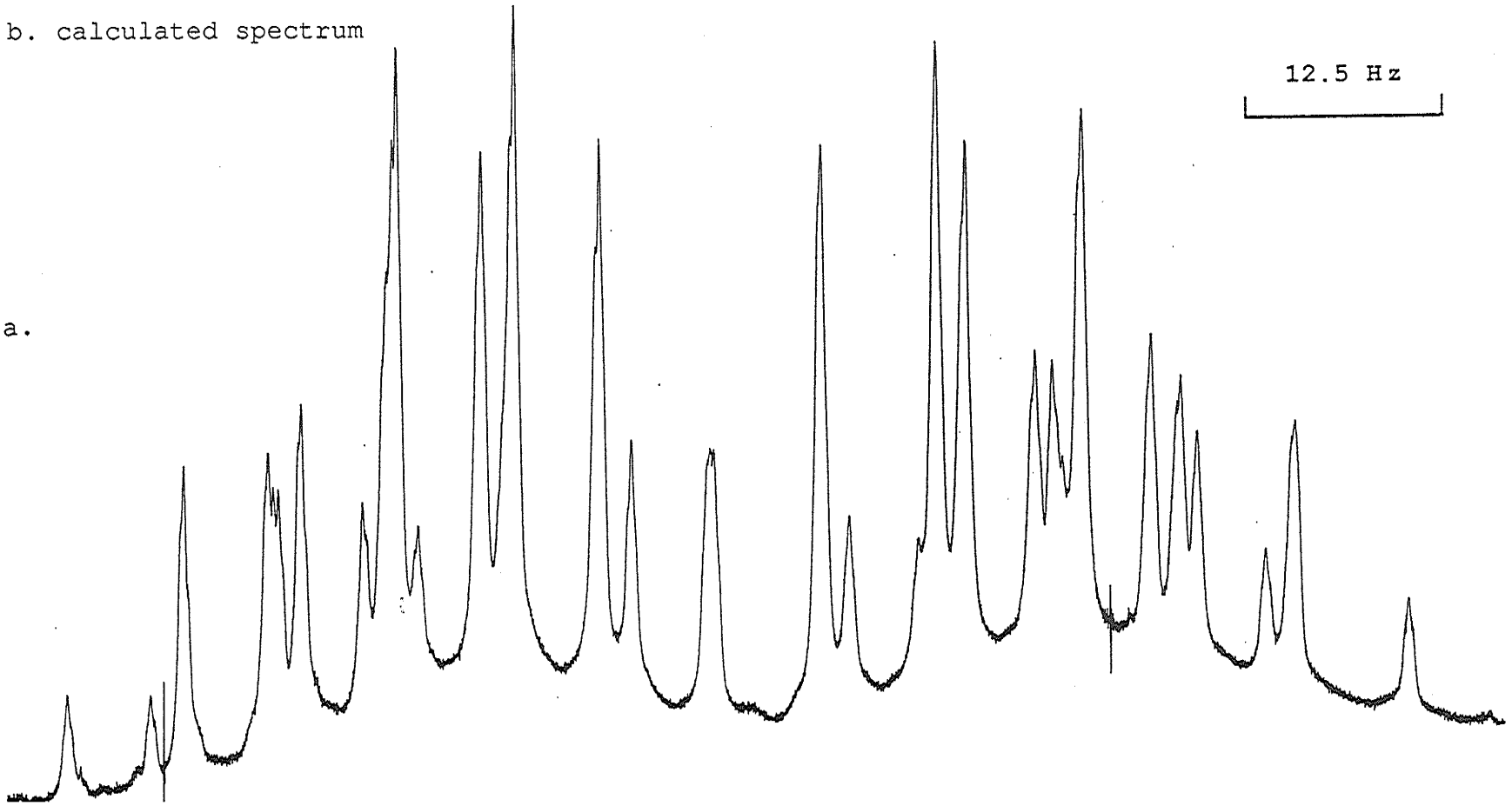

b.

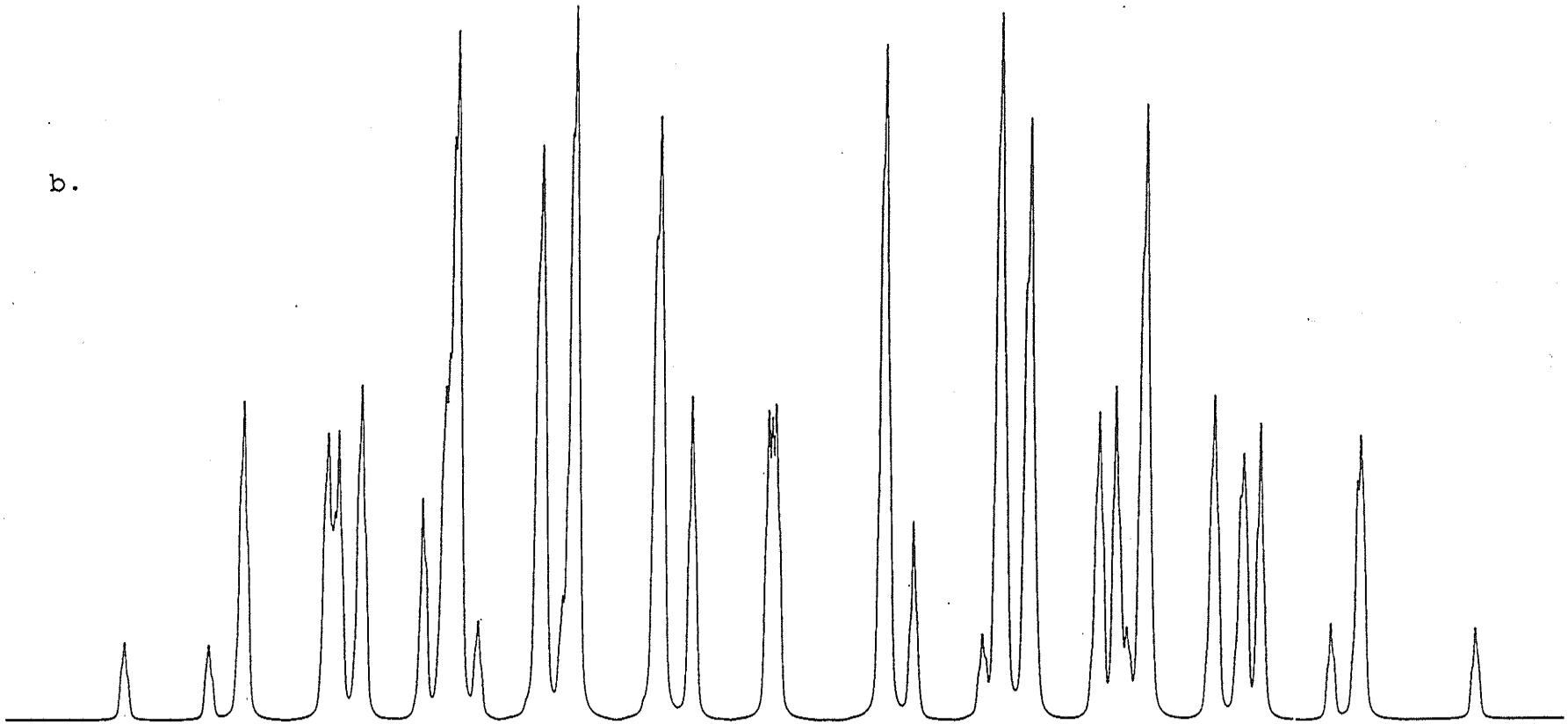

Figure 13

The methyl proton region of a 4.7 mol% solution of 3-phenylpentane in CS_2/C_6D_{12}/TMS.

a. observed spectrum

b. calculated spectrum with $^4J(CH_3,CH)=-0.272$ Hz

c. calculated spectrum with $^4J(CH_3,CH)=+0.272$ Hz

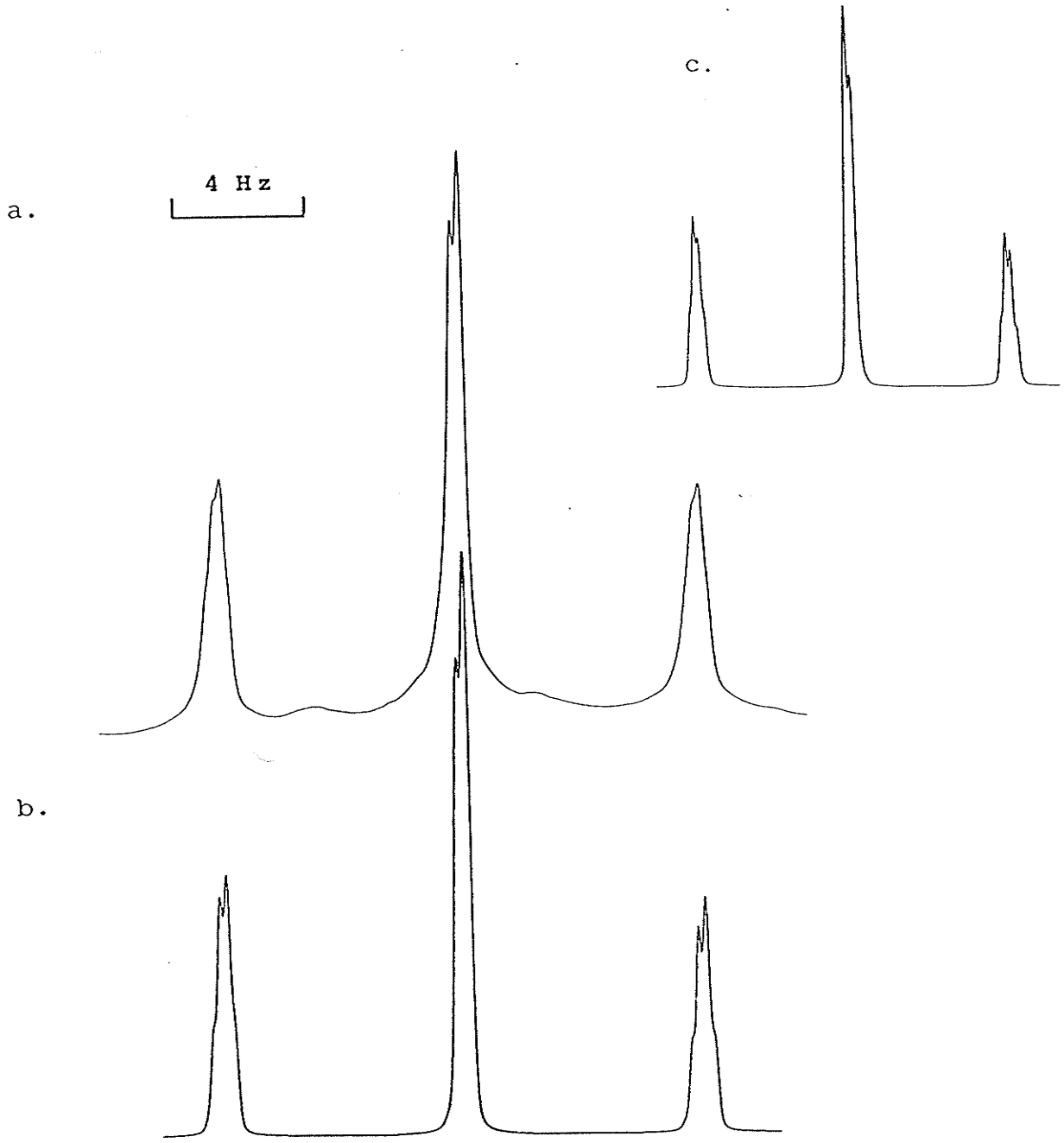

3.2. Computational parameters

3.2.1. 3-iodoanisole at the STO-3G MO level

The relative energies and the dipole moments of 3-iodoanisole at 15° intervals of the dihedral angle, θ, between the methoxy group and the ring, appear in Table 6. The potential energy curve for the rotation of the methoxy group about the C_{sp^2}-O bond appears in Figure 14. The structures of the *cis* and the *trans* conformer appear in Figure 15 and 16, respectively. All the bond angles (°) and bond lengths (Å) reported were optimized, but with the nuclei of the benzene moiety constrained to a plane.

Table 6

The relative energies and the dipole moments of 3-iodoanisole at 15° intervals of the dihedral angle, θ, computed at the STO-3G MO level. The total energy for the *cis* and *trans* conformers are -7190.430 139 and -7190.430 238 a.u., respectively.

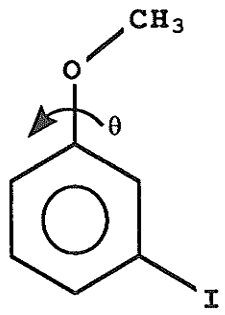

θ°	Relative energy (kJ mol^{-1})	Dipole moment (D)
0	0.000	0.975
15	0.843	1.006
30	3.153	1.103
45	6.007	1.256
60	7.394	1.447
75	7.369	1.674
90	7.355	1.906
105	7.288	2.123
120	7.242	2.322
135	6.313	2.496
150	3.459	2.636
165	0.769	2.729
180	-0.262	2.762

Figure 14

The potential energy curve for the internal rotation of the methoxy group about the C_{sp^2}-O bond in 3-iodoanisole. The relative energies, calculated at the STO-3G MO level, are given as triangles in the figure. The solid line represents the best fit[§] potential function as in [16].

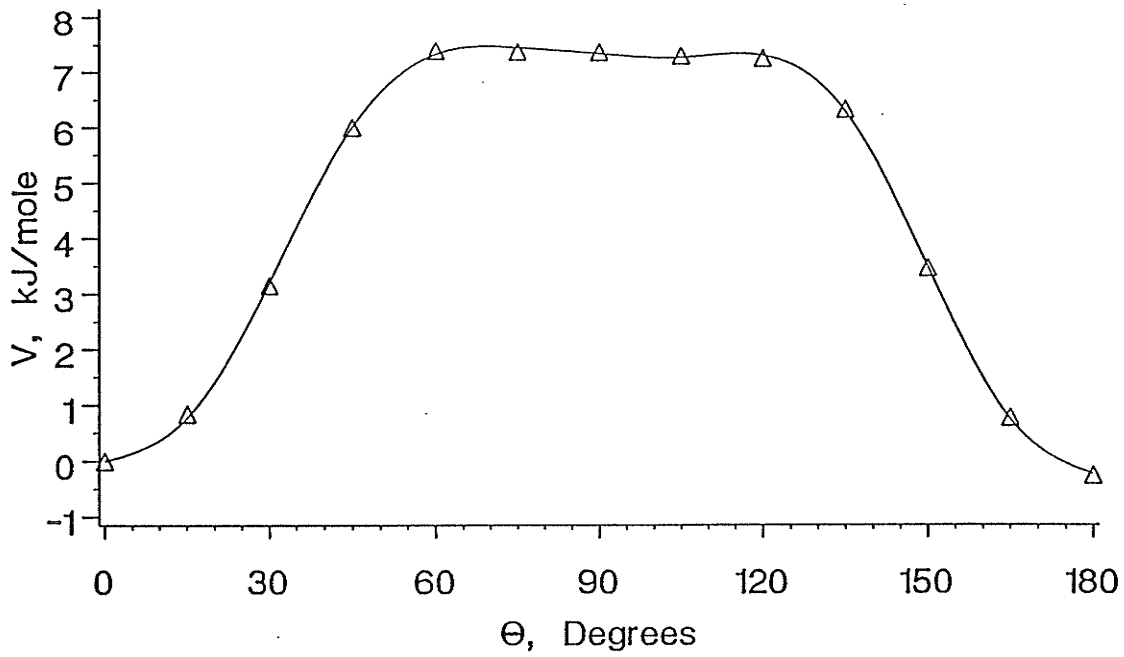

$$V(\theta) = 0.07(5)\sin^2(\tfrac{\theta}{2}) + 7.61(5)\sin^2\theta - 0.06(5)\sin^2(\tfrac{3\theta}{2}) + 2.54(5)\sin^2 2\theta - 0.25(5)\sin^2(\tfrac{5\theta}{2}) - 0.16(5)\sin^2 3\theta - 0.25(5)\sin^2 4\theta \ (\text{kJ mol}^{-1}) \qquad [16]$$

[§] The potential function including only the first two terms, has standard errors as large as 0.61, which drop to 0.14 when the third and fourth terms are also included. However, the error may not decrease or may even increase if too many terms are included. Thus, the best fit function is chosen, with the least number of terms and a reasonable or the lowest standard error.

Figure 15

The STO-3G structure of the *cis* conformer of 3-iodoanisole. All the bond angles (°) and bond lengths (Å) are optimized; the only constraint is that the nuclei of the benzene moiety remain in a plane.

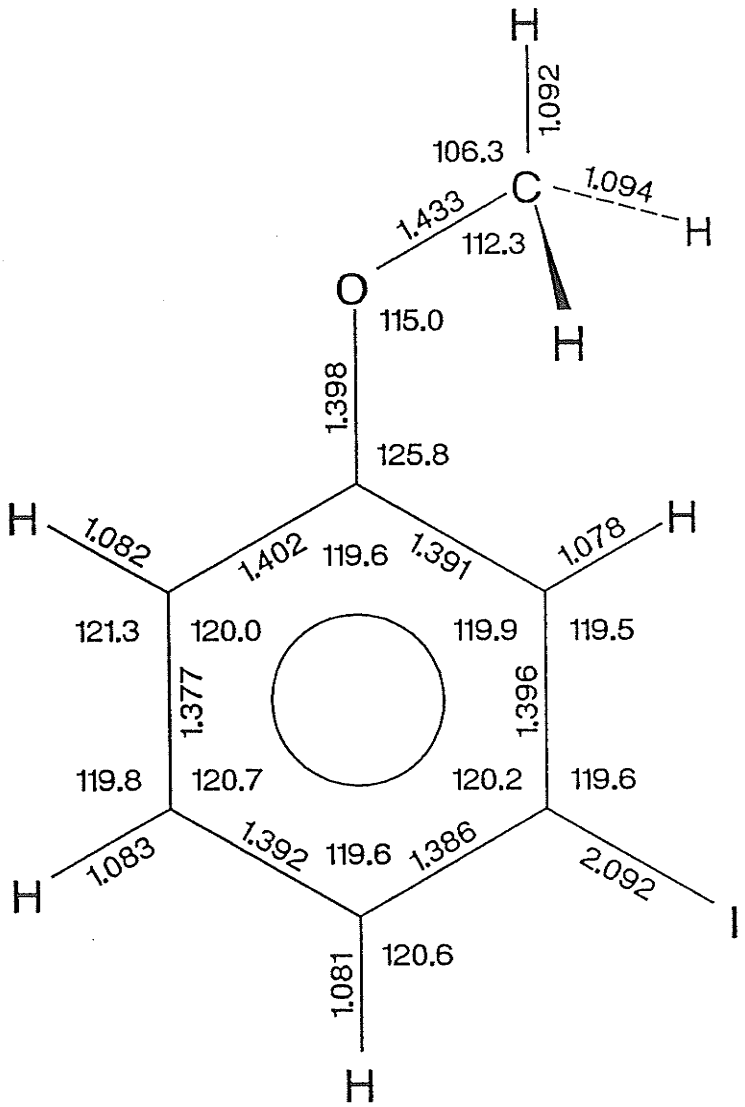

Figure 16

The STO-3G structure of the *trans* conformer of 3-iodoanisole. All the bond angles (°) and bond lengths (Å) are optimized; the only constraint is that the nuclei of the benzene moiety remain in a plane.

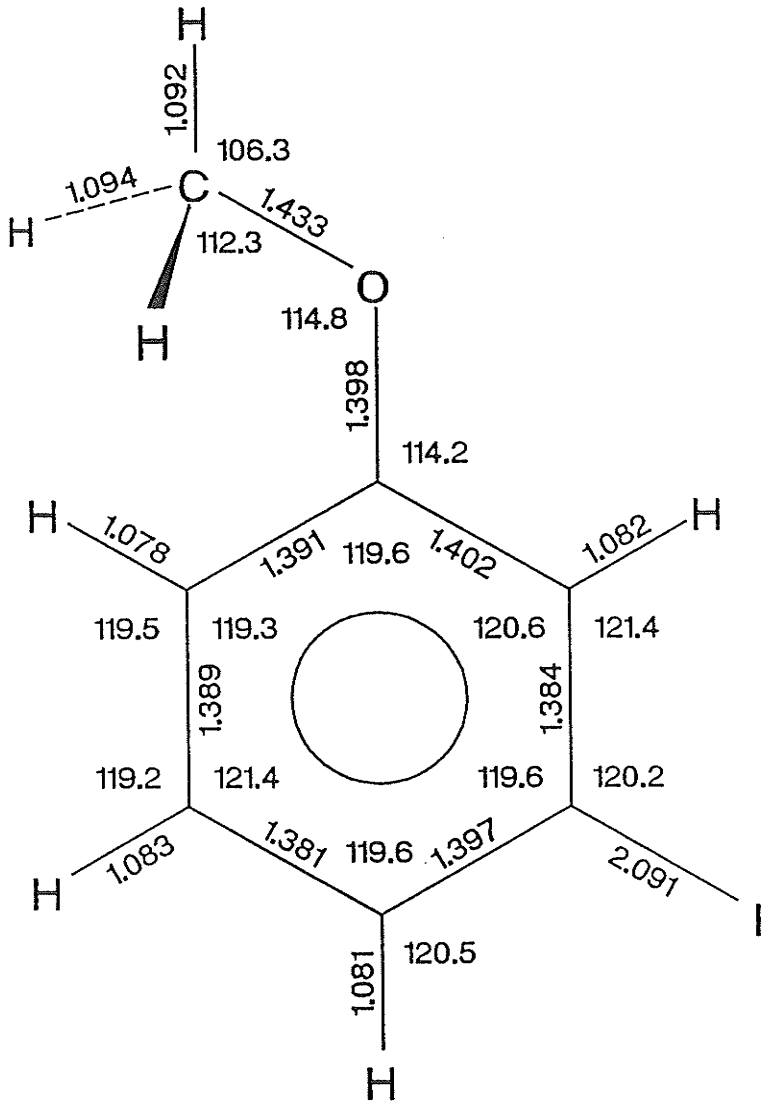

3.2.2. 1,3-dimethoxybenzene at the STO-3G MO level

The relative energies and the dipole moments of 1,3-dimethoxybenzene at 15° intervals of the dihedral angles, θ and ϕ, between the methoxy groups and the ring, appear in Table 7. Computations were done by alternately rotating one methoxy group while confining the other to the plane of the ring. All the bond angles (°) and bond lengths (Å) were optimized, with the nuclei of the benzene moiety confined to a plane. The potential energy curves for the rotation of the methoxy groups about the C_{sp^2}-O bonds appear in Figure 17. The structures of the *trans-cis*, *cis-cis* and *trans-trans* conformers appear in Figure 18, 19 and 20, respectively.

Table 7

The relative energies and the dipole moments of 1,3-dimethoxybenzene at 15° intervals of the dihedral angle, θ and ϕ, computed at the STO-3G MO level. The total energy for the lowest energy conformer (θ=ϕ=0°) depicted below is -452.733 125 a.u..

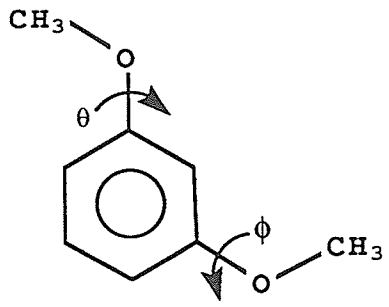

θ°(ϕ°=0)	Relative energy (kJ mol^{-1})	Dipole moment (D)
0(*t*-*c*)	0.000	1.155
15	1.099	1.152
30	3.981	1.155
45	7.123	1.194
60	8.338	1.268
75	8.573	1.366
90	8.780	1.484
105	8.984	1.616
120	9.293	1.755
135	8.197	1.886
150	5.632	1.990
165	3.552	2.055
180(*c*-*c*)	2.795	2.078

$\phi^\circ(\theta^\circ=0)$	Relative energy ($kJ\,mol^{-1}$)	Dipole moment (D)
0 (*t-c*)	0.000	1.155
15	0.961	1.205
30	3.591	1.341
45	6.852	1.530
60	8.642	1.731
75	8.972	1.914
90	9.085	2.035
105	9.004	2.090
120	8.943	2.094
135	8.068	2.080
150	5.310	2.056
165	2.715	2.029
180 (*t-t*)	1.726	2.018

Figure 17

The potential energy curves for the internal rotation of the methoxy groups about the C_{sp^2}-O bonds in 1,3-dimethoxybenzene. The relative energies, calculated at the STO-3G MO level, are given as triangles and squares in the figure. The solid and the broken lines represent the potential functions as in [17] and [18], respectively.

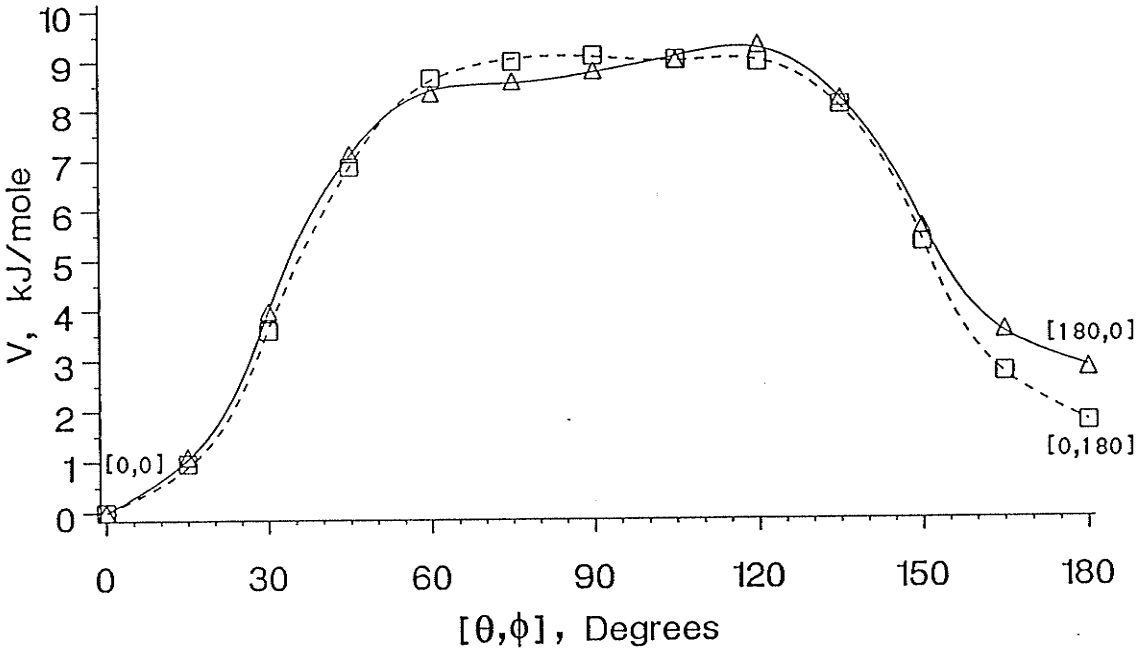

$$V(\theta) = 2.19(5)\sin^2(\tfrac{\theta}{2}) + 7.54(5)\sin^2\theta + 0.38(5)\sin^2(\tfrac{3\theta}{2}) + 2.57(5)\sin^2 2\theta + 0.25(5)\sin^2(\tfrac{5\theta}{2}) - 0.20(5)\sin^2 3\theta - 0.24(5)\sin^2 4\theta \ (\text{kJ mol}^{-1}) \quad [17]$$

$$V(\phi) = 1.70(4)\sin^2(\tfrac{\phi}{2}) + 8.33(4)\sin^2\phi + 0.32(4)\sin^2(\tfrac{3\phi}{2}) + 2.49(4)\sin^2 2\phi - 0.27(4)\sin^2(\tfrac{5\phi}{2}) - 0.14(4)\sin^2 3\phi - 0.25(4)\sin^2 4\phi \ (\text{kJ mol}^{-1}) \quad [18]$$

Figure 18

The STO-3G structure of the *trans-cis* conformer ($\theta=0^\circ, \phi=0^\circ$) of 1,3-dimethoxybenzene. All the bond angles ($^\circ$) and bond lengths (Å) are optimized; the only constraint is that the nuclei of the benzene moiety remain in a plane.

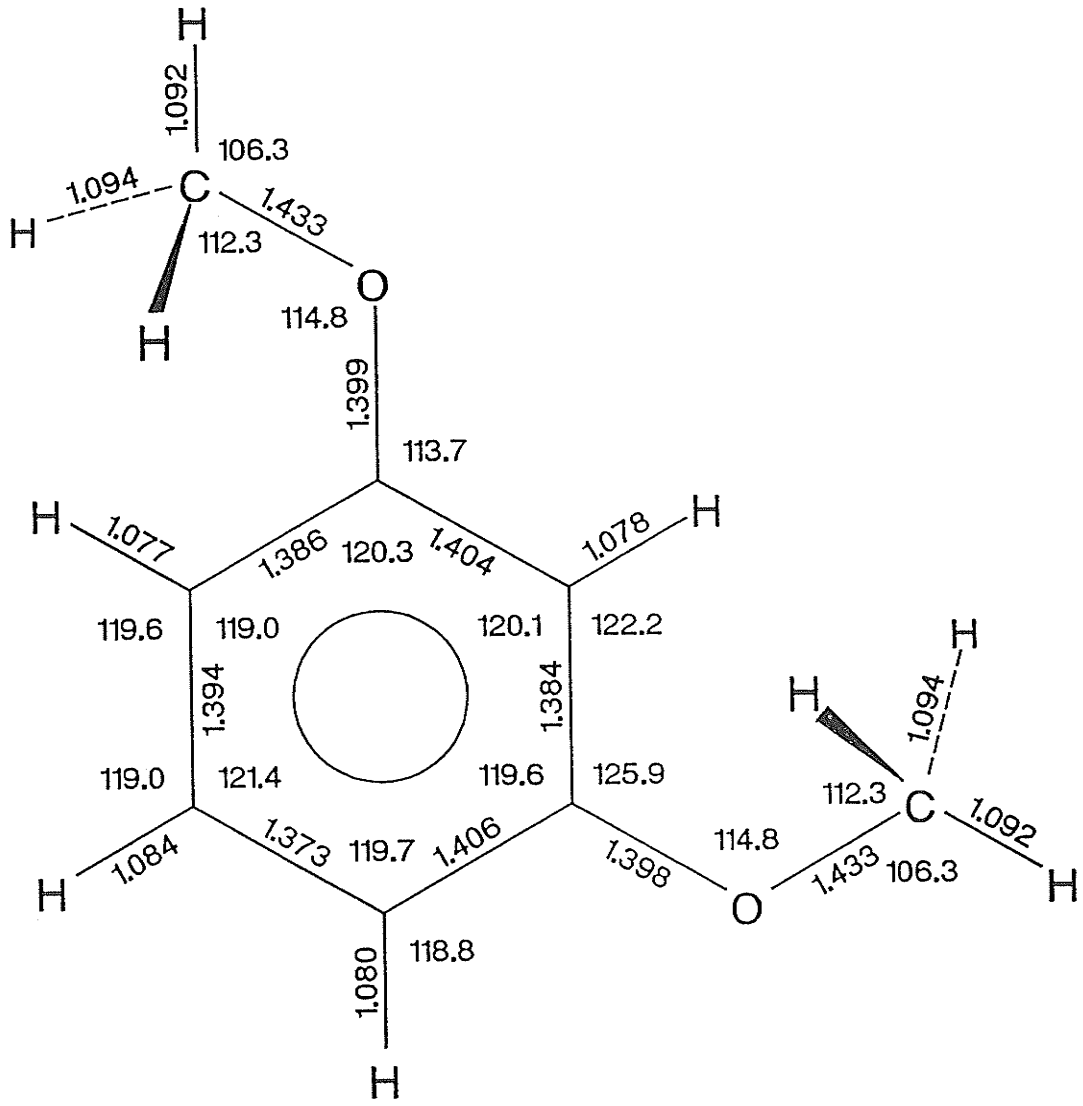

Figure 19

The STO-3G structure of the *cis-cis* conformer ($\theta=180^{\circ}, \phi=0^{\circ}$) of 1,3-dimethoxybenzene. All the bond angles ($^{\circ}$) and bond lengths (Å) are optimized; the only constraint is that the nuclei of the benzene moiety remain in a plane.

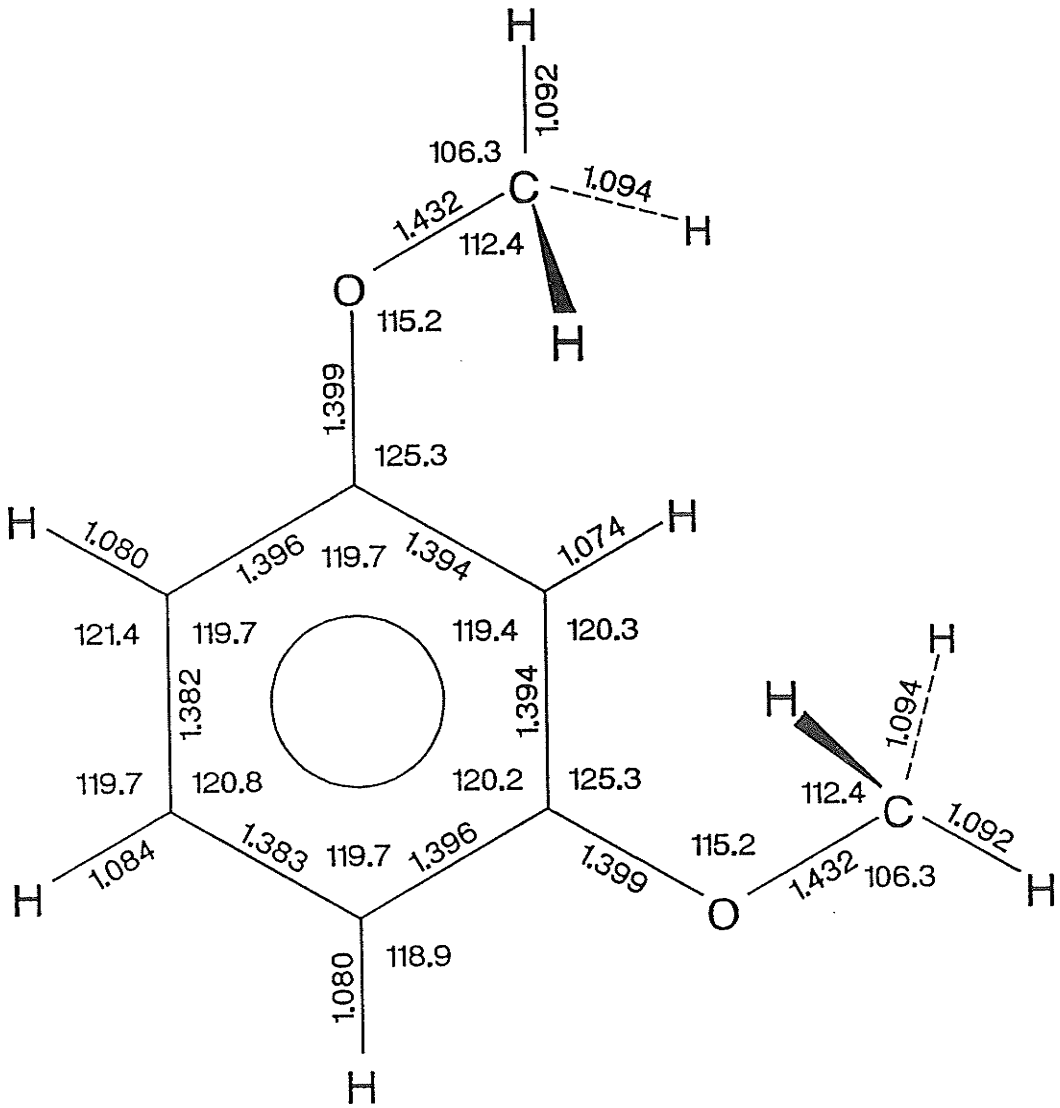

Figure 20

The STO-3G structure of the *trans-trans* conformer ($\theta=0^{\circ}, \phi=180^{\circ}$) of 1,3-dimethoxybenzene. All the bond angles ($^{\circ}$) and bond lengths (Å) are optimized; the only constraint is that the nuclei of the benzene moiety remain in a plane.

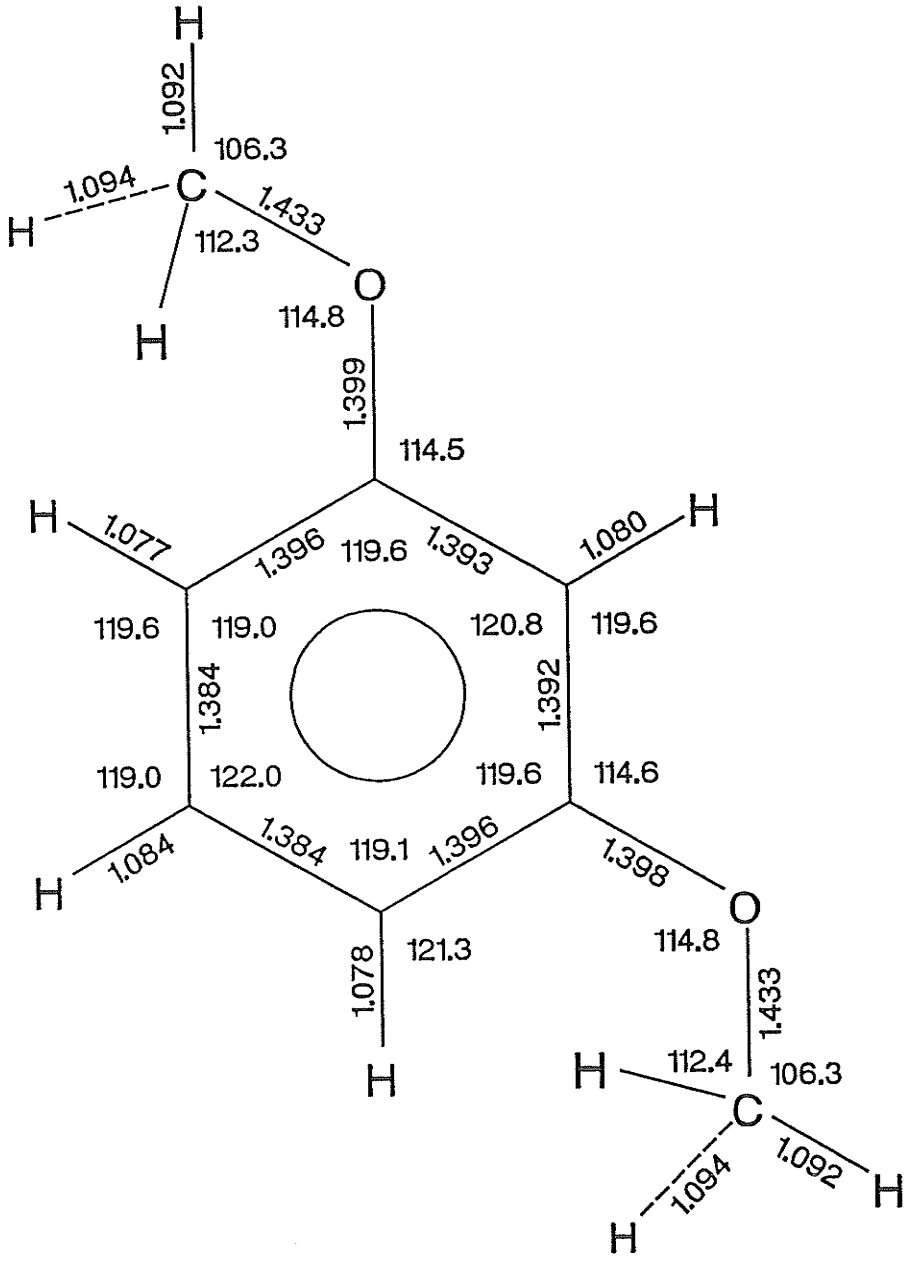

3.2.3. Isobutylbenzene at the AM1 and the STO-3G MO levels

The relative energies and the dipole moments of isobutylbenzene at 15° intervals of the dihedral angle, β, between the isobutyl group and the ring, appear in Tables 8 and 9. The optimized dihedral angles C1C7C8H8, ϕ, are also given. The potential energy curves for internal rotation about the this bond appear in Figure 21.

The angles ϕ are defined as positive for the C8-H8 bond (C8 is behind C7) rotated anti-clockwise, or as negative for clockwise, from the plane containing C1, C7 and C8 (see pictures below).

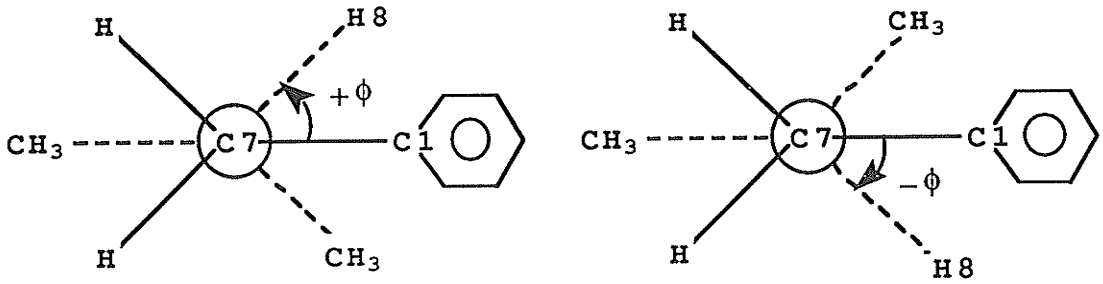

Table 8

The relative energies and the dipole moments of isobutylbenzene at 15° intervals of the dihedral angle, β, computed at the AM1 level. The signs of the dihedral angles C1C7C8H8, ϕ, are defined on p.72.

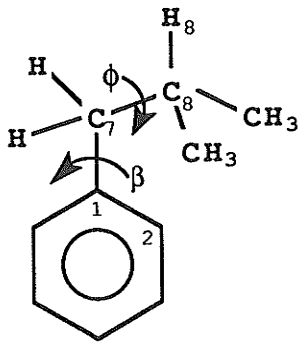

β°	ϕ°	Relative energy (kJ mol^{-1})	Dipole moment (D)
0	-44.0	0.000	0.132
15	-52.7	-0.598	0.124
30	-57.9	-1.402	0.114
45	-56.8	-2.674	0.103
60	-46.9	-4.314	0.096
75	-46.1	-4.690	0.093
90	±45.8	-4.330	0.096

Table 9

The relative energies and the dipole moments of isobutylbenzene at 15° intervals of the dihedral angle, β, computed at the STO-3G MO level. The calculations at β=45° and did not converge and were discarded. The signs of ϕ are defined on p.72. The conformer has a total energy of -382.210 867 a.u. at β=0°(ϕ=-44.4°).

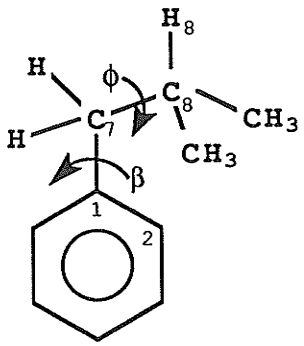

β°	ϕ°	Relative energy (kJ mol^{-1})	Dipole moment (D)
0	-44.4	0.000	0.340
15	-52.4	-3.006	0.331
30	-57.0	-5.610	0.312
60	-56.1	-11.388	0.284
75	-55.7	-12.454	0.281
90	±56.2	-11.084	0.284

Figure 21

The potential energy curves for internal rotation about the C_{sp^2}-C_{sp^3} bond in isobutylbenzene. The relative energies, calculated at the AM1 and the STO-3G MO level, are given as triangles and squares, respectively, in the figure. The solid and the broken lines represent the potential functions as in [19] and [20], respectively.

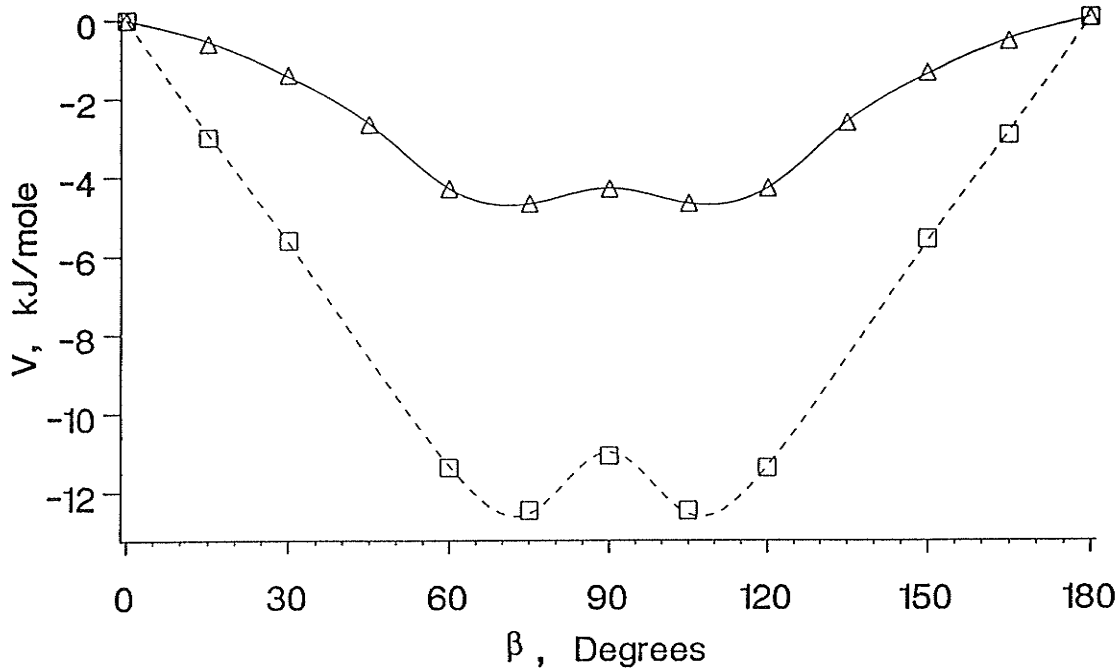

$$V(\beta) = -4.79(2)\sin^2\beta - 0.50(2)\sin^2 2\beta + 0.48(2)\sin^2 3\beta - 0.46(2)\sin^2 4\beta \ (kJ\,mol^{-1}) \quad [19]$$

$$V(\beta) = -11.11(6)\sin^2\beta - 1.54(11)\sin^2 2\beta + 0.12(6)\sin^2 3\beta - 2.47(10)\sin^2 4\beta \ (kJ\,mol^{-1}) \quad [20]$$

3.2.4. 3-phenylpentane at the AM1 level

The relative energies and the dipole moments of 3-phenylpentane at 15° intervals of the dihedral angle, θ, between the 3-pentyl group and the ring, appear in Table 10. The optimized dihedral angles H7C7C8C9, ϕ, and H7C7C10C11, Ψ, are also given. The potential energy curve for internal rotation about the C_{sp^2}-C_{sp^3} bond appears in Figure 22.

The angles ϕ (or Ψ) are defined as positive for the C8-C9 (or C10-C11) bond rotated anti-clockwise, or as negative for clockwise, from the plane containing H7, C7 and C8 (or H7, C7 and C10).

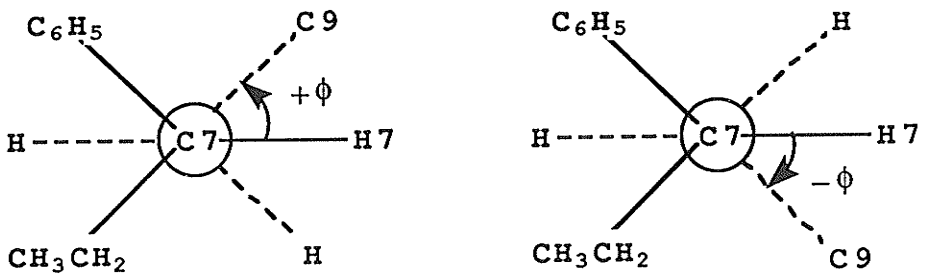

C8 is behind C7

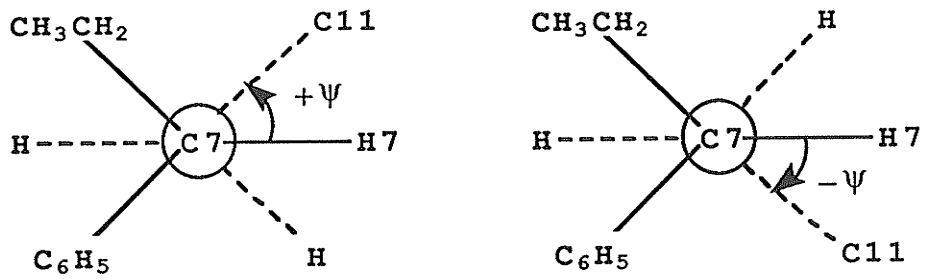

C10 is behind C7

Table 10

The relative energies and the dipole moments of 3-phenylpentane at 15° intervals of the dihedral angle, θ, computed at the AM1 level. The signs of the dihedral angles H7C7C8C9, ϕ, and H7C7C10C11, Ψ, are defined on p.76.

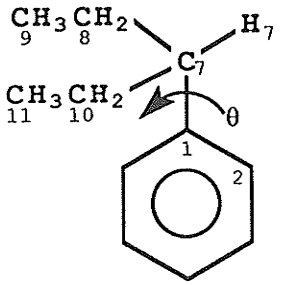

θ°	ϕ°	Ψ°	Rel. energy (kJ mol^{-1})	Dipole moment (D)
0	47.5	39.2	0.000	0.094
15	46.6	36.9	0.015	0.097
30	44.6	38.0	1.293	0.109
45	51.3◊	38.9	4.127	0.119
60	42.4	34.5	6.804	0.132
75	-1.0¤	56.3*	11.590	0.147
90	3.4	20.8◊	13.907	0.136

◊ relieves CH_2 and ring repulsion
¤ relieves CH_3 and ring repulsion
* relieves CH_3 and CH_3 repulsion

Figure 22

The potential energy curve for internal rotation about the C_{sp^2}-C_{sp^3} bond in 3-phenylpentane. The relative energies, calculated at the AM1 level, are given as triangles in the figure. The solid line represents the best fit potential function as in [21].

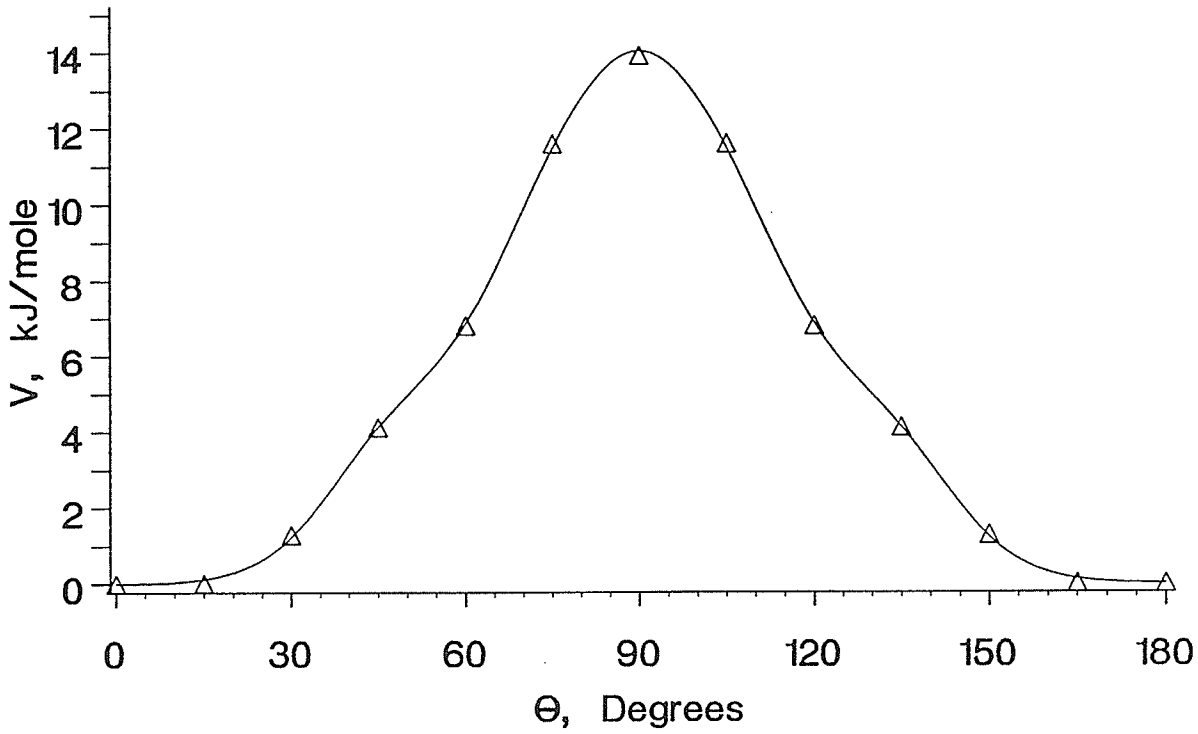

$$V(\theta) = 13.11(7)\sin^2\theta - 3.10(7)\sin^2 2\theta + 0.92(7)\sin^2 3\theta - 0.86(7)\sin^2 4\theta + 0.21(5)\sin^2 6\theta \ (\text{kJ mol}^{-1}) \qquad [21]$$

4. DISCUSSION

4.1. 3-iodoanisole, 1,3-dimethoxybenzene and 5-chloro-1,3-dimethoxybenzene

4.1.1. Summary on the conformation of anisoles

The orientation of the methoxy group in anisole and many of its derivatives has been studied by means of dipole moments and molar Kerr constants (36-39), as well as by spectroscopic (1-6,25,26,40-54), electron diffraction (55) and theoretical (26,44,56-61) methods. Agreement, that the planar heavy atom skeleton, **XII**, is the stable conformer, has

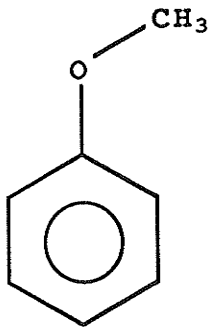

XII

been reached by microwave (25,42,43), nmr (1,2,4,46-51), photoelectron (44), supersonic jet laser spectroscopic (53,54) and theoretical (26,44,56-58,61) studies. The existence of a secondary stable orthogonal conformer has been suggested by photoelectron (45), Raman (26) and theoretical (26,57,61) studies. Statistical analyses (62,63) of X-ray crystal structure data have indicated that the preferred conformation of the methoxy group and the phenyl ring is coplanar. In the presence of two *ortho* substituents other than hydrogen, the methoxy group is orthogonal to the ring

(63). For 1,3-dimethoxybenzene, both experimental and theoretical studies have indicated that the preferred conformation is planar (44,51,54,58,59,64,65). The *trans-trans* conformation is suggested to be the most stable in the vapour phase by photoelectron study (44), whereas molecular mechanics (58) and STO-3G MO (59) calculations are in favour of the *trans-cis* (58,59) conformation.

The rotational characteristics of the methoxy group about the C_{sp^2}-O bond has also been investigated intensively (4-7,25,26,39,44,48,57,60,61,66-68). The barrier to rotation is uncertain, and apparently ranges from 6 kJ mol^{-1} in the vapour phase to 48 kJ mol^{-1} in the solid state (7).

A nonplanar methoxy and ring conformation was proposed by Aroney and coworkers (36-38). By comparing the measured and calculated dipole moments and molar Kerr constants of anisole in CCl_4 at 298 K, they concluded that the methoxy group is twisted 18° out of the benzene plane (38). For 1,3-dimethoxybenzene, a mixture of nonplanar forms with intervalency angles and component moments comparable to that of anisole are postulated (36,37).

From dipole moment measurements and molecular mechanics calculations (39), Allinger et al. suggested free rotation for the methoxy group about the C_{sp^2}-O bond. This contradicts the results from most spectroscopic and theoretical studies (4-7,25,26,41-44,55,57,60,61,66-68) in which hindered rotation is implied.

Steric hindrance between the methoxy and the *ortho* C-H

bonds destabilizes the planar conformation of the methoxy group. Maximum conjugation of the oxygen atom with the ring requires a planar conformation. The two opposing interactions led Horák, Lippincott and Khanna (40) and Josefi et al. (41) to propose that the methoxy group is twisted out of the benzene plane. In a vibrational study of liquid 3-halogenoanisoles (41), Josefi et al. observed two distinguishable isomers, suggesting hindered rotation about the C_{sp^2}-O bond.

In an analysis of the infrared and Raman spectra of liquid anisole at ambient temperature, the planar heavy atom skeleton and C_s symmetry were assumed by Owen and Hester (66). From the torsional frequency of 108 cm^{-1}, the twofold torsional barrier to the methoxy group rotation about the C_{sp^2}-O bond was deduced as 25.2 kJ mol^{-1}, compared to 22.2 kJ mol^{-1} for methyl vinyl ether.

A number of infrared (67) and Raman (26,68) studies have shown that the methoxy and the methyl torsional frequencies are not pure vibrational modes. In other words, the barriers obtained from these frequencies are only apparent.

Allen and Fewster (67) studied the infrared spectra of anisole, anisole-d_3 and anisole-d_5 in the gas phase. The spectra for anisole and anisole-d_5 are similar but unlike that of anisole-d_3. The methoxy torsional frequencies for the two former molecules are close, at 81.5 and 80.0 cm^{-1}, respectively, but that for the latter is 77.5 cm^{-1}. The twofold barriers are 15.1 kJ mol^{-1} for the two former molecules

and 17.1 kJ mol^{-1} for the latter. The discrepancy is explained as due to the mixing of the low frequency out-of-plane ring vibration into the torsional mode and the inadequacy of the use of only two degrees of freedom.

Tylli and Konschin (68) studied the Raman spectra of anisole and anisole-d_3 in the solid state at 130 K. The barriers to methoxy group rotation were deduced as 48.2 ± 1.3 and 49.0 ± 1.5 kJ mol^{-1}, respectively. These values are identical within experimental accuracy, indicating that the coupling of low frequency modes to the methoxy torsional mode in both cases is of the same order of magnitude. The apparent barrier to methyl group rotation decreases from 22.1 ± 0.2 kJ mol^{-1} in anisole to 17.5 ± 0.2 kJ mol^{-1} in anisole-d_3. The reduction upon deuteration is not due to isotopic substitution, but to the coupling of another low frequency mode to the methyl torsional mode.

The planar framework of heavy atoms has been suggested by Lister and Owen (25,42) from microwave studies of *p*-fluoroanisole in the vapour phase. From the spectral appearance (42), a lower limit of 7 kJ mol^{-1} is placed on the barrier to the threefold rotation of the methoxy group. The barrier height is suggested to be similar to that found for methyl vinyl ether, 16.7 kJ mol^{-1}.

Seip and Seip (55) reported the electron diffraction results for gaseous anisole at 328 and 523 K. On comparing the experimental and theoretical intensities, they obtained good agreement for a planar skeleton at the lower

temperature. At the higher temperature, a best result was obtained for a methoxy torsional angle of 40°. The large deviation from planarity at the higher temperature and the large difference between the mean vibrational amplitudes at the two temperatures led them to suggest a secondary potential minimum in addition to that for the planar conformer. The barrier described by equation [22] was suggested as inadequate.

$$V(\theta) = \frac{V_2(1-\cos 2\theta)}{2} \quad (\text{kJ mol}^{-1}) \qquad [22]$$

Later, Lister studied the microwave spectrum of the six lowest torsional states of the methoxy group in *p*-fluoroanisole at 273 K (25). The torsional vibration is reasonably harmonic with a frequency of 70 cm^{-1}. The potential well containing the planar rotamer has at least six pairs of energy levels, indicating that the lower limit of the barrier is at least 4.6 kJ mol^{-1}, and that the energy difference between two rotamers, if a second one exists in less than 20% at 273 K, is at least 3.6 kJ mol^{-1}. The simplest potential function will include a fourfold term in addition to a twofold term as in equation [23].

$$V(\theta) = \frac{V_2(1-\cos 2\theta)}{2} + \frac{V_4(1-\cos 4\theta)}{4} \quad (\text{kJ mol}^{-1}) \qquad [23]$$

Onda et al. (43) measured the microwave spectrum of anisole in the ground vibrational and the first excited torsional states at temperatures near 258 K. The preferred

conformation is the planar heavy atom skeleton and the methoxy torsional frequency is 83.0(3.7) cm^{-1}.

The STO-3G MO calculations of Anderson, Kollman, Domelsmith and Houk (44) have predicted four local minima on the potential function of anisole, with the planar conformations (0° and 180°) favoured over the perpendicular conformations (90° and 270°) by 3.9 kJ mol^{-1}. When the steric replusion between the methoxy and the *ortho* hydrogen atoms in the planar conformation is relieved by the opening of the C_{sp^2}-C_{sp^2}-O angle from 120° to 125.5°, the rotational barrier becomes 5.6 kJ mol^{-1}. Their photoelectron spectra implied planar conformation of the methoxy groups in anisole, 1,3- and 1,4-dimethoxybenzenes. The 1,3-dimethoxybenzene has the two methoxy groups pointing away from each other. Substitution of a second methoxy group at the *meta* position in anisole stabilizes the molecule, as indicated by the isodesmic energy and a higher rotational barrier, 9.4 kJ mol^{-1}, compared to anisole. The predicted π charges on the carbon bonding to the methoxy group correlate with the rotational barrier: π charges of 0.035, 0.017 and -0.016 for 1,3-dimethoxybenzene, anisole and 1,4-dimethoxybenzene with barriers of 9.4, 3.9 and 0.7 kJ mol^{-1}, respectively. The less stable orthogonal conformer of anisole has been assessed by Friege and Klessinger (45) in their photoelectron study as 5.7 ± 0.6 kJ mol^{-1} less stable than the planar conformer.

Emsley and coworkers (46,47) studied the ^1H nmr spectra of substituted anisoles in the nematic phase. The 2,6- and

3,5- derivatives were used in order to simplify the spectra. However, the dipolar couplings from the remaining protons do not yield enough conformational information, and reasonable assumptions about the geometries of the ring and methoxy group had to be made (46). Only the couplings between the methoxy protons were independent of the methyl group motion. With a ^{13}C labelled methoxy group, more couplings of this type could be obtained (47). The calculated and the observed dipolar couplings between the methoxy protons showed that molecular reorientation was faster than the rotation about the C_{sp^2}-O bond (46), which had a barrier of more than 12 kJ mol^{-1} (47). The stable conformer had a planar structure with one C-H bond pointing away from the ring on the plane (46,47). In the case of 2,6-dichloroanisole, the minimum energy conformation had an orthogonal methoxy group (47).

Diehl and coworkers (48), using ^1H, ^2H, $^1H\{^1H\}$ and $^2H\{^1H\}$ experiments, have obtained all dipolar couplings but are unable to decide on the depth and shape of the methoxy and the methyl group potentials.

^{13}C nmr chemical shifts give information about the π electron density distribution in the molecular system (69). Dhami and Stothers (70) studied the effects of steric substitution on the methoxy group and the ring conjugation. For mono-*ortho* substitution, the *ortho* carbon *cis* to the methoxy group is more shielded than the *trans*. Biekofsky and coworkers (71) have estimated the average *cis*- and *trans-ortho* carbon substituent chemical shift (SCS) effects

to be -17.7 and -10.1 ppm, respectively, in agreement with their Individual Gauge for Localized Orbitals (IGLO) calculations. The interaction between the methoxy group and the *trans-ortho* carbon is mainly an electronic effect, whereas that with the *cis-ortho* carbon involves both electronic and steric effects. Kitching and coworkers (64) have observed an increase in the *para* carbon SCS effect from -7.68 ppm in anisole to -7.93 ppm in 2-methylanisole. The steric enhancement of resonance is attributed to an increase in population of the planar conformer. For di-*ortho* substitution, all aromatic ^{13}C nuclei are deshielded due to the reduction of electron-release by the methoxy group to the ring (70). In the presence of two *ortho* methyl groups, the *para* carbon SCS effect is reduced to -4.45 ppm, demonstrating the steric inhibition of resonance as the population of nonplanar conformers is increased (64). In terms of additivity of substituent effects, deviations from the calculated values are observed for both *ortho* carbon atoms in mono-*ortho* substituted anisoles and for all aryl carbon atoms in di-*ortho* substituted anisoles, which depend on the conformation of the methoxy group (64,70,71). The rule holds satisfactorily for 1,3-dimethoxybenzene, implying that the methoxy groups lie in the benzene plane (64). The methoxy ^{13}C nmr chemical shift is insensitive to mono substitution at any position on the ring. The methoxy carbon is deshielded upon di-*ortho* substitution, and the deshielding increases as the size of the substituent increases (70). This observation

is puzzling because the presence of two *ortho* substituents will reduce the electron-release by the oxygen to the ring, thereby causing an increase in shielding (70). The study of ^{13}C chemical shift tensors in single crystals of methoxybenzenes by Carter et al. suggested that the isotropic methoxy ^{13}C nmr chemical shift is 54 ppm for an in-plane methoxy conformation and is increased to 60.3 ppm for an out-of-plane methoxy conformation (72).

Based on the methoxy ^{13}C nmr chemical shifts and spin-lattice relaxation times (T_1), Makriyannis and coworkers (49-51) are able to conclude that the methoxy groups are planar in 1,2-, 1,3- and 1,4-dimethoxybenzenes, and in methoxybenzenes with one or no *ortho* substituent. These methoxy groups have ^{13}C nmr chemical shifts very similar to unsubstituted anisole (54 ppm). For out-of-plane methoxy groups, such as the 2-methoxy group in 1,2,3-trimethoxybenzene, the methoxy ^{13}C nmr chemical shift increases to 60.7 ppm, with a longer T_1, 61 s.

Kruse, Debrosse and Kruse (52) studied the conformational preference of the methoxy groups in certain anisole deriratives, using nuclear Overhauser enhancement, NOE, and *ortho* proton T_1 measurements. It was postulated that the methoxy group seeks the *ortho* position of highest π electron density. They pointed out that the ratio of NOEs does not necessarily give the ratio of conformational populations correctly for such complex spin systems. Both NOE and T_1 measurements had to be considered. The

deuteration/T_1 technique, independent of NOE, gave comparable results.

From ^1H nmr studies on anisole (23), Schaefer et al. obtained a $^5J_o(H,CH_3)$ of -0.152(0) Hz in CS_2 and -0.155(0) Hz in acetone-d_6, close to the mean value of their INDO MO FPT computations (1) on $^5J_o(H,CH_3)$ at $\theta=0^\circ$ and 180° (-0.292 and 0.037 Hz, respectively). They concluded that the methoxy group and the ring are coplanar with a substantial barrier to internal rotation (2). Their ^{13}C DNMR experiment (5) showed no broadening of the peaks of the two *ortho* carbon nuclei in dimethyl ether solution at 120 K. The difference in chemical shifts between these nuclei in the planar conformation could not be less than 6 ppm (5); therefore the free energy barrier to the methoxy group rotation about the C_{sp^2}-O bond was less than 19.7 kJ mol^{-1}. Further $T_{1\rho}$ measurements gave a maximum of 18.4 kJ mol^{-1} on the assumption that the shift difference is 6 ppm (5).

Schaefer et al. have studied the rotational barrier with the J-method (12). Their INDO MO FPT computations indicate that both $^5J(^{13}C,^{13}C)$ (6) and $^6J_p(^1H,^{13}C)$ (5) are $\sin^2\theta$ dependent as in [24] and [25]

$$^5J(^{13}C,^{13}C) = 1.53(1)\sin^2\theta \text{ (Hz)} \qquad [24]$$

$$^6J_p(^1H,^{13}C) = -0.01 - 0.626\sin^2\theta \text{ (Hz)} \qquad [25]$$

Experimentally (5,6), a $^5J^{\pi}_{90}(^{13}C,^{13}C)$ of 0.98±0.03 Hz and a $^6J^{\pi}_{90}(^1H,^{13}C)$ of 0.625±0.005 Hz are obtained (see eq. [2],[3] on

p.9). $^{5}J(^{13}C,^{13}C)$ is not observed and may be less than 0.03 Hz, which implies a $\langle\sin^2\theta\rangle$ of 0.03 or less (6). For $^{6}J_p(^{1}H,^{13}C)$, the observed value is ±0.030±0.005 Hz, which gives a $\langle\sin^2\theta\rangle$ of 0.048(8) (7). These values of $\langle\sin^2\theta\rangle$ imply a rotational barrier close to 40 and 28.0 kJ mol^{-1}, respectively, if the barrier is purely twofold (6,7). Both results indicate that a fourfold term with the same sign as the twofold term must be present in order to give a barrier height consistent with the DNMR result (5-7).

$^{6}J_p(^{1}H,^{13}C)$ implies a V_2 of 15.0±2.0 kJ mol^{-1} and a V_4 of 5.6±2.2 kJ mol^{-1} for the V_4/V_2 ratio of 0.44 indicated by the 6-31G*(5D) computations (7). The computed potential energy functions at the STO-3G MO level, [26], and the 6-31G MO level, [27], are

$$V(\theta) = 5.8(2)\sin^2\theta + 2.4(2)\sin^2 2\theta - 0.6(2)\sin^2 3\theta \ (\text{kJ mol}^{-1}) \qquad [26]$$

$$V(\theta) = 7.78(5)\sin^2\theta + 2.41(5)\sin^2 2\theta - 0.54(5)\sin^2 3\theta \ (\text{kJ mol}^{-1}) \qquad [27]$$

Seeman, Secor, Breen and Bernstein (53,54) observe the minimum energy conformer of methoxybenzenes by supersonic jet laser spectroscopy. Only one conformer of anisole is detected. The stable conformer is identified by comparing the number of observed origins to that predicted by the symmetry of each conformation. The time of flight mass spectroscopy (TOFMS) of the electronic origin transition

region for the first excited singlet state ($S_1 \leftarrow S_0$) of jet-cooled anisole, 1,2-, 1,3- and 1,4-dimethoxybenzene display one, one, three and two origins, respectively, which are consistent with planar methoxy moieties. The observed methoxy group torsional transitions of 1,2- and 1,3-dimethoxybenzene are suggested to arise from the change of the geometry of the minimum energy conformation upon electron excitation from S_0 to S_1. The potential barrier to methoxy group rotation for 1,3-dimethoxybenzene is roughly approximated as 2000-5000 cm^{-1} or with 23.9-59.8 $kJ\,mol^{-1}$. These numbers (for the free molecule) are rather larger than expected on the basis of other data discussed above.

In the following sections, the long-range coupling constants between the methoxy protons and the *ortho* ring protons, $^5J_o(H,CH_3)$, are applied to the problem of the conformational distributions of 3-iodoanisole, 1,3-dimethoxybenzene and 5-Cl-1,3-dimethoxybenzene, for which disagreement exists in the literature.

4.1.2. Conformational distribution of 3-iodoanisole

If the rotational barrier of the methoxy group about the C_{sp^2}-O bond in anisole in the liquid state or in solution at room temperature is much greater than kT (4-7,66) and the preferred conformation is planar (1,2,4,49-52,64,65), then 3-iodoanisole can exist in two distinguishable forms, *trans* and *cis*.

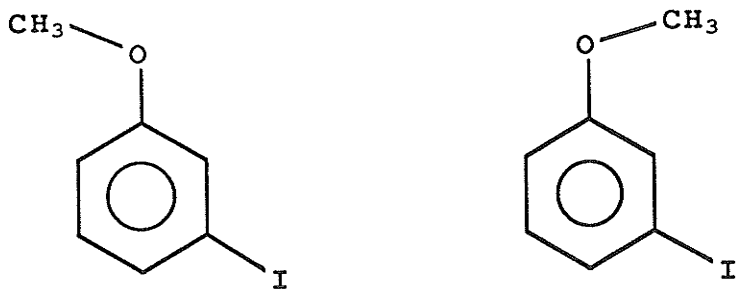

The two isomers in a liquid sample are identified from some vibrational bands (41). On cooling to 93 K, one conformer has frozen out and the *trans* conformation is assigned as the more stable. The conformational preferences of all 3-halogenoanisoles are suggested (66) to be similar (see conclusion). In a vibrational study (66) of liquid 3-halogenoanisoles, the changes in the optical densities at 940 and 915 cm^{-1} between 290 and 373 K indicate that the *trans* conformer of 3-fluoroanisole is 2.4 ± 0.6 kJ mol^{-1} more stable than the *cis*. By way of contrast, an ^1H nmr study (4) of 3-fluoroanisole has shown that the *cis* conformer is slightly more stable in both CS_2 and acetone-d_6 solutions at 300 K, with a fractional population of 0.51 and 0.54, respectively.

At the STO-3G MO level, the energy difference between the two planar conformers is 0.46 kJ mol^{-1}, with a fractional *cis* population of 0.55.

From infrared intensities at ambient temperature (73), 3-iodoanisole is concluded to exist solely in the *cis*-form in CCl_4. It seems unlikely that 3-iodoanisole exists only in the *cis*-form at ambient temperature. The *cis/trans* equilibrium of 3-iodoanisole is expected to be very similar to that of 3-fluoroanisole (4) which has the *cis* conformer as slightly more abundant.

Conformational equilibrium from $^5J_o(H,CH_3)$

$^5J_o(H,CH_3)$ in anisole and its derivatives is stereospecific (1-3), which enables the *cis/trans* equilibrium to be estimated. In Table 1 (p.28), $^5J_o(H,CH_3)$ for H-2 and H-6 of 3-iodoanisole are -0.176(1) and -0.134(1) Hz in CS_2 and -0.167(1) and -0.141(1) Hz in acetone-d_6, respectively. Assuming that the coupling for the *trans* arrangement, $^5J_t(H,CH_3)$, vanishes, and that for the *cis* arrangement, $^5J_c(H,CH_3)$, is the same in the two planar conformers, then $^5J_c(H,CH_3)$ is -0.176(1)-0.134(1)=-0.310(2)$^{\Delta}$ Hz in CS_2 and is -0.308(2) Hz in acetone-d_6. These numbers imply a fractional

---

$^{\Delta}$ The errors in the parentheses are estimated as follows:
(i) For a sum or difference of two or more values, eg. A(a)±B(b)=C(c), the error is c=a+b.
(ii) The error in a product, A(a)xB(b)=C(c), or a quotient, $\frac{A(a)}{B(b)}$=C(c), is $c=[\frac{a}{A}+\frac{b}{B}]xC$.

cis population of $-0.176(1)/-0.310(2)=0.57(1)^{\Delta}$ in CS_2 and 0.54(1) in acetone-d_6 at 300 K. In other words, the free energy of the *cis* conformer is $0.70(10)^{\Delta}$ and 0.40(10) kJ mol^{-1} lower than that of the *trans* in CS_2 and acetone-d_6, respectively. The population distributions in the two solvents indicate that the less polar *cis* conformer is slightly more stable in the less polar solvent.

If $^5J_t(H,CH_3)$ is non-zero, say 0.05 Hz, then $^5J_c(H,CH_3)$ is $-0.176(1)-0.134(1)-0.05=-0.360(2)$ Hz in CS_2 and $-0.358(2)$ Hz in acetone-d_6. The fractional population of the *cis* conformer becomes 0.55(1) in CS_2 and 0.53(1) in acetone-d_6. Again, the *cis* conformer is slightly more abundant in both solutions at 300 K.

Molecular orbital results

The relative energies and the dipole moments of 3-iodoanisole at 15° intervals of the dihedral angle between the methoxy group and the ring, computed at the STO-3G MO level, appear in Table 6 (p.61). The potential energy curve for the rotation of the methoxy group about the C_{sp^2}-O bond is least-squares fitted to the function in [16] and is displayed in Figure 14 (p.62). The top of the curve around 90° is quite flat, as in those of anisole (7) and 3-fluoroanisole (4). The STO-3G MO geometries of the *cis* and the *trans* conformers are given in Figure 15 and 16 (p.63 and 64), respectively. The geometries of the methoxy moieties are

very close to those in anisole (57).

The rotational barrier is dominated by a twofold term of 7.61(5) kJ mol^{-1} in $\sin^2\theta$, and a fourfold term of 2.54(5) kJ mol^{-1} in $\sin^2 2\theta$. These terms are higher than those for anisole at the same level, being 5.8(2) and 2.4(2) kJ mol^{-1}, respectively (60). The twofold term has increased by 1.8(2) kJ mol^{-1} in 3-iodoanisole. The STO-3G MO predicts the *trans* conformer as 0.26 kJ mol^{-1} more stable than the *cis*. These results suggest a slight shift of the *cis/trans* equilibrium of 3-iodoanisole in solution.

Conclusion

Judging from the sums of $^5J_o(H,CH_3)$ in anisole and 3-iodoanisole, the perturbation of this coupling interaction by the iodine substituent is rather small. The populations of the *cis* and the *trans* conformers of 3-iodoanisole are very nearly equal. The near equality probably holds for all 3-halogenoanisoles. In fact, for 3-chloro and 3-bromoanisole in acetone-d_6 solutions (2), $^5J_o(H,CH_3)$ values for H-2 are -0.135(4) and -0.139(4) Hz, and those for H-6 are -0.156(5) and -0.145(4) Hz, respectively; implying a fractional *cis* population of 0.46(3) and 0.49(3), respectively.

The population distributions and energy barriers of 3-halogenoanisoles found from various spectroscopic methods are summarized in Table 11 (p.96 and 97).

Table 11

Summary of the population distributions and internal barriers

	Method	(Ref.)	Fractional *cis* population
3-fluoroanisole	IR torsional freq.	(66)	---
	IR optical density	(66)	0.28±0.05
	IR intensities	(73)	0.72
	^{1}H nmr, $^5J_o(H,CH_3)$	(4)	0.51(1)
	^{1}H nmr, $^5J_o(H,CH_3)$	(4)	0.54(1)
	STO-3G MO	(4)	0.55
	6-31G MO	(4)	0.58
3-chloroanisole	IR torsional freq.	(66)	---
	IR intensities	(73)	0.44
	^{1}H nmr, $^5J_o(H,CH_3)$	(2)	0.46(3)
3-bromoanisole	IR torsional freq.	(66)	---
	IR intensities	(73)	0.50
	^{1}H nmr, $^5J_o(H,CH_3)$	(2)	0.49(3)
3-iodoanisole	IR intensities	(73)	1.00
	^{1}H nmr, $^5J_o(H,CH_3)$		0.57(1)
	^{1}H nmr, $^5J_o(H,CH_3)$		0.54(1)
	STO-3G MO		0.47

---

* the energy difference between the *cis* and *trans* conformers (note that the $^5J_o(H,CH_3)$ values give free energy differences, and MO calculations yield approximate enthalpy differences)

‡ the barrier to methoxy group rotation function

§ the twofold component

of 3-halogenoanisoles from various spectroscopic methods.

State	Energy* (kJ mol^{-1})	Barrier† (kJ mol^{-1})
liquid, ambient temp.	---	29.4
liquid, 290-373 K	2.4±0.6	---
CCl_4, ambient temp.	---	---
CS_2, 300 K	0.10(10)	---
acetone-d_6, 300 K	0.40(10)	---
free molecule	0.46	8.32[§]
free molecule	0.85	---
liquid, ambient temp.	---	28.9
CCl_4, ambient temp.	---	---
acetone-d_6, 305 K	0.42(31)	---
liquid, ambient temp.	---	31.8
CCl_4, ambient temp.	---	---
acetone-d_6, 305 K	0.12(31)	---
CCl_4, ambient temp.	---	---
CS_2, 300 K	0.71(10)	---
acetone-d_6, 300 K	0.40(10)	---
free molecule	0.26	7.61(5)[§]

4.1.3. Conformational distributions of 1,3-dimethoxybenzene and 5-chloro-1,3-dimethoxybenzene

A number of studies have shown that the conformation of the methoxy groups in 1,3-dimethoxybenzene is in-plane (44,51,54,58,59,64,65). The methoxy ^{13}C nmr chemical shift and ^{13}C spin-lattice relaxation time of 1,3-dimethoxybenzene are 55.2 ppm and 3.7 s, respectively, similar to those of unsubstituted anisole and indicating that the methoxy group conformation is planar (51). The planar conformation is also evident as the additivity of methoxy substituent effects on all the ring carbons holds satisfactorily for 1,3-dimethoxybenzene (64). ^{13}C and ^{17}O nmr chemical shifts of the methoxy groups in 1,3-dimethoxybenzene and 5-chloro-1,3-dimethoxybenzene are 55.9 and 54.8 ppm, and 56.2 and 59.9 ppm, respectively (65). These methoxy groups have similar conformations, in the plane of the ring, and the increase in chemical shifts is caused by the inductive effect of the electronegative chlorine.

The four possible planar conformations of 1,3-dimethoxybenzene and 5-chloro-1,3-dimethoxybenzene are *cis-cis*, *cis-trans*, *trans-cis* and *trans-trans*; *cis-trans* and *trans-cis* are a pair of degenerate conformers and will be referred to as *trans-cis* hereafter.

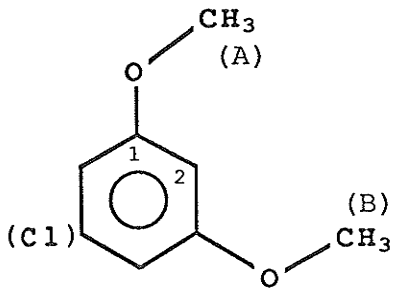

cis-cis

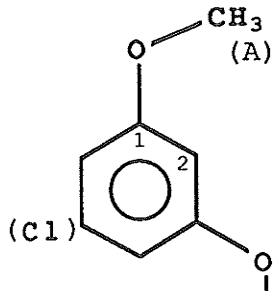

cis-trans

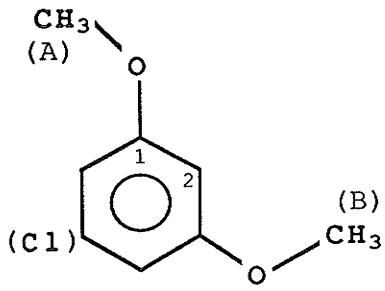

trans-cis

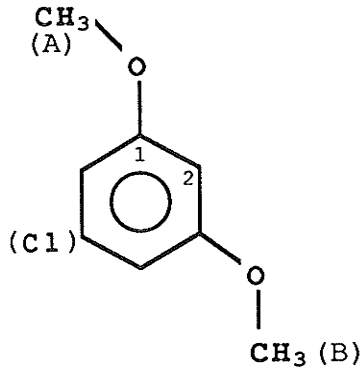

trans-trans

The dipole moment in CCl_4 solution at 298 K has been interpreted to mean that 1,3-dimethoxybenzene exists predominantly as *trans-cis* and *trans-trans* in a ratio of 3:1, with a very small amount of *cis-cis* (36,37). Similar measurements in the benzene solution suggest that the dipole moment is compatible with a mixture of planar conformations, where *trans-cis* is the most abundant, with smaller contributions from *cis-cis* and *trans-trans* (74). Comparison of the dipole moment in benzene solution, 1.61 D, and the estimated values for equimolecular mixture of all planar conformers, 1.77 D, suggests that *cis-cis* is disfavoured (75). In the photoelectron study (44) of

1,3-dimethoxybenzene in the vapour state, *trans-trans* is assigned as the most stable conformer. The STO-3G MO computations, with standard geometries of anisole, have *trans-trans* as 9.4 kJ mol^{-1} more stable than the conformation with one methoxy group rotated 90° out-of-plane (44). The authors also suggest that the *trans-cis* and the *trans-trans* conformations have approximately identical energies. Molecular mechanics calculations (58) imply the co-existence of all three conformers. The free energies of *cis-cis* and *trans-trans* relative to *trans-cis* at 300 K are 3.1 and 1.9 kJ mol^{-1}, respectively, suggesting that the fractional populations are 0.10, 0.17 and 0.73, respectively (58). The calculated values indicate no change of the dipole moment upon an increase in temperature: 1.51 D at 573 K and 1.52 D at 673 K. This is also demonstrated for a decalin solution where the dipole moment is constant at 1.48 D over the temperature range of 293-403 K (76). An unfavourable entropy factor, counteracting the increase of population of the less stable conformers at higher temperature, is given as an explanation (58). Fully optimized STO-3G MO calculations (59) also predict the *trans-cis* as the most stable conformer. In the TOFMS of the supersonic jet-cooled 1,3-dimethoxybenzene molecule, three origins associated with the three stable planar conformers are observed (54). The first torsional transition appears ~190 cm^{-1} from the first origin, implying that the rotational barrier of the methoxy group is within 23.9-59.8 kJ mol^{-1}. In the solid state, the

crystal structure of 2-ethynyl-1,3-dimethoxybenzene has the methoxy groups *trans* to each other (77). The ethynyl group at position 2 determines the orientation of the methoxy groups sterically. In solution, the presence of solvent molecules, if polar enough, will stablize the conformer with the largest dipole moment.

Conformational equilibrium from $^5J_o(H,CH_3)$

The ^1H nmr spectrum of the ring region corresponds to an AB_2C system for 1,3-dimethoxybenzene, or an AB_2 system, for 5-chloro-1,3-dimethoxybenzene, which implies rapid interconversion among the conformers on the chemical shift time scale. $^5J_o(H,CH_3)$ values for H-2 and H-6 are conformationally averaged parameters, and are represented by equations [28] and [29],

$$^5J(H2,CH_3(A)) = {}^5J_c(H,CH_3)\,(P_{c\text{-}c}+P_{c\text{-}t}) + {}^5J_t(H,CH_3)\,(P_{t\text{-}c}+P_{t\text{-}t}) \quad \text{(Hz)} \qquad [28]$$

$$^5J(H6,CH_3(A)) = {}^5J_t(H,CH_3)\,(P_{c\text{-}c}+P_{c\text{-}t}) + {}^5J_c(H,CH_3)\,(P_{t\text{-}c}+P_{t\text{-}t}) \quad \text{(Hz)} \qquad [29]$$

where $P_{c\text{-}c}$, $P_{c\text{-}t}$, $P_{t\text{-}c}$ and $P_{t\text{-}t}$ are the fractional populations of the corresponding conformers with $P_{c\text{-}t}$ the same as $P_{t\text{-}c}$ (written as $\frac{1}{2}P^{total}_{t\text{-}c}$ hereafter). Equations [28] and [29] are compatible with the conditions in equation [30] and [31],

$$P_{c\text{-}c} + P^{total}_{t\text{-}c} + P_{t\text{-}t} = 1 \qquad [30]$$

$$^5J(H2,CH_3(A)) + {}^5J(H6,CH_3(A)) = {}^5J_c(H,CH_3) + {}^5J_t(H,CH_3) \quad (Hz) \qquad [31]$$

In Table 2 (p.32), the two $^5J_o(H,CH_3)$ values of 1,3-dimethoxybenzene are -0.153(0) and -0.097(1) Hz in CS_2 and -0.160(0) and -0.104(1) Hz in acetone-d_6. If $^5J_t(H,CH_3)$ is 0.037 Hz, as calculated for anisole by Schaefer and Laatikainen (1), then $^5J_c(H,CH_3)$ is $-0.153(0)-0.097(1)-0.037=-0.287(1)^{\Delta}$ Hz in CS_2 and -0.301(1) Hz in acetone-d_6. Therefore, in the CS_2 solution, [28] and [29] become $-0.153(0)=-0.287(1)\,(P_{c-c}+\frac{1}{2}P_{t-c}^{total})+0.037\,(\frac{1}{2}P_{t-c}^{total}+P_{t-t})$ and $-0.097(1)=0.037\,(P_{c-c}+\frac{1}{2}P_{t-c}^{total})-0.287(1)\,(\frac{1}{2}P_{t-c}^{total}+P_{t-t})$ Hz. It follows that $P_{c-c}+\frac{1}{2}P_{t-c}^{total}=0.59(1)^{\Delta}$ and $\frac{1}{2}P_{t-c}^{total}+P_{t-t}=0.41(1)$. In the acetone-$d_6$ solution, $P_{c-c}+\frac{1}{2}P_{t-c}^{total}=0.58(1)$ and $\frac{1}{2}P_{t-c}^{total}+P_{t-t}=0.42(1)$.

Now, if $^5J_t(H,CH_3)$ vanishes, then $^5J_c(H,CH_3)$ is $-0.153(0)-0.097(1)=-0.250(1)$ Hz in CS_2 and -0.264(1) Hz in acetone-d_6. Hence $P_{c-c}+\frac{1}{2}P_{t-c}^{total}=0.61(1)$ and $\frac{1}{2}P_{t-c}^{total}+P_{t-t}=0.39(1)$ in both CS_2 and acetone-d_6 solutions. These two sets of fractional populations imply that $P_{c-c}+\frac{1}{2}P_{t-c}^{total}=0.60(2)$, $\frac{1}{2}P_{t-c}^{total}+P_{t-t}=0.40(2)$ and $P_{c-c}-P_{t-t}=0.20(4)$ in CS_2, indicating that *cis-cis* is more abundant than *trans-trans* by a fractional population difference of 0.20(4). In acetone-d_6, $P_{c-c}+\frac{1}{2}P_{t-c}^{total}=0.59_5(2)$, $\frac{1}{2}P_{t-c}^{total}+P_{t-t}=0.40_5(2)$ and $P_{c-c}-P_{t-t}=0.19(4)$, impling that *cis-cis* is more favoured than *trans-trans* by a fractional population difference of 0.19(4).

$^{\Delta}$ The method of error estimation is given on p.93.

If $^5J_t(H,CH_3)$ is as large as 0.05 Hz, $^5J_c(H,CH_3)$ is $-0.153(0)-0.097(1)-0.05=-0.300(1)$ Hz in CS_2 and $-0.314(1)$ Hz in acetone-d_6. Then $P_{c-c}+\frac{1}{2}P_{t-c}^{total}=0.58(1)$ and $\frac{1}{2}P_{t-c}^{total}+P_{t-t}=0.42(1)$ in both solvents, giving $P_{c-c}-P_{t-t}=0.16(2)$. In other words, *cis-cis*, the conformer with the largest dipole moment, is more favoured than *trans-trans* by a fractional population difference of at least 0.16(2) in either solvent. At the STO-3G MO level, conformers *cis-cis*, *trans-cis* and *trans-trans* have dipole moments of 2.078, 1.155 and 2.018 D, respectively (Table 7 on P.66). The values given by the 3-21G basis set are 3.12, 1.65 and 2.55 D, respectively. The STO-3G basis generally gives lower values and the 3-21G basis gives higher values than those from experiment (78).

In Table 3 (p.39), the two $^5J_o(H,CH_3)$ values of 5-chloro-1,3-dimethoxybenzene are $-0.146(0)$ and $-0.098(5)$ Hz in CS_2 and $-0.157(0)$ and $-0.100(2)$ Hz in acetone-d_6. $^5J_c(H,CH_3)$ is $-0.281(5)$ Hz in CS_2 and $-0.294(2)$ Hz in acetone-d_6 for $^5J_t(H,CH_3)=0.037$ Hz. If $^5J_t(H,CH_3)=0$ Hz, then $^5J_c(H,CH_3)=-0.244(5)$ Hz in CS_2 and $-0.257(2)$ Hz in acetone-d_6. The same treatment, as for 1,3-dimethoxybenzene, will give $P_{c-c}+\frac{1}{2}P_{t-c}^{total}=0.58(4)$ and $\frac{1}{2}P_{t-c}^{total}+P_{t-t}=0.42(4)$ in CS_2, and $P_{c-c}+\frac{1}{2}P_{t-c}^{total}=0.59(2)$ and $\frac{1}{2}P_{t-c}^{total}+P_{t-t}=0.41(2)$ in acetone-d_6, for $^5J_t(H,CH_3)=0.037$ Hz. Then $P_{c-c}-P_{t-t}$ is 0.16(8) in CS_2 and 0.18(4) in acetone-d_6. For $^5J_t(H,CH_3)=0$ Hz, $P_{c-c}+\frac{1}{2}P_{t-c}^{total}=0.60(3)$ and $\frac{1}{2}P_{t-c}^{total}+P_{t-t}=0.40(3)$ in CS_2, and $P_{c-c}+\frac{1}{2}P_{t-c}^{total}=0.61(1)$ and $\frac{1}{2}P_{t-c}^{total}+P_{t-t}=0.39(1)$ in acetone-d_6. It follows that $P_{c-c}-P_{t-t}$ is

0.20(6) in CS_2 and 0.22(2) in acetone-d_6. These fractional population differences also indicate that *cis-cis* is more abundant than *trans-trans* in both solutions, and the population differences seem to be independent of solvent. The substitution of a chlorine atom at the *meta* position does not appear to change the population differences. It is evident that population studies of 1,3-dimethoxybenzene, based on the magnitude of the dipole moment, may be wrong (36,37,74,75) in that they discount the significant presence of the *cis-cis* conformer in solution.

Molecular orbital results

Table 7 (p.66) shows the relative energies and the dipole moments of 1,3-dimethoxybenzene at 15° intervals of the dihedral angles between the methoxy groups and the ring at the STO-3G MO level. The *trans-cis* conformer is computed as 2.795 and 1.726 kJ mol^{-1} more stable than the *cis-cis* and the *trans-trans*, respectively, which suggests that the fractional populations of the three conformers at 300 K are 0.71, 0.11 and 0.18, respectively. The energies of *cis-cis* and *trans-trans* relative to *trans-cis*, calculated at the 3-21G MO level, are 3.910 and 2.548 kJ mol^{-1}, respectively. The fractional populations of the three conformers are then 0.08, 0.14 and 0.78, respectively. In other words, the STO-3G MO implies that $P_{c\text{-}c}+\frac{1}{2}P_{t\text{-}c}^{total}=0.46_5$, $\frac{1}{2}P_{t\text{-}c}^{total}+P_{t\text{-}t}=0.53_5$ and

$P_{c-c}-P_{t-t}=-0.07$. The 3-21G MO implies that $P_{c-c}+\frac{1}{2}P_{t-c}^{total}=0.47$, $\frac{1}{2}P_{t-c}^{total}+P_{t-t}=0.53$ and $P_{c-c}-P_{t-t}=-0.06$. In both CS_2 and acetone-d_6 solutions, the values of $^5J_o(H,CH_3)$ indicate that $P_{c-c}+\frac{1}{2}P_{t-c}^{total}=0.58(1)$, $\frac{1}{2}P_{t-c}^{total}+P_{t-t}=0.42(1)$ and $P_{c-c}-P_{t-t}=0.16(2)$.

Obviously, these population distributions do not hold in solution, but the calculations give a strong hint as to which conformer will be the most abundant. The potential energy curves (Figure 17 on P.68) for the rotation of the methoxy groups about the C_{sp^2}-O bonds resemble those for anisole (7) and derivatives (4), with a flat top around 90°. The rotational barriers for the two methoxy groups have a dominant V_2 of 7.54(5) and 8.33(4) kJ mol^{-1} and a V_4 of 2.57(5) and 2.49(4) kJ mol^{-1} (eq. [17],[18] on P.68). These values are higher than those for anisole (60), which are 5.8(2) and 2.4(2) kJ mol^{-1}, respectively, at the same level of molecular orbital theory. 1,3-dimethoxybenzene is considered more stable than anisole in terms of isodesmic energies (44). The rotational barrier for 1,3-dimethoxybenzene was estimated by supersonic jet laser spectroscopy as 23.9-59.8 kJ mol^{-1}, a dubiously high value (54). However, a decision on the relative populations of the three conformers was precluded due to the complications involved in the interpretation of the relative intensities of the transition origins.

Conclusion

The measured values of $^5J_o(H,CH_3)$ give the sums of the fractional populations of either two of the three conformers, and the fractional population difference between the *cis-cis* and the *trans-trans* conformers. It is noteworthy that the equations of the sums of fractional populations are still consistent with $P_{t-c}^{total}=0$ or $P_{t-t}=0$. However, P_{c-c} must be at least 0.16(2). This result is the first indicative of the significance of the *cis-cis* conformer in solution.

Experimentally, the sums of $^5J_o(H,CH_3)$ for 1,3-dimethoxybenzene in CS_2 and acetone-d_6 are comparatively smaller in magnitude than those for anisole (23), 3-fluoroanisole (4) and 3-methoxybenzaldehye (79). Furthermore, the magnitude of the sum of $^5J_o(H,CH_3)$ in 3-chloroanisole (2) has decreased from (-)0.291(9) to (-)0.257(2) Hz in 5-chloro-1,3-dimethoxybenzene in acetone-d_6. The sums of $^5J_o(H,CH_3)$ in anisole and its *meta* derivatives with F, CHO and OCH_3 substituents are shown.

	CS_2	acetone-d_6
anisole	-0.304(0)	-0.310(0)
3-methoxybenzaldhyde	-0.298(2)	-0.301(2)
3-fluoroanisole	-0.297(2)	-0.304(1)
1,3-dimethoxybenzene	-0.257(1)	-0.264(1)
{$^5J_t(H,CH_3)$=0.037 Hz	-0.287(1)	-0.301(1)}

The presence of a small positive $^5J_t(H,CH_3)$, say 0.037 Hz, may cause the relatively small magnitude of the sums of $^5J_o(H,CH_3)$ in 1,3-dimethoxybenzene.

The population distributions of 1,3-dimethoxybenzene found from various methods are summarized in Table 12 (p.108).

Table 12

Summary of the population distributions of 1,3-dimethoxybenzene from various methods.

Method	(Ref.)	State	Fractional population P_{c-c}	P_{t-c}	P_{t-t}	$P_{c-c}+\frac{1}{2}P_{t-c}^{total}$	$\frac{1}{2}P_{t-c}^{total}+P_{t-t}$	$P_{c-c}-P_{t-t}$
dipole moment	(36,37)	CCl_4, 298 K	*	0.75	0.25			
dipole moment	(74)	C_6H_6	*	¤	*			
dipole moment	(75)	C_6H_6, 303 K	◊	‡	‡			
MM2	(58)	free molecule	0.10	0.73	0.17	0.46_5	0.53_5	-0.07
STO-3G MO		free molecule	0.11	0.71	0.18	0.46_5	0.53_5	-0.07
3-21G MO		free molecule	0.08	0.78	0.14	0.47	0.53	-0.06
^{1}H nmr, $^5J_o(H,CH_3)$		CS_2, 300 K				0.60(2)	0.40(2)	0.20(2)
^{1}H nmr, $^5J_o(H,CH_3)$		acetone-d_6, 300 K				0.59_5(2)	0.40_5(2)	0.19(4)

* present in small amount
¤ most abundant
◊ disfavoured
‡ present

4.2. Conformational distribution and internal rotational potential in isobutylbenzene

The conformation of isobutylbenzene is described with two dihedral angles, β, between the side chain and the phenyl ring, and ϕ, between the methine C-H bond and the C_{sp^2}-C_{sp^3} bond. The orientation of the isobutyl group relative to the ring in the minimum energy conformation could be one of **V**, **VI**, **VII** and **VIII**.

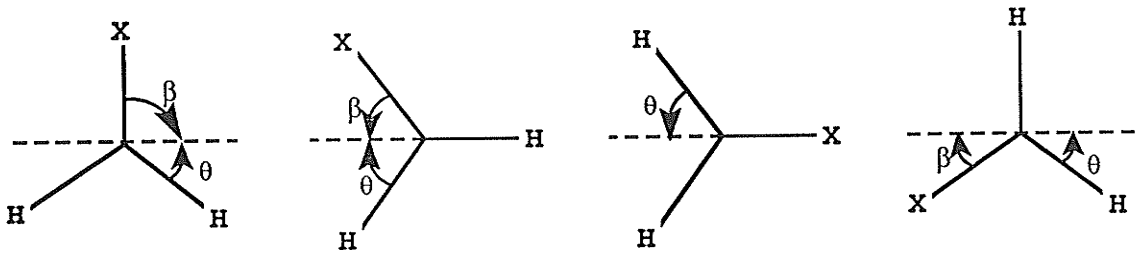

V **VI** **VII** **VIII**

The isobutyl group can assume two conformations, **XIII** and **XIV**, where **XIV** is possibly unstable due to steric repulsion between the methyl and phenyl groups.

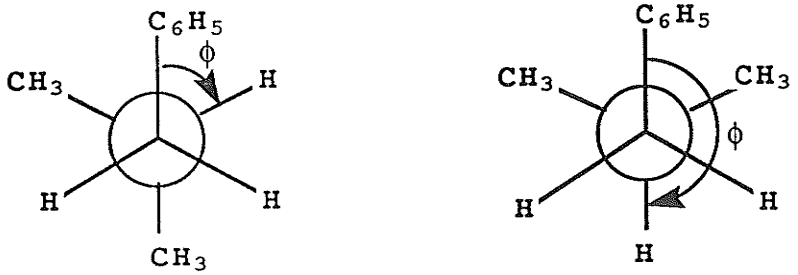

ϕ=−60° ϕ=±180°

XIII **XIV**

In a recent jet-cooled laser spectroscopic study (80), **V** is assigned as the minimum energy conformation, with the isopropyl group perpendicular to the ring. The number of origin transitions observed in the TOFMS of isobutylbenzene and the asymmetrically substituted 1-isobutyl-3-methylbenzenes display one and two origins, respectively, implying that the methine C-H bond is oriented *gauche* to the ring as in **XIII**. The result is further supported by the molecular orbital-molecular mechanics (MOMM) calculations, that **XIII** is more stable than **XIV** by 2.93 kJ mol^{-1}. In another computational study, the energy difference between **XIII** and **XIV** is calculated as 8.4 kJ mol^{-1} by the CAMSEQ method, whereas MM2 indicates no energy difference (81).

The perpendicular orientation of the isobutyl group, with the methine C-H bond oriented *gauche* to the ring, is also observed in some isobutyl-substituted heterocyclic compounds (82-84).

Molecular orbital studies

Table 8 and 9 (p.73 and 74) show the relative energies, the dipole moments and the conformations of the side chain for seven conformations about the C_{sp^2}-C_{sp^3} bond, computed at the semi-empirical AM1 and STO-3G MO levels. The conformation about the C_{sp^2}-C_{sp^3} bond is indicated by the angle β. The conformation of the side chain is indicated by the

dihedral angle, ϕ, between the C_{sp^2}-C_{sp^3} bond and the methine C-H bond. Both levels of computation predict that the minimum energy conformation occurs for β=75° or 105°, with the methine C-H bond placed *gauche* to the phenyl ring as in **XIII**. This conformation has some steric repulsion between the methyl and phenyl groups, so that the molecule is computed as more stable at 75° rather than 90°. The angle ϕ is predicted as -46.1° by AM1 and -55.7° by STO-3G MO at β=75°. The *gauche* conformation (**XIII**, optimized ϕ=45.8°) at β=90° is calculated as 4.85 kJ mol^{-1} more stable than the *trans* (**XIV**, optimized ϕ=180°) at the AM1 level. The STO-3G basis gives an energy difference of about 2.96 kJ mol^{-1} [§], which is the same as that given by the MOMM calculations (80).

The barrier height for rotation about the C_{sp^2}-C_{sp^3} bond computed by STO-3G is 12.45 kJ mol^{-1}, almost three times that predicted by AM1, 4.69 kJ mol^{-1}. The STO-3G MO computations are probably more reliable than the AM1, as suggested by the calculations on ethylbenzene which has similar conformational parameterization around the C_{sp^2}-C_{sp^3} bond. The STO-3G MO calculations for ethylbenzene predict a twofold rotational barrier of 6.58(11) kJ mol^{-1} as compared to 4.85-9.2 kJ mol^{-1} in the vapour phase (85,86) or about 5 kJ mol^{-1} in solutions (16). The AM1 value is 2.25 kJ mol^{-1}, being underestimated by more than half. The AM1 and STO-3G MO relative energies are

---

[§] The computation for the conformation β=90°, ϕ=180° did not converge; however, the energy difference between the last two iterations is only 4.2x10^{-5} kJ mol^{-1}.

least-squares fitted to the functions in [19] and [20], respectively (p.75). At the 95% confidence level, the twofold components of the barrier at the AM1 and the STO-3G MO levels are 4.79(2) and 11.11(6) kJ mol^{-1}, respectively. There are significant V_4, V_6 and V_8 components in the AM1 potential function, which are of similar magnitude, -0.50(2), +0.48(2) and -0.46(2) kJ mol^{-1}, respectively. The V_4 component in the STO-3G MO potential is -1.54(11) kJ mol^{-1}, and surprisingly, the magnitude of the V_8 term is as large as 2.47(10) kJ mol^{-1}. The signs of the corresponding components are the same at both levels.

At 300 K, the AM1 potential implies a $\langle\sin^2\beta\rangle$ of 0.707 and $\langle\beta\rangle$ of 59.8° by a classical averaging method. Under the same conditions, the STO-3G MO potential yields a $\langle\sin^2\beta\rangle$ of 0.833 and $\langle\beta\rangle$ of 68.4°.

Barrier implied by ^6J_p(H,H)

^6J_p(H,H) is -0.374(1) Hz in isobutylbenzene in CS_2 at 300 K (Table 4 on p.45). The coupling in toluene is represented by equation [5] (p.11). $^6J^{\pi}_{90}$ is -1.204(4) Hz in toluene and is reduced by electronegative substituents attached to the α-carbon (12,16,17,87). The electronegative substituent polarizes the C_α-H bonds and decreases hyperconjugation, thereby reducing the magnitude of $^6J^{\pi}_{90}$ (12). Assuming a linear dependence of $^6J^{\pi}_{90}$ on electronegativity, the presence of one methyl group in ethylbenzene reduces the

magnitude to -1.16 Hz (16). The electronegativities of the methyl and isopropyl groups are the same (88); therefore $^{6}J^{\pi}_{90}$ is also taken as -1.16 Hz for isobutylbenzene. The measured $^{6}J_{p}(H,H)$ gives a $\langle\sin^2\theta\rangle$ of 0.322(1), or a $\langle\sin^2\beta\rangle$ of 0.856(3). The value of $\langle\sin^2\theta\rangle$ implies that the minimum energy conformation has the side chain perpendicular to the plane of the ring (**V** on p.109). If the rotational barrier about the C_{sp^2}-C_{sp^3} bond is twofold, then $\langle\sin^2\theta\rangle$, in terms of the hindered rotor model, implies that it has a magnitude of 10.4(1) kJ mol^{-1}. The classical averaging procedure gives the same result at 300 K. In the AM1 and STO-3G MO calculations, the V_4/V_2 ratio is indicated as ~0.10. The experimental value of $\langle\sin^2\theta\rangle$ is compatible with a number of possible combinations of V_2 and V_4 and also suggests that the STO-3G MO approximation is superior to the AM1 in the isobutylbenzene computations. The internal barrier in ethylbenzene is solvent independent (16), which suggests that isobutylbenzene will behave similarly.

A list of some possible combinations of V_2 and V_4 for the experimental value of $\langle\sin^2\theta\rangle$, at 300 K, is given in Table 13 (p.114).

Table 13

The possible combinations of V_2 and V_4 for the measured $\langle \sin^2\beta \rangle$ of isobutylbenzene at 300 K.

	$\langle \sin^2\beta \rangle$	Barrier* (kJ mol^{-1}) V_2	V_4	V_4/V_2
AM1	0.707	-4.79(2)	-0.50(2)	0.104
STO-3G	0.837	-11.08(8)	-1.25(8)	0.113
^6J_p(H,H)	0.856(3)	-10.4(1)	---	---
		-12.06	-1.25	0.104
		-12.14	-1.30	0.107
		-12.21	-1.35	0.111
		-12.28	-1.40	0.114
		-12.43	-1.50	0.121

* The negative sign of the barrier indicates that the minimium energy conformation has the C_α-C_β bond perpendicular to the benzene plane.

The coupling constants $^4J_o(H,H)$ and $^5J_m(H,H)$

$^4J_o(H,H)$ in toluene is represented by equation [15] (p.17). If the σ-π component, in the presence of the isopropyl group, is reduced by the same factor as is $^6J^{\pi}_{90'}$ -1.16/-1.20, then

$$^4J_o(H,H) = -1.04\langle\sin^2\theta\rangle - 0.32\langle\cos^2\theta\rangle \text{ (Hz)} \qquad [32]$$

In Table 4 (p.45), $^4J_o(H,H)$ is -0.538(1) Hz in CS_2 at 300 K, which is smaller in magnitude than those of toluene, -0.702(1) Hz (9), and ethylbenzene, -0.649(1) Hz (16), but larger than that of neopentylbenzene, -0.453(3) Hz (18). For a $\langle\sin^2\theta\rangle$ of 0.396 from the AM1 potential, $^4J_o(H,H)$ is calculated as -0.605 Hz. The $\langle\sin^2\theta\rangle$ of 0.332 from the STO-3G MO computations give a $^4J_o(H,H)$ of -0.559 Hz. The $^4J_o(H,H)$ from the experimental $\langle\sin^2\theta\rangle$ is -0.552 Hz. To obtain agreement with the measured $^4J_o(H,H)$, the coefficient of $\langle\cos^2\theta\rangle$ should be -0.30 Hz and the equation representing $^4J_o(H,H)$ of isobutylbenzene is

$$^4J_o(H,H) = -1.04\langle\sin^2\theta\rangle - 0.30\langle\cos^2\theta\rangle \text{ (Hz)} \qquad [33]$$

The equation representing $^5J_m(H,H)$ in toluene (eq. [13] on p.15) includes a σ-π and a σ electron component. If the σ-π component is reduced by the same factor as for $^6J^{\pi}_{90'}$ then

$$^5J_m(H,H) = 0.325\langle\sin^2\theta\rangle + 0.322\langle\sin^2(\tfrac{\theta}{2})\rangle \text{ (Hz)} \qquad [34]$$

Since $\langle\sin^2(\frac{\theta}{2})\rangle$ is 0.5 for all evenfold barriers, the $\langle\sin^2\theta\rangle$ from the AM1 potential gives a $^5J_m(H,H)$ of 0.290 Hz; the

STO-3G MO potential implies a value of 0.269 Hz. The measured $\langle \sin^2\theta \rangle$ will give $^5J_m(H,H)$ as 0.266 Hz. To reproduce the experimental value of 0.272(1) Hz, the coefficient of $\langle \sin^2(\frac{\theta}{2}) \rangle$ has to be 0.335 Hz. The equation representing $^5J_m(H,H)$ of isobutylbenzene is then

$$^5J_m(H,H) = 0.325\langle \sin^2\theta \rangle + 0.335\langle \sin^2(\frac{\theta}{2}) \rangle \text{ (Hz)} \qquad [35]$$

In summary, $^4J_o(H,H)$ and $^5J_m(H,H)$ are roughly consistent with the STO-3G MO potential, but not with the AM1 potential.

$^3J(H,H)$ and conformation of side chain

The conformations **XIII** and **XIV** should display quite different magnitudes of $^3J(H,H)$ because of the *gauche* and *trans* orientations of the coupling protons. In isopropylcyclopropane, the *gauche* and the *trans* couplings, ^3J_g and ^3J_t, are estimated as $2.0 \leq {}^3J_g \leq 3.0$ and $11.0 \leq {}^3J_t \leq 13.0$ Hz (89). These couplings are obtained as 2.5 ± 0.1 and 12.5 ∓ 0.1 Hz, respectively, in 2,4-diphenylpentane, with the assumption that $^3J_t - {}^3J_g = 10$ Hz (90). At room temperature, where **XIII** and **XIV** interconvert rapidly, the measured $^3J(H,H)$ is an average value. $^3J(H,H)$ is given by equation [36] for the conformation in **XIII**.

$$^3J(H,H) = \frac{1}{2}(^3J_t + {}^3J_g) \text{ (Hz)} \qquad [36]$$

For conformation **XIV**, the average $^3J(H,H)$ is the same as ^3J_g.

$$^3J(H,H) = \frac{1}{2}(^3J_g + {}^3J_g) = {}^3J_g \text{ (Hz)} \qquad [37]$$

In isobutylbenzene, $^3J(H,H)$ is 7.154(1) Hz, clearly indicating that the isobutyl group predominantly assumes conformation **XIII**. The coupling in a rigid **XIII** can be approximated by $^3J(H,H)=\frac{1}{2}[12.5(1)+2.5(1)]=7.5(1)$ Hz. Were **XIV** the preferred conformation of the isobutyl group, the measured coupling would be as small as 2.5 Hz. Alternatively, the population distribution of the two conformers can be approximated by [38],

$$^3J(H,H) = P_{XIII}{}^3J_{XIII} + P_{XIV}{}^3J_{XIV} \text{ (Hz)} \qquad [38]$$

where P_{XIII} and P_{XIV} are the fractional populations of the conformers **XIII** and **XIV**, respectively, and $P_{XIII}+P_{XIV}=1$. $^3J_{XIII}$ and $^3J_{XIV}$ are obtained with equations [36] and [37]. The measured $^3J(H,H)$ gives P_{XIII} as 0.93(6) at 300 K, implying a free energy preference of $6.4^{-1.7}_{+5.5}$ kJ mol^{-1}.

$^4J(CH_3,H)$ was not observed in isobutylbenzene. The use of this coupling in the determination of the conformation is complicated by the structural and substituent dependence of the coupling. It will be discussed in section 4.3.

Conclusion

The minimum energy conformation of isobutylbenzene in CS_2 solution, implied by $^6J_p(H,H)$, has the side chain perpendicular to the benzene plane. The magnitude of $^3J(H,H)$

indicates that the methine C-H bond lies *gauche* to the ring. Both AM1 and STO-3G MO computations predict that the minimum energy conformation is at β=75° instead of 90°. The STO-3G MO result is perhaps a better approximation to the internal rotational barrier of isobutylbenzene, probably for all α-monoalkyl substituted toluenes (cf. ethylbenzene (16)). The STO-3G MO twofold barrier, 11.08(8) kJ mol^{-1}, is fairly close to the apparent twofold barrier of 10.4(1) kJ mol^{-1} in solution. In fact, STO-3G MO also gives a better dipole moment. The minimum energy conformer has a dipole moment of 0.28 and 0.10 D according to STO-3G and AM1, respectively, whereas the experimental value is 0.34 D (91). The internal barrier in isobutylbenzene may be solvent independent, as in ethylbenzene (16).

The apparent twofold rotational barriers for some α-alkyl substituted toluenes are listed in Table 14 (p.119). The barrier increases sharply from effectively zero in toluene (9) to higher than 20 kJ mol^{-1} in neopentylbenzene (18), as the size of the substituent increases. For comparison, the barriers for benzyl silane (92) and benzyl trimethylsilane (18) are also listed. The barrier for benzyl trimethylsilane is much lower than that for the corresponding benzyl trimethylmethane (neopentylbenzene), while the barrier for benzyl silane is higher than that for ethylbenzene. It is suggested that the internal rotational barriers of the silanes are dominated by the hyperconjugation between the C-Si bond and the aromatic π electron system (18,92).

Table 14

The apparent twofold rotational barrier of some benzyl alkanes and silanes obtained by the J-method at 300 K.

	Ref.	^6J_p (Hz)	$^6J^{\pi}_{90}$ (Hz)	$\langle\sin^2\theta\rangle$	V_2 (kJ mol^{-1})
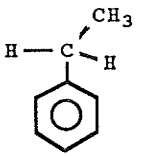	16	-0.450(5)§	-1.16	0.388(4)	5.1(2)
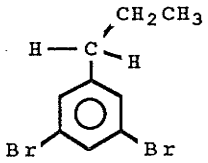	15*	-0.423(8)$^{\Diamond}$	-1.16	0.365(7)	6.5(5)
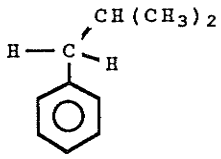		-0.374(1)$^{\Diamond}$	-1.16	0.322(1)	10.4(1)
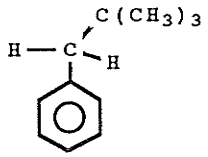	18	-0.300(3)‡	-1.16	0.259(5)	>20.0
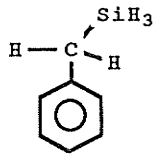	92	-0.444(5)$^{\Delta}$	-1.27(7)	0.350(23)	7.4(1.6)
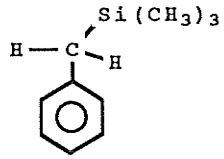	18	-0.418(3)‡	-1.26	0.332(2)	9.4(2)

§ the mean of acetone-d_6, CCl_4, CS_2, and $C_6F_{11}CF_3$ results

* at 305 K

$^{\Diamond}$ in CS_2

‡ in CCl_4

$^{\Delta}$ the mean of CS_2 and C_6D_6 results

4.3. Conformational distribution and internal rotational potential in 3-phenylpentane

The conformational analysis of 3-phenylpentane includes the studies of the conformation of the alkyl side chain and of the orientation of the phenyl group relative to the chain. For n-pentane, the possible conformations are the TT, $TG^{\pm}$ and $G^{\pm}G^{\pm}$ (see pictorial T, G^{+} and G^{-} below), where TT is the all *trans* or zig-zag conformation and is considered the most stable. The $TG^{+}(TG^{-})$, $G^{+}G^{+}(G^{-}G^{-})$ and $G^{+}G^{-}(G^{-}G^{+})$ are pairs of degenerate conformers. The degeneracy is lifted upon substitution by a phenyl group to form 3-phenylpentane. For steric reasons, $G^{+}G^{-}(G^{-}G^{+})$ are considered energetically unfavourable (84,93-95).

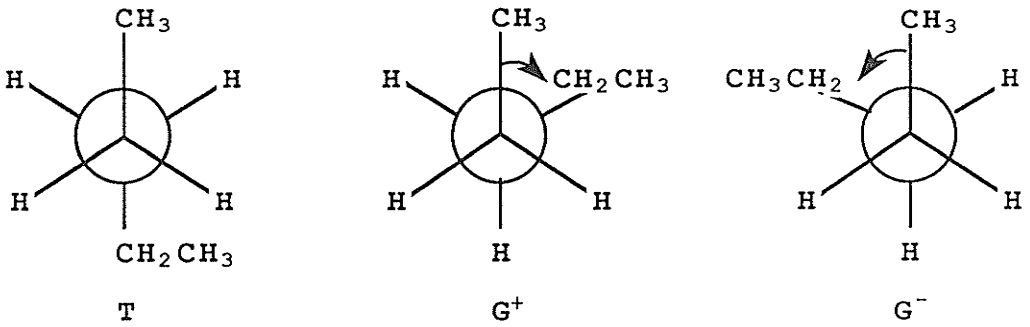

A number of molecular mechanics (93,94,96) and semi-empirical (95) calculations on n-pentane have shown that the relative stabilities of these conformations decrease in the order TT > $TG^{+}(TG^{-})$ > $G^{+}G^{+}(G^{-}G^{-})$ > $G^{+}G^{-}(G^{-}G^{+})$; the respective energies relative to the TT conformation are calculated as 1.1-2.7, 3.4-4.9 and 10.7-13.4 kJ mol^{-1} by molecular mechanics calculations (93,94,96). CNDO/2

calculations (95) give the energies of $TG^+(TG^-)$ and $G^+G^+(G^-G^-)$ relative to TT as 1.84 and 6.06 kJ mol^{-1}, respectively. The *ab initio* molecular orbital calculations (97), using the 6-31G* basis set, the MP3 correction for electron correlation, and zero point energy correction, give an energy difference for $TG^+(TG^-)$ relative to TT as 3.6 kJ mol^{-1} at 0 K, and as 3.4 kJ mol^{-1} at 298 K. Those for $G^+G^+(G^-G^-)$ are roughly twice as high. Molecular mechanics calculations (98) give the strain energy differences for $TG^+(TG^-)$ and $G^+G^+(G^-G^-)$ relative to TT as 3.77 and 6.78 kJ mol^{-1}, respectively. The Monte Carlo simulations of liquid n-pentane at 298 K indicate only minor condensed-phase effects on the conformational equilibrium (99). The fractional populations of the TT, $TG^+(TG^-)$, $G^+G^+(G^-G^-)$, and $G^+G^-(G^-G^+)$ conformers in the gas(liquid) phases are calculated as 46.5(47.0), 47.1(45.7), 5.4(6.0) and 1.0(1.3), respectively. The respective energies relative to the TT conformation are -0.03(0.07), 5.3(5.1) and 9.5(8.9) kJ mol^{-1}. In a Raman study (100) of n-pentane in the liquid state, two vibrational bands were assigned to the TT and $TG^+(TG^-)$ conformers. The enthalpy difference of these two forms, obtained from the temperature dependence of the intensities of these bands, is 1.88±0.25 kJ mol^{-1}. Upon cooling, one conformer remains in the solid phase and is assumed to be TT. The electron diffraction measurement (101) in the gaseous state imply an free energy difference of about 2.55±0.42 kJ mol^{-1}. In the study of the conformational equilibrium of n-pentane, using high pressure infrared

spectroscopy, the relative concentrations of the more globular conformers increase upon compression, with $G^+G^+(G^-G^-)$ > $TG^+(TG^-)$ > TT. The accompanied changes in volume at 293 K for $TG^+(TG^-)$ and $G^+G^+(G^-G^-)$ relative to TT are -1.0 ± 0.2 and -2.1 ± 0.3 $cm^3\,mol^{-1}$, respectively (102). For the high pressure solid, the only isomer that exists is in the TT form.

The side chain in 3-phenylpentane has nine possible conformations of the all-staggered form (see Figure 23 on p.123). In the infrared spectrum (103) of neat 3-phenylpentane, two bands, at 550 and 540 cm^{-1}, are assigned to the TT and TG^+(or G^-T) conformations. On lowering the temperature, the band at 550 cm^{-1} disappears and the energetically less favourable TG^+(or G^-T) remains in the crystalline state. The enthalpy difference between TT and TG^+(or G^-T), obtained from the temperature dependence of the intensities of these bands, is 1.7 $kJ\,mol^{-1}$. That obtained from the temperature dependence of the vicinal proton-proton coupling constants, on the assumption that only these two forms exist, is 1.5 $kJ\,mol^{-1}$ (103). The molecular mechanics calculations of Štokr et al. yield the energy differences of 1.84, 11.30 and 11.55 $kJ\,mol^{-1}$ for TG^+(or G^-T), TG^-(or G^+T) and G^+G^- with respect to TT (103). The region at 1100-1200 cm^{-1}, representing the conformation about the C_{sp^2}-C_{sp^3} bond, does not change upon crystallization, indicating that the probably coplanar orientation of the C_α-H bond and the ring persists in both states (103). In a molecular mechanics study (104)

Figure 23

The nine possible all-staggered conformations of the side G^+G^+(or G^-G^-), G^-G^+ and G^+G^-. The carbon atoms of the side of the paper. A wedge indicates that the bond extends out of the plane of the paper.

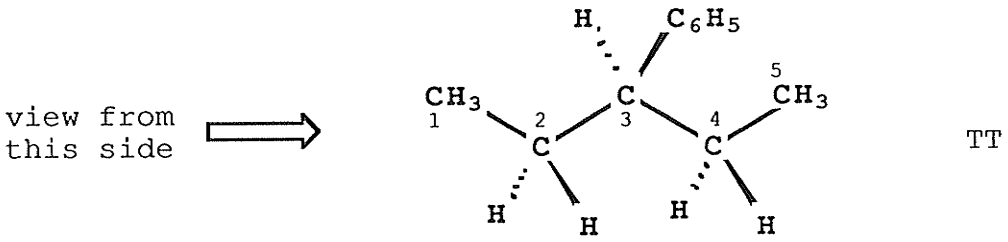

TT

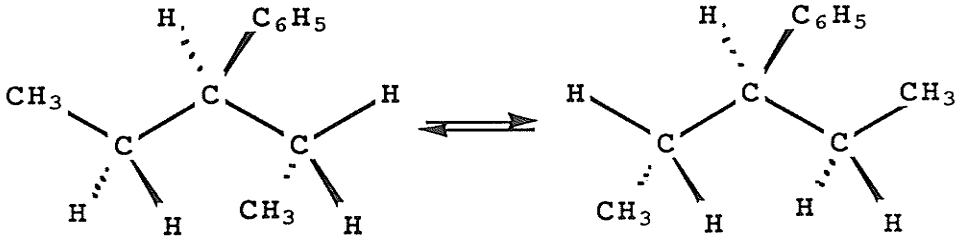

TG^+ G^-T

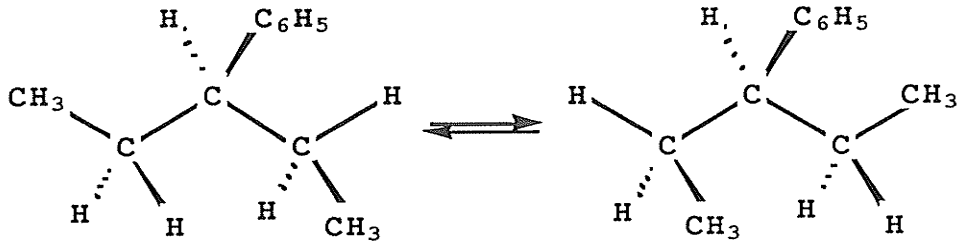

TG^- G^+T

chain in 3-phenylpentane: TT, TG^+(or G^-T), TG^-(or G^+T), chain, C(1) to C(5), in the TT conformation lie in the plane the paper. A broken line represents a bond pointing behind

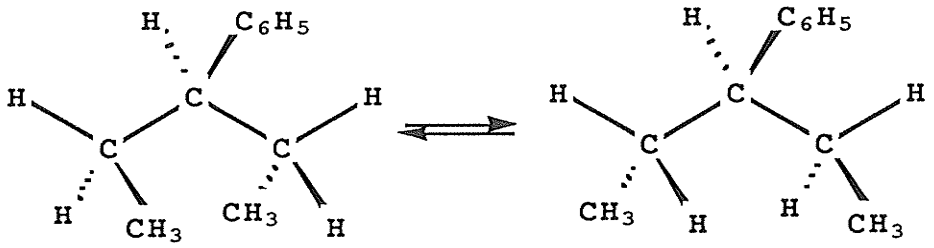

G^+G^+ G^-G^-

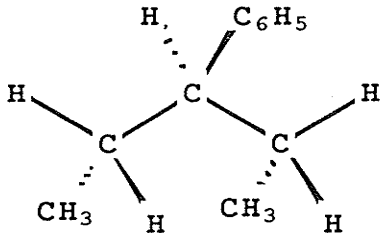

G^-G^+

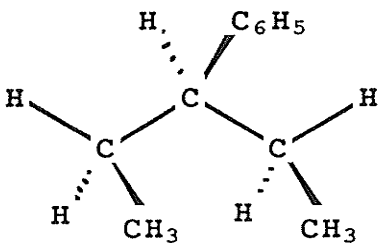

G^+G^-

of the conformation of 3-phenylpentane, the minimum energy conformation has a perpendicular orientation of the ring and the side chain (ie. the methine C-H bond lies in the plane of the ring). This rotamer is present to the extent of 99% at 298 K, from a Boltzmann statistical analysis.

3-phenylpentane is sometimes considered as a monomer unit of polystyrene. Other polystyrene model molecules, such as 2,4-diphenylpentane, 2,4,6-triphenylheptane and 2,4,6,8-tetraphenylnonane have been studied (105-108). The reorientation times of the phenyl groups of a 20.0 wt% solution of 2,4-diphenylpentane in $CHCl_3$, from a Raman line-shape analysis (183-313 K), give potential barriers of 13.8±1.3 and 8.4±1.3 kJ mol^{-1} for the rotation of the phenyl groups in the *meso* and the *racemic* compounds, respectively (105). The *meso* compound exists predominantly in the TG^+(or G^-T) form, whereas the *racemic* compound is composed of 75% of the TT and 25% of the G^-G^- at room temperature (105).

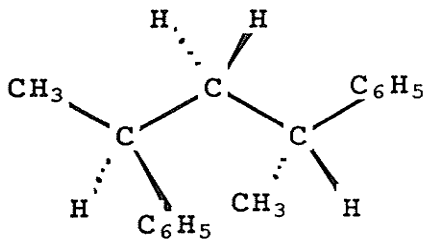

meso TG^+(or G^-T)

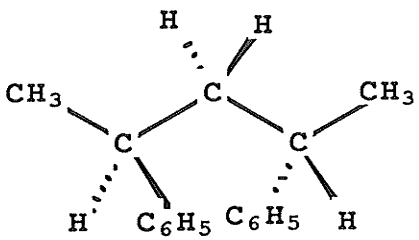

racemic TT

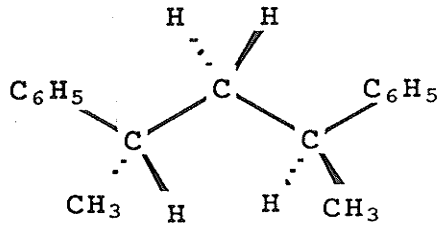

racemic G^-G^-

The crystal structures of syndiotactic 2,4,6-triphenylheptane and 2,4,6,8-tetraphenylnonane indicate a perpendicular orientation of the phenyl groups to the alkyl side chain (106,107). The calculated energies indicate that the minimum energy conformation of polystyrene has the phenyl rings perpendicular to the backbone and bisecting the C_β-C_α-C_β bond angles (108).

In 3-phenylpentane, the alkyl side chain resembles the polystyrene backbone.

The AM1 barrier for 3-phenylpentane

Table 10 (p.77) shows the computed relative energies, the dipole moments and the conformations of the side chain for seven conformations about the C_{sp^2}-C_{sp^3} bond. The conformation of the side chain is indicated by the dihedral angles, ϕ and Ψ, between the methine C-H bond and the two C_α-C_β bonds. The conformation about the C_{sp^2}-C_{sp^3} bond is indicated by θ. Computations were done at the AM1 level for various ϕ and Ψ, at 15° intervals of θ. The minimum energy conformation occurs at θ=0°, ϕ=47.5° and Ψ=39.2°, which

implies that the 5-pentyl group is in the TG^+ conformation (see Figure 23 on p.123). The values of ϕ and Ψ in Table 10 indicate that the two ethyl groups move in such a way as to minimize repulsions between the *ortho* C-H bonds and those in the methylene and methyl groups; CH_3, CH_3 repulsions are also involved (see footnote in Table 10 on p.77). The AM1 calculations predict that the TT conformer (optimized ϕ=50.4°, Ψ=-50.6°) is about 0.81 kJ mol^{-1} less stable than the TG^+. The G^-G^+ (optimized ϕ=-52.9°, Ψ=15.4°) is 2.66 kJ mol^{-1} less stable than the TG^+. The relative energies are best fit to the internal rotational potential $V(\theta)$ (eq. [21] on p.78). At the 95% confidence level, the V_2 and V_4 components of the barrier are 13.12(5) and -3.09(5) kJ mol^{-1}, respectively. There are significant V_6 and V_8 magnitudes of 1.04(5) and 0.86(5) kJ mol^{-1}, respectively. V_4 is of opposite sign to V_2, and its magnitude is almost 25% of that of V_2. The twofold barrier is comparable in magnitude to that of *meso* 2,4-diphenylpentane in $CHCl_3$, 13.8±1.3 kJ mol^{-1}, obtained from Raman line-shape analysis (105). The AM1 level has proved successful in establishing the internal rotational barrier of isopropylbenzene. The computed barrier height is 6.57 kJ mol^{-1}, which agrees very well with the experimental value of 6.5 kJ mol^{-1} in solution (17). The conformation around the α-carbon is similar in isopropylbenzene and 3-phenylpentane. Thus, as can be seen below, the predicted and experimental twofold potentials are also very close for 3-phenylpentane. However, the calculations on the side chain

are not as reliable, given that the AM1 prediction on the rotational barrier in ethane, 5.22 kJ mol^{-1}, is not compatible with the experimental value of 12.1(1) kJ mol^{-1} (84).

At 300 K, the potentials imply a $\langle \sin^2\theta \rangle$ of 0.158 and $\langle \theta \rangle$ of 20.1° via a classical averaging procedure. The MO calculations indicate the foldedness of the internal rotational barrier about the C_{sp^2}-C_{sp^3} bond. With the presence of librating groups in the side chain, substantial magnitudes of the higher terms are induced into the potential function (14). If the theoretical potential is purely twofold, the value of $\langle \sin^2\theta \rangle$, corresponding to a barrier height of 13.91 kJ mol^{-1}, will be 0.104.

Barrier implied by ^6J_p(H,H)

^6J_p(H,H) is -0.107(1) Hz in 3-phenylpentane in CS_2 at 300 K (Table 5 on p.53). The coupling in toluene is represented by equation [5] (p.11) and $^6J^{\pi}_{90}$ is -1.204(4) Hz (9). In α-substituted toluenes, the magnitude of $^6J^{\pi}_{90}$ is altered according to the electronegativities of the substituents (12,16,17,87). An electronegative substituent on the side chain will polarize the C_α-H bonds, hence decreasing the σ-π interaction and reducing the magnitude of $^6J^{\pi}_{90}$ (12). Assuming a linear dependence of $^6J^{\pi}_{90}$ on electronegativity and additivity, $^6J^{\pi}_{90}$ is -1.16 Hz in ethylbenzene for the presence of one methyl group (16), and

is -1.12 Hz in isopropylbenzene for two methyl groups (17). The electronegativities of the ethyl and the methyl groups are the same (88), therefore $^6J^{\pi}_{90}$ is also -1.12 Hz in 3-phenylpentane. The measured $^6J_p(H,H)$ gives $\langle\sin^2\theta\rangle$ as 0.096(1). This implies that the minimum energy conformation has the C_α-H bond in the benzene plane (**I** on p.13). If the rotational barrier about the C_{sp^2}-C_{sp^3} bond is twofold, $\langle\sin^2\theta\rangle$, in terms of the hindered model, corresponds to a V_2 of 14.9(1) kJ mol^{-1}. The classical averaging procedure gives the same result at 300 K. If the substitution of a second ethyl group at the α-carbon is only half as effective as the first, then $^6J^{\pi}_{90}$ is -1.14 Hz and $\langle\sin^2\theta\rangle$ is 0.094(1), giving a V_2 of 15.2(1) kJ mol^{-1}. The apparent twofold barrier agrees reasonably well with that from the AM1 calculations. The AM1 computations indicate that the V_4/V_2 ratio is ~-0.24. The presence of V_4 modifies the rotational barrier. By a classical averaging procedure, this V_4/V_2 ratio with the $\langle\sin^2\theta\rangle$ from $^6J_p(H,H)$ gives a number of possible combinations of V_2 and V_4. A list of these values at 300 K is given below.

	$\langle\sin^2\theta\rangle$	Barrier (kJ mol^{-1}) V_2	V_4	$-V_4/V_2$
AM1	0.158	13.12(5)	-3.09(5)	0.236
$^6J_p(H,H)$	0.096(1)	15.0(3)	----	----
		29.09	-6.40	0.220
		29.85	-6.70	0.224

Because AM1 underestimates the energy necessary to cause rotations about the C_{sp^3}-C_{sp^3} bonds in the side chains, it follows that, if rotation of the phenyl group entails the former rotations, then AM1 will underestimate the barrier to rotation of the latter. Hence the sign and magnitude of V_4, which presumably arises from accomodations of the side chain ethyl groups to the rotation of the phenyl group, are uncertain. However, if the AM1 computations do give the correct ratio of V_4 to V_2, then the measured value of $^6J_p(H,H)$ implies that DNMR measurements are possible. A V_2 of 29 kJ mol^{-1} (V_4 will not contribute to the barrier height) is accessible to ^{13}C DNMR measurements, particularly at 125 MHz.

The coupling constants $^4J_o(H,H)$ and $^5J_m(H,H)$

$^4J_o(H,H)$ in toluene is represented by equation [15] (p.17). If the σ-π component, in the presence of two ethyl groups, is reduced by the same factor as is $^6J^{\pi}_{90}$, -1.12/1.20, then

$$^4J_o(H,H) = -1.01\langle\sin^2\theta\rangle - 0.32\langle\cos^2\theta\rangle \text{ (Hz)} \qquad [39]$$

In Table 5 (p.53), $^4J_o(H,H)$ is -0.454(1) Hz in CS_2 at 300 K, much smaller in magnitude than those of toluene, -0.702(1) Hz (9) and isopropylbenzene, -0.559(1) Hz (17) in the same solvent; hence a much higher barrier. With a $\langle\sin^2\theta\rangle$ of 0.158 from the theoretical potential, $^4J_o(H,H)$ is calculated as -0.429 Hz. Alternatively, the $\langle\sin^2\theta\rangle$ from $^6J_p(H,H)$ gives

$^4J_o(H,H)$ as -0.386 Hz. To obtain agreement with the measured $^4J_o(H,H)$, the coefficient of $\langle\cos^2\theta\rangle$ should be -0.40 Hz and the equation representing $^4J_o(H,H)$ of 3-phenylpentane is

$$^4J_o(H,H) = -1.01\langle\sin^2\theta\rangle - 0.40\langle\cos^2\theta\rangle \text{ (Hz)} \qquad [40]$$

It may be noted that the magnitude of $^4J_o(H,H)$ is uncertain for θ near 0° in compounds of this kind (see point 39 in Figure 3 of ref. 28).

The equation representing $^5J_m(H,H)$ in toluene, [13] (p.15), includes a σ-π and a σ electron component. If the σ-π component is reduced by the same factor as is $^6J^{\pi}_{90}$, then

$$^5J_m(H,H) = 0.314\langle\sin^2\theta\rangle + 0.322\langle\sin^2(\tfrac{\theta}{2})\rangle \text{ (Hz)} \qquad [41]$$

where $\langle\sin^2(\frac{\theta}{2})\rangle$ is 0.5 for all evenfold barriers. The theoretical $\langle\sin^2\theta\rangle$ gives a $^5J_m(H,H)$ of 0.211 Hz. The $\langle\sin^2\theta\rangle$ from $^6J_p(H,H)$ will give a $^5J_m(H,H)$ of 0.191 Hz. The measured $^5J_m(H,H)$ of 0.279(1) Hz requires the equation for $^5J_m(H,H)$ in 3-phenylpentane as

$$^5J_m(H,H) = 0.314\langle\sin^2\theta\rangle + 0.498\langle\sin^2(\tfrac{\theta}{2})\rangle \text{ (Hz)} \qquad [42]$$

The large increase in the σ component, relative to that proposed for toluene, raises the question of the validity of equation [13] (p.15).

Couplings and conformation of side chain

It was suggested in the study of Štokr et al. (103) that of the nine possible all-staggered conformations of the side chain in 3-phenylpentane (Figure 23 on p.123), those with the methyl group(s) close to the ring (ie. TG^-(or G^+T) and G^+G^+(or G^-G^-)) and those with the two methyl groups close to each other (ie. G^+G^- and G^-G^+) are energetically unfavorable. This is further supported by their molecular mechanics calculations (103) that TG^-(or G^+T) and G^+G^- are 11.30 and 11.55 kJ mol^{-1}, respectively, higher in energy than TT. Hence TT and TG^+(or G^-T) are the only significant conformations of the side chain in 3-phenylpentane.

The TT and TG^+(or G^-T) conformers, viewed along the C(2)-C(3) bond, can be considered as ethane derivatives of type CH_2X-CHYZ. The Newman projections are indicated as the ***trans*** and the ***gauche***, respectively, where the ***trans*** has the CH_3 and the CH_3CH_2 groups *trans* to each other, and the ***gauche*** has the two groups *gauche* to each other. Another method (103) to illustrate these two rotamers is also shown below.

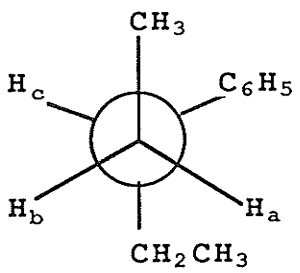

trans

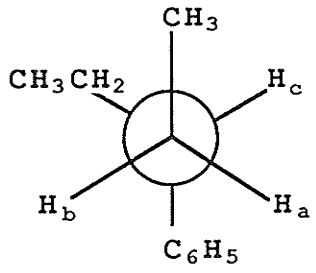

gauche

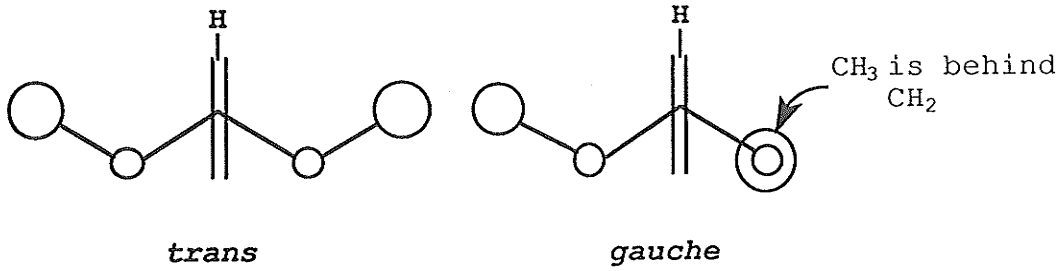

trans ***gauche***

view from *para* position

In the TT or ***trans*** conformation, H_a in both ethyl groups lies *trans* to H_c while H_b in both ethyl groups lies *gauche* to H_c. In the TG^+(or G^-T) or ***gauche*** conformation, H_c is *gauche* to H_a in one ethyl group but is *trans* to H_a in the other. Therefore, if the *trans* couplings, ^3J_t, are the same and the *gauche* couplings, ^3J_g, are the same in these two conformations, then [43] and [44] follow.

$$^3J_{ac} = P_T{}^3J_t + P_G(^3J_g + {}^3J_t) \quad \text{(Hz)} \qquad [43]$$

$$^3J_{bc} = P_T{}^3J_g + P_G(^3J_t + {}^3J_g) \quad \text{(Hz)} \qquad [44]$$

P_T and P_G are fractional populations and $P_T+P_G=1$; hence

$$^3J_{ac} - {}^3J_{bc} = P_T(^3J_t - {}^3J_g) \quad \text{(Hz)} \qquad [45]$$

$^3J_{ac}$ is 9.207(3) Hz and $^3J_{bc}$ is 5.250(2) Hz in 3-phenylpentane in CS_2 at 300 K (Table 5 on p.53). If $^3J_t-{}^3J_g=10.0$ Hz as in 2,4-diphenylpentane (90) and the uncertainty in this difference is 10%, then P_T is 0.40(4) and P_G is 0.60(4). These fractional populations entail a free energy difference of 1.0(4) kJ mol^{-1}, favouring the ***gauche*** conformer. The TG^+(or G^-T) conformation is more abundant than the TT in

solution at room temperature because the former is doubly degenerate. An entropy term of Rln2 implies that the enthalpy difference between ***gauche*** and ***trans*** is $-0.7(4)$ kJ mol^{-1}, TT being of lower energy. In the nmr study of Štokr et al. (103), only the spectrum of the pentyl group was analysed and was treated as a K_3ABX system. $^3J_{ac}$ and $^3J_{bc}$ were obtained as 8.7 and 5.5 Hz at 293 K and 8.2 and 6.0 Hz at 453 K, respectively. The enthalpy difference between TT and TG^+(or G^-T) then was 1.5 kJ mol^{-1}. However, the uncertainties in these couplings were not stated and the latter were obtained from the methylene peaks with only fair resolution.

Turning to $^4J(H,H)$, Barfield's calculations indicate that this coupling is positive for only a narrow range of dihedral angles near the zig-zag arrangement of the coupling protons (109). In Table 5 (p.53), $^4J(H,H)$ between the four methylene protons are $-0.233(3)$, $-0.231(0)$ and $-0.228(2)$ Hz, for $(H_a,H_{a'})$, $(H_a,H_{b'})$ and $(H_b,H_{b'})$, respectively. These values support the assumption that G^+G^+(or G^-G^-), G^+G^- and G^-G^+ are unstable forms, since only these forms involve zig-zag arrangement of the coupling protons and give a positive $^4J(H,H)$ instead of what has been measured.

The four bond couplings involving a methyl group, $^4J(CH_3,H)$, are usually observed as 0.7 to 1.0 Hz when $\varphi'=180°$ (see diagram below) and as -0.3 Hz when $\varphi'=60°$. They are calculated as 0.49 and -0.22 Hz, respectively (109).

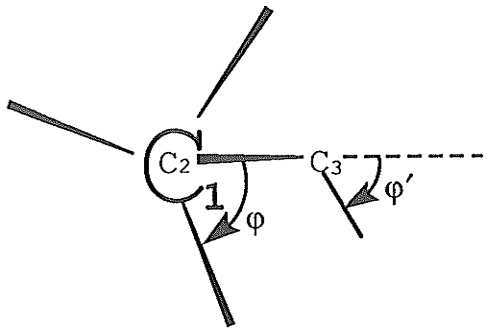

In 3-phenylpentane, $^4J(CH_3,H)$ is -0.272 Hz (see Figure 13 on p.59). This result is consistent with the TT and TG^+(or G^-T) conformations, in which φ' is 60° for the methine C-H bond.

Conclusion

The AM1 computations and the measured $^6J_p(H,H)$ both agree that the minimum energy conformation of 3-phenylpentane has the C_α-H bond in the plane of the ring. $^3J_{ac}$ and $^3J_{bc}$ imply that the side chain exists in the TT and TG^+(or G^-T) conformations in a ratio of 2:3 in solution. The measured $^4J(CH_3,H)$ is consistent with the TT and TG^+(or G^-T) conformations of the side chain.

A list of α,α-disubstituted toluenes and their twofold rotational barriers, obtained by the J-method, appears in Table 15 (p.137). These barriers increase from effectively zero in toluene (9) to 14.9(1) kJ mol^{-1} in 3-phenylpentane, and are expected to be much higher as the α-substituents become bulkier, such as the isobutyl and t-butyl groups. The rotational barriers about the C_{sp^2}-C_{sp^3} bonds in

3-(3-nitro-4-acetamidophenyl)-2,2,4,4-tetramethylpentane (110) and 3-(3,4,5-trimethoxyphenyl)-2,2,4,4-tetramethylpentane (111) are 92 and 93.3 kJ mol^{-1}, respectively.

Table 15

The apparent twofold rotational barrier of some α,α-disubstituted toluenes obtained by the J-method at 300 K.

	Ref.	^6J_p (Hz)	$^6J^{\pi}_{90}$ (Hz)	$\langle\sin^2\theta\rangle$	V_2 (kJ mol^{-1})
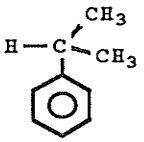	17	-0.254(2)[§]	-1.12	0.227(2)	6.6(7)
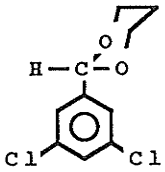	13*	-0.399(11)[◊]	-0.96(5)	0.416(33)	1.7(8)
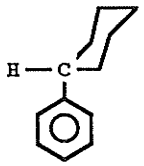	19	-0.243(4)[‡]	-1.12	0.217(4)	7.0(2)
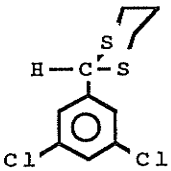	13*	-0.218(7)[‡]	-1.14	0.191(6)	9.2(1.3)
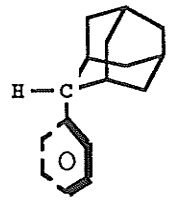	19	-0.889(5)[‡,¤]	-1.12	0.794(4)	7.5(1)
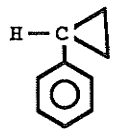	112*	-0.23(2)[‡]	-1.11(10)	0.21(4)	8.4(1.3)
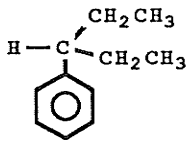		-0.107(1)[‡]	-1.12	0.096(1)	14.9(1)

[§] the mean of acetone-d_6 and CS_2 results

* at 305 K

[◊] in benzene-d_6

[‡] in CS_2

[¤] The C-H bond lies near a plane perpendicular to the benzene ring, analogous to axial phenylcyclohexane.

5. SUGGESTIONS FOR FUTURE RESEARCH

The STO-3G MO calculations suggest that the barrier to the methoxy group rotation in 1,3-dimethoxybenzene is about 8 kJ mol^{-1} and is higher than in anisole (60). The size of this barrier is accessible by the J-method through the use of long-range coupling constants between the methoxy carbon and the *para* carbon or proton, $^{5}J(^{13}C,^{13}C)$ and $^{6}J_{p}(^{1}H,^{13}C)$, respectively. It will be interesting to measure and compare this barrier with the theoretical value.

The substitution of a chlorine atom at the *meta* position does not affect the population distribution (or more precisely, the sums of the fractional populations of either two of the conformers) of 1,3-dimethoxybenzene. The influence of different types of substituent at this position on the population may furnish a more definite conclusion.

The H4 and H6 regions of the ^{1}H nmr spectrum of 1,3-dimethoxybenzene are not as well-resolved as those of H-2, which implies that $^{5}J_{o}(H4{=}H6,CH_3)$ and $^{7}J_{p}(H4{=}H6,CH_3)$ are less certain than $^{5}J_{o}(H2,CH_3)$. If the size of $^{5}J_{o}(H4{=}H6,CH_3)$ is being underestimated, so is the fractional population of the *trans-trans* conformer. In order to investigate how reliable the present results are, $^{5}J_{o}(H4{=}H6,CH_3)$ and $^{7}J_{p}(H4{=}H6,CH_3)$ have to be determined independently. To accomplish this, the two methoxy groups can be made nonequivalent by enriching one methoxy carbon with ^{13}C. The different types of methoxy proton resonances now enable $^{12}CH_3$ to be decoupled, thereby giving the methoxy-ring coupling constants of the other with greater reliability.

If the barrier in 3-phenyl-2,2,4,4-tetramethylpentane is as high as those suggested in the literature (110,111), $^{6}J_{p}$(H,H) of the methine proton will become negligible. The rotational barrier of 3-phenyl-2,4-dimethylpentane, which may be in the insensitive region of the J-method, is expected to lie between those of 3-phenylpentane and 3-phenyl-2,2,4,4-tetramethylpentane. The AM1 barriers of these methyl-substituted pentanes will provide further tests of AM1 as a suitable algorithm for α,α-dialkyl substituted toluenes.

The barrier to the phenyl groups rotation in *meso* 2,4-diphenylpentane, from a Raman line-shape study (105), is about the same size as the internal rotational barrier of 3-phenylpentane, and can be measured by the J-method. An ^{1}H nmr analysis of the whole molecule has not been done so far.

REFERENCES

(1) T. Schaefer and R. Laatikainen. Can. J. Chem. **61**, 224 (1983).

(2) T. Schaefer, T.A. Wildman, and J. Peeling. J. Magn. Reson. **56**, 144 (1984).

(3) T. Schaefer, S.R. Salman, T.A. Wildman, and G.H. Penner. Can. J. Chem. **63**, 782 (1985).

(4) T. Schaefer and R. Sebastian. Can. J. Chem. **67**, 1027 (1989).

(5) T. Schaefer, R. Laatikainen, T.A. Wildman, J. Peeling, G.H. Penner, J. Baleja, and K. Marat. Can. J. Chem. **62**, 1592 (1984).

(6) T. Schaefer and G.H. Penner. Can. J. Chem. **66**, 1635 (1988).

(7) T. Schaefer and R. Sebastian. Can. J. Chem. **67**, 1148 (1989).

(8) T. Schaefer, R. Sebastian, A. Lemire, and G.H. Penner. Can. J. Chem. **68**, 1393 (1990).

(9) T. Schaefer, R. Sebastian, and G.H. Penner. Can. J. Chem. **63**, 2597 (1985).

(10) R.B. Rowbotham and T. Schaefer. Can. J. Chem. **52**, 489 (1974).

(11) T. Schaefer and R. Laatikainen. Can. J. Chem. **61**, 2785 (1983).

(12) W.J.E. Parr and T. Schaefer. Acc. Chem. Res. **13**, 400 (1980).

(13) T. Schaefer, W. Niemczura, and W. Danchura. Can. J. Chem. **57**, 355 (1979).

(14) T. Schaefer and C. Takeuchi. Can. J. Chem. **67**, 1022 (1989).

(15) T. Schaefer, L.J. Kruczynski, B. Krawchuk, R. Sebastian, J.L. Charlton, and D.M. McKinnon. Can. J. Chem. **58**, 2452 (1980).

(16) T. Schaefer, G.H. Penner, and R. Sebastian. Can. J. Chem. **65**, 873 (1987).

(17) T. Schaefer, R. Sebastian, and G.H. Penner. Can. J. Chem. **66**, 1495 (1988).

(18) T. Schaefer, G.H. Penner, C.S. Takeuchi, and C. Beaulieu. Can. J. Chem. **67**, 1283 (1989).

(19) T. Schaefer, C. Beaulieu, and R. Sebastian. Can. J. Chem. **69**, 503 (1991).

(20) J. Kowalewski. Progress in NMR Spectroscopy. **11**, 1 (1977).

(21) H.A. Gaur, J. Vriend, and W.G.B. Huysmans. Tetrahedron Lett. 1999 (1969).

(22) D.G. de Kowalewski, R.H. Contreras, A.R. Engelman, J.C. Facelli, and J.C. Durán. Org. Magn. Reson. **17**, 199 (1981).

(23) T. Schaefer and R. Sebastian. J. Magn. Reson. **73**, 541 (1987).

(24) K.N. Trueblood and J.D. Dunitz. Acta Cryst. **B39**, 120 (1983).

(25) D.G. Lister. J. Mol. Struct. **68**, 33 (1980).

(26) H. Konschin, H. Tylli, and C. Grundfelt-Forsius. J. Mol. Struct. **77**, 51 (1981).

(27) R. Wasylishen and T. Schaefer. Can. J. Chem. **50**, 1852 (1972).

(28) M. Barfield, C.J. Fallick, K. Hata, S. Sternhell, and P.W. Westerman. J. Am. Chem. Soc. **105**, 2178 (1983).

(29) W. Danchura. Ph.D. Thesis, 1983. University of Manitoba, Winnipeg, Canada.

(30) J.S. Martin, A.R. Quirt, and K.E. Worvill. The NMR program library, Daresbury Laboratory, Daresbury, U.K.

(31) M.J. Frisch, J.S. Binkley, H.B. Schlegel, K. Raghavachari, C.F. Melius, R.L. Martin, J.J.P. Steward, F.W. Bobrowicz, C.F. Rohlfing, L.R. Kahn, D.J. Defrees, R. Seeger, R.A. Whiteside, D.J. Fox, E.M. Fluder, and J.A. Pople. Carnegie-Mellon Quantum Publishing Unit, Pittsburgh PA, 1984.

(32) SAS User's Guide : Statistics, A.A. Ray (ed), Statistical Analysis System Institute, 1985.

(33) SAS/Graph User's Guide. K.A. Council and J.T. Helwig (ed), Statistical Analysis System Institute, 1985.

(34) V.A. Chertkov and N.M. Sergeyev. J. Magn. Reson. **52**, 400 (1983).

(35) Handbook of NMR Spectral Parameters. Edited by W. Brügel. Heyden & Son Ltd., London. 1979.

(36) M.J. Aroney, R.J.W. Le Fèvre, and S-S. Chang. J. Chem. Soc. 3173 (1960).

(37) M.J. Aroney, M.G. Cornfield, and R.J.W. Le Fèvre. J. Chem. Soc. 2954 (1964).

(38) M.J. Aroney, R.J.W. Le Fèvre, R.K. Pierens, and M.G.N.

The. J. Chem. Soc. B, 666 (1969).

(39) N.L. Allinger, J.J. Maul, and M.J. Hickey. J. Org. Chem. **36**, 2747 (1971).

(40) M. Horák, E.R. Lippincott, and R.K.Khanna. Spectrochim. Acta, Part A: **23**, 1111 (1967).

(41) R. Josefi, E.Drahorádová, and M. Horák. Collect. Czech. Chem. Commun. **39**, 1541 (1974).

(42) D.G. Lister and N.L. Owen. J. chem. Soc. Faraday Trans. 2, **69**, 1304 (1973).

(43) M. Onda, A. Toda, S. Mori, and I. Yamaguchi. J. Mol. Struct. **144**, 47 (1986).

(44) G.M. Anderson III, P.A. Kollman, L.N. Domelsmith, and K.N. Houk. J. Am. Chem. Soc. **101**, 2344 (1979).

(45) H. Friege and M. Klessinger. Chem. Ber. **112**, 1614 (1979).

(46) J.W. Emsley, J.C. Lindon, and J.M. Street. J. Chem. Soc. Perkin Trans. 2, 805 (1976).

(47) J.W. Emsley, C.M. Exon, S.A. Slack, and A-M Giroud. J. Chem. Soc. Perkin Trans. 2, 928 (1978).

(48) P. Diehl, H. Huber, A.C. Kunwar, and M. Reinhold. Org. Magn. Reson. **9**, 374 (1977).

(49) A. Makriyannis and J.J. Knittel. Tetrahedron Lett. 2753 (1979).

(50) J.J. Knittel and A. Makriyannis. J. Med. Chem. **24**, 906 (1981).

(51) A. Makriyannis and S. Fesik. J. Am. Chem. Soc. **104**, 6462 (1982).

(52) L.I. Kruse, C.W. DeBrosse, and C.H. Kruse. J. Am. Chem. Soc. **107**, 5435 (1985).

(53) J.I. Seeman, H.V. Secor, P.J. Breen, and E.R. Bernstein. J. Chem. Soc. Chem. Commun. 393 (1988).

(54) P.J. Breen, E.R. Bernstein, H.V. Secor, and J.I. Seeman. J. Am. Chem. Soc. **111**, 1958 (1989).

(55) H.M. Seip and R. Seip. Acta Chem. Scand. **27**, 4024 (1973).

(56) E. Helgstrand. Acta Chem. Scand. **24**, 3687 (1970).

(57) M. Klessinger and A. Zywietz. J. Mol. Struct. **90**, 341 (1982).

(58) H. Dodziuk. Polish J. Chem. **57**, 535 (1983).

(59) H. Konschin. J. Mol. Struct. (Theochem), **110**, 311 (1984).

(60) T. Schaefer and G.H. Penner. J. Mol. Struct. (Theochem), **152**, 179 (1987).

(61) D.C. Spellmeyer, P.D.J. Grootenhuis, M.D. Miller, L.F. Kuyer, and P.A. Kollman. J. Phys. Chem. **94**, 4483 (1990).

(62) S.C. Nyburg and C.H. Faerman. J. Mol. Struct. **140**, 347 (1986).

(63) W. Hummel, K. Huml, and H-B. Bürgi. Helv. Chim. Acta. **71**, 1291 (1988).

(64) W. Kitching, I. de Jonge, W. Adcock, and A.N. Abeywickrema. Org. Magn. Reson. **14**, 502 (1980).

(65) J. Knuutinen and E. Kolehmainen. Magn. Reson. Chem. **28**, 315 (1990).

(66) N.L. Owen and R.E. Hester. Spectrochim. Acta, Part A: **25**, 343 (1969).

(67) G. Allen and S. Fewster. *In* Internal rotation in molecules. Edited by W.J. Orville-Thomas. J. Wiley & Sons, London. 1974. pp.274-276.

(68) H. Tylli and H. Konschin. J. Mol. Struct. **42**, 7 (1977).

(69) H. Spiesecke and W.G. Schneider. J. Chem. Phys. **35**, 731 (1961).

(70) K.S. Dhami and J.B. Stothers. Can. J. Chem. **44**, 2855 (1966).

(71) R.R. Biekofsky, A.B. Pomilio, R.H. Contreras, D.G. de Kowalewski, and J.C. Facelli. Magn. Reson. Chem. **27**, 158 (1989).

(72) C.M. Carter, J.C. Facelli, D.W. Alderman, D.M. Grant, N.K. Dalley, and B.E. Wilson. J. Chem. Soc. Faraday Trans. 1, **84**, 3673 (1988).

(73) A.R. Katritzky, M.V. Sinnot, T.T. Tidwell, and R.D. Topsom. J. Am. Chem. Soc. **91**, 628 (1969).

(74) V.A. Granzhan, S.F. Manole, and S.K. Laktinova. Izv. Akad. Nauk Mold. SSR, Ser. Biol. Khim. Nauk. **4**, 72 (1972).

(75) H. Lumbroso, Ch. Liégeois, L. Testaferri, and M. Tiecco. J. Mol. Struct. **144**, 121 (1986).

(76) L.M. DiBello, H.M. McDevitt, and D.M. Roberti. J. Phys. Chem. 72, 1405 (1968).

(77) K.L. Evans, G.W. Horn, F.R. Fronczek, R.D. Gandour, and S.F. Watkins. Acta Cryst. **C46**, 331 (1990).

(78) S. Marriott, T. Silvestro, and R.D. Topsom. J. Mol. Struct. (Theochem), **151**, 15 (1987).

(79) T. Schaefer, R. Sebastian, H.Y. Li, and T. Quach. Can. J. Chem. **68**, 996 (1990).

(80) J.I. Seeman, H.V. Secor, P.J. Breen, V.H. Grassian, and E.R. Bernstein. J. Am. Chem. Soc. **111**, 3140 (1989).

(81) G.L. Grunewald, M.W. Creese, and H.J.R. Weintraub. J. Comp. Chem. **9**, 315 (1988).

(82) C. Roussel, R. Gallo, J.Metzger, and J. Sandström. Org. Magn. Reson. **14**, 120 (1980).

(83) I. Pettersson, K. Rang, and J. Sandström. Acta Chem. Scand. **B40**, 751 (1986).

(84) U. Berg and J. Sandström. Adv. Phys. Org. Chem. **25**, 1 (1989).

(85) A. Miller and D.W. Scott. J. Chem. Phys. **68**, 1317 (1978).

(86) P. Scharfenberg. J. Chem. Phys. **77**, 4791 (1982).

(87) T. Schaefer, J. Peeling, and R. Sebastian. Can. J. Chem. **63**, 3219 (1985).

(88) J.E. Huheey. J. Phys. Chem. **69**, 3284 (1965).

(89) T. Schaefer, R. Sebastian, and R.E. Wasylishen. Can. J. Chem. **60**, 845 (1982).

(90) F.A. Bovey, F.P. Hood III, E.W. Anderson, and L.C. Snyder J. Chem. Phys. **42**, 3900 (1965).

(91) A.P. Altshuller. J. Phys. Chem. **58**, 392 (1954).

(92) T. Schaefer, R. Sebastian, and G.H. Penner. Can. J. Chem. **69**, 496 (1991).

(93) A. Abe, R.L. Jernigan, and P.J. Flory. J. Am. Chem. Soc. **88**, 631 (1966).

(94) R.A. Scott and H.A. Scheraga. J. Chem. Phys. **44**, 3054 (1966).

(95) I. Ando and A. Nishioka. Bull. Chem. Soc. Jap. **46**, 1040 (1973).

(96) S. Sýkora. Collect. Czech. Chem. Commun. **33**, 3514 (1968).

(97) K.B. Wiberg and M.A. Murcko. J. Am. Chem. Soc. **110**, 8029 (1988).

(98) S. Nikolić, N. Trinajstić, Z. Mihalić, and S. Carter. Chem. Phys. Lett. **179**, 21 (1991).

(99) W.L. Jorgensen, J.D. Madura, and C.J. Swenson. J. Am. Chem. Soc. **106**, 6638 (1984).

(100) N. Sheppard and G.J. Szaz. J. Chem. Phys. **17**, 86 (1949).

(101) L.S. Bartell and D.A. Kohl. J. Chem. Phys. **39**, 3097 (1963).

(102) M. Katō and Y. Taniguchi. J. Chem. Phys. **94**, 4440 (1991).

(103) J. Štokr, H. Pivcová, B. Schneider, and S. Dirlikov. J. Mol. Struct. **12**, 45 (1972).

(104) M.Simonetta, B. Calcagno, R. Santi and P. Schwarz. Chim. Ind. (Milan) **55**, 226 (1973).

(105) S. Koda, H. Nomura, and Y. Miyahara. Bull. Chem. Soc. Jap. **52**, 1828 (1979).

(106) R. Fourme, D. Andre, L. Bosio, and B. Jasse. J. Mol.

Struct. **71**, 245 (1981).

(107) D. Andre, L. Bosio, and B. Jasse. J. Mol. Struct. **140**, 339 (1986).

(108) F. Heatley. Prog. NMR Spectr. **13**, 44 (1979).

(109) M. Barfield, A.M. Dean, C.J. Fallick, R.J. Spear, S. Sternhell, and P.W. Westerman. J. Am. Chem. Soc. **97**, 1482 (1975).

(110) J.M.A. Baas. Recl. Trav. Chim. Pays-Bas. **91**, 1287 (1983).

(111) L.M. Jackman and F.A. Cotton. Dynamic Nuclear Magnetic Resonance Spectroscopy. Academic Press Inc., New York. 1975. p.p.177.

(112) W.J.E. Parr and T. Schaefer. J. Am. Chem. Soc. **99**, 1033 (1977).